

*CSU*

# HYDRAULIC TEST TO DEVELOP DESIGN CRITERIA FOR THE USE OF RENO MATTRESSES

PREPARED FOR

**MACCAFERRI  
STEEL WIRE PRODUCTS LTD.**

130 MITNER AVENUE  
AGINCOURT, ONTARIO, CANADA



PREPARED BY

**DARYL B. SIMONS**

**YUNG HAI CHEN**

**LAWRENCE J. SWENSON**

**CIVIL ENGINEERING DEPARTMENT, ENGINEERING RESEARCH CENTER  
COLORADO STATE UNIVERSITY, FORT COLLINS, COLORADO**

and

**SIMONS, LI & ASSOCIATES, INC.**

**P. O. BOX 1816, FORT COLLINS, COLORADO**

# TABLE OF CONTENTS

	<u>Page</u>
LIST OF FIGURES . . . . .	iv
LIST OF TABLES . . . . .	vi
FORWARD . . . . .	vii
EXECUTIVE SUMMARY . . . . .	viii
I. INTRODUCTION	
1.1 <u>The Problem</u> . . . . .	1.1
1.2 <u>Objectives</u> . . . . .	1.1
1.3 <u>Organization of the Report</u> . . . . .	1.2
II. GABIONS AND MATTRESSES: A LITERATURE REVIEW	
2.1 <u>Introduction</u> . . . . .	2.1
2.2 <u>Applications</u> . . . . .	2.2
2.3 <u>Behavior and Design</u> . . . . .	2.6
III. MATTRESS TEST PROGRAM	
3.1 <u>Introduction</u> . . . . .	3.1
3.2 <u>Scale-Model Mattress Test Program</u> . . . . .	3.1
3.2.1 Test Facilities and Test Scales . . . . .	3.1
3.2.2 Instrumentation . . . . .	3.13
3.2.3 Test Procedure . . . . .	3.16
3.2.4 Test Conditions and Data Collected in the 8-Foot Flume . . . . .	3.20
3.2.5 Test Conditions and Data Collected in the 4-Foot Flume . . . . .	3.28
3.3 <u>Full-Size Mattress Test Program</u> . . . . .	3.28
3.3.1 Test Facilities . . . . .	3.28
3.3.2 Instrumentation . . . . .	3.35
3.3.3 Test Conditions . . . . .	3.37
3.3.4 Problems Pertaining to Full-Scale Mattress Tests . . .	3.37
IV. ANALYSIS OF RESULTS	
4.1 <u>Introduction</u> . . . . .	4.1
4.2 <u>Hydraulic of Mattress Channels</u> . . . . .	4.1
4.2.1 Roughness Coefficients . . . . .	4.1
4.2.2 Velocity Distribution . . . . .	4.2
4.2.3 Relation Between Shear Stress and Velocities . . . . .	4.6
4.2.4 Velocity at the Mattress and Filter Interface and at the Filter and Soil Interface . . . . .	4.9
4.2.5 Pressure Variation . . . . .	4.10

TABLE OF CONTENTS (continued)

	<u>Page</u>
4.3 <u>Incipient Motion Conditions</u> . . . . .	4.12
4.4 <u>Deformation of the Mattress</u> . . . . .	4.21
V. DEVELOPMENT OF DESIGN CRITERIA	
5.1 <u>Development Approach</u> . . . . .	5.1
5.2 <u>Determination of Hydraulic Conditions</u> . . . . .	5.1
5.3 <u>Determination of Mattress Requirement Based on Incipient Motion Criteria</u> . . . . .	5.2
5.4 <u>Determination of Velocity at the Mattress/Filter (or Base Soil) Interface</u> . . . . .	5.3
5.5 <u>Determination of Filter Requirement</u> . . . . .	5.4
5.6 <u>Determination of Potential Deformation</u> . . . . .	5.6
VI. SUMMARY AND CONCLUSIONS . . . . .	6.1
VII. REFERENCES . . . . .	7.1
APPENDIX - DESIGN EXAMPLES	

## LIST OF FIGURES

	<u>Page</u>
Figure 3.1. Scale-model experiment setup . . . . .	3.2
Figure 3.2. Plan view of scale model mattress configuration . . . . .	3.5
Figure 3.3. Plan view of scale-model mattress configuration in the 4-foot flume . . . . .	3.6
Figure 3.4. Overview of 8-foot tilting flume test setup . . . . .	3.9
Figure 3.5. Overview of the 4-foot tilting flume test setup . . . . .	3.10
Figure 3.6. . . . .	3.12
Figure 3.7. Pressure transducer calibration relationship . . . . .	3.15
Figure 3.8. Configuration of pressure instrumentation . . . . .	3.17
Figure 3.9. A view of 4-foot flume run for $Q = 50$ cfs . . . . .	3.18
Figure 3.10 . . . . .	3.19
Figure 3.11. . . . .	3.27
Figure 3.12. Experimental setup for prototype Maccaferri Mattress tests . . . . .	3.34
Figure 3.13. Pressure tap location diagram for the 9-inch full- scale mattress tests . . . . .	3.36
Figure 3.14. Overall view of outdoor flume setup. $Q = 80$ cfs . . . . .	3.41
Figure 3.15. View of flume in vicinity below nozzle for $Q = 56$ cfs. . . . .	3.42
Figure 4.1. Comparison between the measured and computed Manning's roughness coefficient . . . . .	4.3
Figure 4.2. Velocity distribution for selected model-scale mattress tests in the 4-foot flume . . . . .	4.4
Figure 4.3. Average velocity for selected model-scale mattress tests in the 4-foot flume . . . . .	4.5
Figure 4.4. Relationship between shear stress, velocity and hydraulic radius . . . . .	4.7
Figure 4.5. $\frac{d_{50}}{D} =$ vs. Froude number (from Fiuzat, et al. 1982) . . . . .	4.8

LIST OF FIGURES (continued)

	<u>Page</u>
Figure 4.6. Comparison between the measured and computed velocity in the mattress and filter interface . . . . .	4.11
Figure 4.7. Variation of specific head immediately below the full-scale mattresses . . . . .	4.13
Figure 4.8. Variation of specific head immediately below the full-scale mattresses . . . . .	4.14
Figure 4.9. Critical velocity that initiates rock movement as a function of rock size . . . . .	4.16
Figure 4.10. Critical velocity that initiates rock movement as a function of mattress thickness . . . . .	4.17
Figure 4.11. Critical shear stress versus rock sizes for the with and without mattress cases . . . . .	4.19
Figure 4.12. Shields parameter as a function of the shear Reynolds number for with and without mattress cases . . . . .	4.20
Figure 4.13. Critical shear stress versus mattress thickness . . . . .	4.22
Figure 4.14. General pattern of rock movement within a mattress compartment . . . . .	4.23
Figure 4.15. Comparison of deformation of 6-inch and 9-inch full-scale mattress units for a velocity of 12 fps . . . . .	4.25
Figure 4.16. Comparison of deformation of 6-inch and 9-inch full-scale mattress units for a velocity of 20 fps . . . . .	4.26
Figure 4.17. Deformation of mattresses (9") due to rock movement (looking downstream). $V = 16.4$ fps. . . . .	4.27
Figure 4.18. Deformation of mattresses (9") due to rock movement (looking downstream). $V = 17.6$ fps . . . . .	4.27
Figure 4.19.	4.28
Figure 4.20.	4.29
Figure 4.21. Relationship between the deformation factor and effective Shields parameter . . . . .	4.30
Figure 5.1. Permissible unit tractive force for canals in cohesive material as converted from the U.S.S.R. data on permissible velocities . . . . .	5.5

## LIST OF TABLES

	<u>Page</u>
Table 2.1. Thickness of Reno Mattress Related to Water Velocity . . .	2.10
Table 3.1. Model-to-Prototype Scaling Ratios . . . . .	3.3
Table 3.2. Dimensions of Model-Scale and Full-Scale Mattresses Tested . . . . .	3.4
Table 3.3. Scale-Model Mattress Test Data in the 8-Foot Flume . . . .	3.21
Table 3.4. Manning's Roughness Coefficient for the Model-Scale Mattresses Tests Conducted in the 8-Foot Flume . . . . .	3.26
Table 3.5a. Run Sequence for Test A 6-Inch Mattress . . . . .	3.29
Table 3.5b. Run Sequence for Test B 9-Inch Mattress . . . . .	3.30
Table 3.5c. Run Sequence for Test C 12-Inch Mattress . . . . .	3.31
Table 3.5d. Run Sequence for Test D 18-Inch Mattress . . . . .	3.32
Table 3.5e. Run Sequence for Test E 6-Inch Mattress With Mastic . . . .	3.33
Table 3.6. Test Run Sequence - Discharge, Depth, Velocity Measurements for the 9-Inch Full-Scale Mattress Tests . . .	3.38
Table 3.7. Determination of 9-Inch Mattress Properties, Roughness Coefficient, $n_b$ - Bed Shear Stress, $\tau_b$ . . . . .	3.39
Table 3.8. Determination of 9-Inch Mattress Properties, Roughness Coefficient, $n_b$ - Bed Shear Stress, $\tau_b$ . . . . .	3.40

## FOREWARD

This study was performed under a contract entitled "Hydraulic Tests to Develop Design Criteria for the Use of Mattresses." The tests were conducted at the Hydraulics Laboratory, Engineering Research Center, Colorado State University. This report includes the analysis of data collected during the study and the conclusions drawn accordingly. The investigation was conducted by Dr. Daryl B. Simons, Professor of Civil Engineering, Colorado State University, Dr. Yung Hai Chen, Associate Principal Engineer, and Mr. Lawrence J. Swenson, Hydraulic Engineer of Simons, Li & Associates, Inc. (SLA). Dr. Ruh-Ming Li, Principal Hydraulic Engineer of SLA, was the Technical Reviewer to review the test program and results.

Mr. Alan D. Crowhurst, Dr. Eng. R. Agostini and Mr. E. Allen Dye of Maccaferri Gabions, Inc. served as the contracting representatives, technical consultant and liaison between SLA and the Maccaferri Steel Wire Products, Ltd. Dr. Rebecca M. Summer, Mr. Mark R. Peterson, Mr. James E. Goodman, Mr. Steven R. Townsley and Mr. Michael Mussetter assisted in conducting the study. The study period was from May 1982 to May 1983.

## EXECUTIVE SUMMARY

### Objectives

Various protection measures have been developed to insure the continued flow of water along a preselected path and to stabilize channels and soil slopes. Gabions and reno mattresses are protective devices that have been successfully utilized to meet these needs. Guidelines or methodologies concerning gabion and reno mattress applications have been established primarily through field experience and empirical analysis, aided in some instances by hydraulic model studies. Further research is necessary to generate the required data base from which to develop design criteria for reno mattress applications.

The present study was aimed at evaluating the performance of Maccaferri mattress products when used as river and canal bank and bed revetment. A hydraulic testing program was developed and undertaken to provide experimental data pertaining to the performance of reno mattresses. Test data were utilized to develop reliable design criteria for Maccaferri reno mattresses. Major tasks include:

1. To review the existing design methodologies and field application experience pertaining to gabions and mattresses.
2. To determine the roughness of revet mattresses.
3. To evaluate requirements of underlying granular filters or filter cloth layers.
4. To evaluate the stability of mattresses subjected to various flow conditions.
5. To analyze test results and develop design criteria applicable to mattress protection designs.

### Literature Review

Gabion and mattresses are rock-filled wire devices which have been used for controlling erosion and stabilizing soils for centuries. Gabions or wire-bound rock sausages were introduced by Maccaferri in 1894 to repair the breach of the River Reno at Casalecchio. The use of gabions and mattresses has a number of advantages. The strength and flexibility of the steel wire mesh allows the rock-filled basket to change shape without failure due to unstable ground or scour from moving water. Gabions and mattresses are permeable and

therefore eliminate the problems due to the hydraulic lift forces. Also, they permit plant growth for added stability and trapping efficiency. Climate has no measureable effect on the performance and longevity of gabions and mattresses. Finally, gabions and mattresses are economical to implement and provide a cost-effective means of stabilization and erosion control.

Major applications of gabions and mattresses including the following: revetments to protect river embankments against erosion; stabilization of bridge abutments; groins to deflect and "train" river currents; irrigation and ship canal linings; check dam, weirs and drop structures; culvert protection; protective works to dissipate wave action along coastal and lake shores; road stabilization; sedimentation ponds; stream rehabilitation; retaining walls; and boat launching ramps.

Design charts for placing gabion weirs on sloping and horizontal surfaces were developed by Stephenson (1980). The charts and equations were verified experimentally to determine structural stability against sliding and overturning. Oswald and Maynard (1978) conducted a series of tests to evaluate the effectiveness of several schemes using gabions for bank protection. No results were specified. Brown (1979) investigated various theoretical, experimental and prototype aspects of the use of gabion-type revetments. Many other researchers conducted site-specific model studies of the use of gabions for bank protection or for breakwater. Oswalt, et al. (1975) conducted a hydraulic model study at the Hydraulic Laboratory of the U.S. Army Engineer Waterways Experiment Station to evaluate bank protection requirements for the Fourmile Run local flood-control project. Both the riprap and mattresses were tested in the model. It was found that in several reaches in the channel, the flow conditions resulted in failure of the 36-inch riprap while the 12 x 3 x 1-foot mattresses with proper toe protection would provide necessary protection. The results of their study also indicated that the required mattress thickness is no more than one-third the required riprap thickness. Agostini and Papetti (1978) recommended thickness of Reno Mattress related to flow velocities and proposed the canal side slopes according to soil type. They found that compared with the use of riprap a savings of 25 to 30 percent could be obtained by using the mattresses.

Considering the available information, it is clear that very limited information is available regarding the performance of mattresses under high flow conditions. Additional study is required to answer the following questions:

1. What are the permissible design flow conditions for various types of mattresses?
2. What will be the change in mattress performance when the flow conditions are higher than the critical (incipient motion) conditions?
3. What is the requirement of filter under high flow conditions?

The study results presented in this report will address these questions.

#### Test Program

To evaluate mattress performance over a range of conditions, a two-section test scheme involving full-scale tests complemented by scale-model tests was conducted. Hydraulic tests of scale-model mattresses were conducted using the eight-foot wide flume located in the Hydraulics Laboratory at the Colorado State University Engineering Research Center. This flume is eight feet wide, four feet deep and 200 feet long and can be raised or lowered to produce slopes ranging from zero to about two percent. A maximum flow rate of approximately 100 cfs can be achieved.

Two series of scale-model mattress tests were conducted: one utilized the original eight-foot flume and the other utilized the four-foot flume which was established by installing a 100-foot long partition wall at the center of the eight-foot flume. The mattresses tested in the four-foot flume included 6-inch, 9-inch, 12-inch and 18-inch thick rock mattresses and 6-inch thick grouted mattresses which were converted to model-scale using a model-to-prototype length ratio of 1:3. Because available mesh screen for making scale-model mattresses was limited, it was difficult to achieve dynamic similarity between the model mesh and prototype mesh. A tensile test conducted by Maccaferri Gabions indicated that the model-scale mesh utilized for the model tests in the four-foot flume was more flexible compared to full-scale ones. The results obtained from these model tests would guarantee a safety coefficient. However, comparison between model and prototype tests results indicates that their results are comparable. The characteristics of scale-model mattresses are presented in Table 3.2. Only the 9-inch mattresses which were converted to model scale were tested in the eight-foot flume.

Six-inch and nine-inch thick full-scale mattresses were tested in a seven-foot wide, 75-foot long and four-foot high outdoor flume with a slope of 13 percent. The maximum discharge capacity is 100 cfs. Table 3.2 gives the characteristics of these mattresses.

In order to determine the flow conditions that initiate the movement of filling rocks within the mattresses, the test conditions were always started at relatively low velocity and large depth. These test velocities were increased step by step to determine the incipient flow conditions. Tables 3.3, 3.5 and 3.6 present the test conditions conducted in the eight-foot indoor flume, the four-foot indoor flume and the seven-foot outdoor flume, respectively. The maximum velocities obtained from these three flumes were about 10, 12, and 21 fps. The former two values correspond to prototype velocities of about 17 and 21 fps, respectively.

Data collected for each run included discharge, velocity, stage, mattress bed elevation, and pressure fluctuations at three measuring stations. Attempts were made to measure velocity and pressure at the rock/filter and filter/soil interfaces because these velocities would be control factors affecting stability of base soil. Some measured interface velocities although not very conclusive were analyzed and presented.

#### Analysis of Results

The data collected in the model-scale mattress and full-scale mattress tests were analyzed to determine:

1. Hydraulics of channels protected by mattresses.
2. Incipient motion conditions of filling rocks within mattresses.
3. Deformation of mattresses under high flow conditions.

The hydraulic variables considered in the analysis include: roughness coefficients, velocity distributions, relation between shear stress and velocities, velocity at the mattress and filter interface and at the filter and soil interface, and pressure variation. It was found that the bed roughness of the mattress surface could be determined from the Meyer-Peter and Muller's roughness equation for gravel, and the velocity distribution could be approximated by a log-velocity distribution. This indicates that hydraulic conditions in a mattress channel are similar to the condition in a gravel bed channel and the mattress mesh will not significantly affect channel roughness.

Analysis of hydraulic data also indicates that for the same velocity, shear stress increases with decrease in hydraulic radius or depth. Because shear stress is the major factor that controls the stability of mattress and riprap, for a given velocity, as depth is increased, stability will be increased due to the reduction in shear stress. A similar conclusion was obtained based on the analysis of pressure data collected in this study and based on the riprap tests conducted by Fiuzat, et al. (1982). The study of Fiuzat, et al. indicates that the stable size of rock is inversely proportional to  $D^{1/2}$  while it is proportional to  $V^3$ .

Based on the model-scale mattress tests in the four-foot flume, it was found that the velocity immediately underneath the mattresses remained somewhat unchanged regardless of the flow conditions the mattresses were subjected to and the thickness of mattresses. This situation is only true when the major flow direction is parallel to the mattress surface. The velocity at the mattress/filter interface could be approximately determined using a Manning's equation by assuming that the hydraulic radius approximately equalled one-half of the median rock size and assuming a Manning's n of 0.02. According to the full-scale 9-inch mattress tests, the velocity underneath the filter fabric at the filter and soil interface would be about one-fourth to one-half of the velocity immediately above the filter fabric. This velocity could be sufficiently large to move base material even though the mattress structure remained stable. In this case, a gravel filter layer that can effectively reduce velocity may be a better way to protect the base material.

The ability of the mattress to resist movement by the current relies on its monolithic continuity to resist displacement and not its mass. The rocks inside the mattress are retained by the wire netting. In general, when the velocity and shear stress reach a critical magnitude, the rocks inside the mattress start to move in the main flow direction. The mattress test results clearly indicate that mattress mesh improves the stability of filling rocks by doubling the critical shear stress compared to that for the riprap alone. The Shields parameter  $C_* = 0.10$  for the mattress while  $C_* = 0.047$  for the riprap. These results show that the mattress is more stable than riprap structures of greater thickness if the mattress structure is properly designed and installed.

With further increase in flow velocity and shear stress beyond the critical values, a significant amount of rocks would move from the upstream portion of a mattress compartment to its downstream portion. This resulted in reductions in thickness of rock in the upper portion of a mattress compartment and increase in thickness of rock in the lower portion of the compartment. A deformation factor is therefore defined as the ratio of the height difference between the lowest and highest rock surface within a mattress compartment to the median size of the filling rock. This ratio was related to the effective Shields parameter. This relation can be utilized to determine the mattress deformation as a function of hydraulic conditions and mattress strength.

Based on the full-scale mattress tests, the mattress deformation would not significantly affect the specific head variation underneath the mattress unless the extent of rock movement within the mattress was such that the filter or base materials were exposed. This indicates that the mattress even after deformation provided a similar degree of protection to that provided by an undeformed mattress if the reduced rock thickness section was more than one median size thick. Nine-inch mattresses were found to be effective in protecting soils in a mild slope channel bed under a velocity up to 20 fps. However, gravel filters or a combined geotextile/gravel filter should be utilized to reduce the water velocity at the mattress/filter interface that attacks the base materials, if this interface velocity is sufficiently high to affect the stability of base soil. Additional studies should be conducted to evaluate the effectiveness of various filter designs to improve the ability of mattresses to stabilize channels under extremely high flow conditions.

#### Development of Design Criteria

The following steps are proposed to design the mattress protection works:

1. Determine the hydraulic conditions in the mattress channel for a given design discharge.
2. Determine the mattress requirement based on incipient motion criteria.
3. Determine the velocity at the mattress/filter (or base soils) interface.
4. Determine filter requirement to safely protect base material.
5. Determine potential deformation of mattress when flow discharge is larger than the design discharge.

Detailed descriptions of each major design step are presented in Chapter V. Design examples are given in the Appendix. It should be noted that all the mattress tests were conducted on flume beds. The developed criteria for protecting banks were based on theories and some empirical equations and should be verified whenever possible.

## I. INTRODUCTION

### 1.1 The Problem

Various protection measures have been developed to insure the continued flow of water along a preselected path and to stabilize channels and soil slopes. In canals or channelized water courses protection measures typically embody some type of channel lining. A channel lining permits designing for a larger permissible velocity or tractive force, without channel scour or erosion, than would be possible in an unlined channel. Additionally, linings can be used to reduce or eliminate seepage problems in channels. Gabions and reno mattresses are protective devices that have been successfully utilized to meet these needs.

Guidelines or methodologies concerning gabion and reno mattress applications have been established primarily through field experience and empirical analysis, aided in some instances by hydraulic model studies. Further research is necessary to generate the required data base from which to develop design criteria for reno mattress applications. Such criteria are required to ensure adequate performance of reno mattresses under specific hydraulic and geometric conditions.

To address these needs, Simons, Li & Associates, Inc. (SLA) was awarded a research contract by Maccaferri Steel Wire Products, Ltd. to conduct hydraulic tests of Maccaferri Heavy Duty Reno Mattresses, and to develop design criteria governing utilization of these devices for channel stabilization.

### 1.2 Objectives

The present study was aimed at evaluating the performance of Maccaferri mattress products when used as river and canal bank and bed revetment. A hydraulic testing program was developed and undertaken to provide experimental data pertaining to the performance of reno mattresses. Test data were utilized to develop reliable design criteria for Maccaferri reno mattresses. Major tasks defined in the study program are:

1. To review the existing design methodologies and field application experiences pertaining to gabions and mattresses.
2. To determine the roughness of revet mattresses.
3. To evaluate requirements of underlying granular filters or filter cloth layers.

4. To evaluate the stability of mattresses subjected to various flow conditions.
5. To analyze test results and develop design criteria applicable to mattress protection designs.

### 1.3 Organization of the Report

Chapter II presents a literature review of gabion and mattress applications and discuss their applicabilities. Chapter III describes the laboratory facilities, procedures and test conditions that were applied to evaluate the performance of mattresses. Chapter IV presents the analysis results. A design method was developed based on the analysis results and hydraulic theories. Chapter V presents this design method. Chapter VI summarizes the study program, presents the conclusions and recommends additional studies. Two examples of applying the developed design procedures to design mattress protection works are presented in the Appendix.

## II. GABIONS AND MATTRESSES: A LITERATURE REVIEW

### 2.1 Introduction

Gabions and mattresses are rock-filled wire devices which have been used for controlling erosion and stabilizing soils for centuries. Gabions or wire-bound rock sausages were introduced by Maccaferri in 1894 to repair the breach of the River Reno at Casalecchio. Keutner (1935) presented the results of an exhaustive investigation of the applications of gabions in Germany and Austria. The National Park Service in the United States used gabion training walls as early as 1935 (Parker and Kittredge, 1935) to counteract streambed erosion and the Highway Commission in California (1922) employed gabions as a stream bank protection measure. Modernized versions of gabions and mattresses consist of rectangular compartmented containers made of thick steel wire mesh, woven with a triple twist at intersections. Heavy wire is sometimes added or woven into the mesh before or after filling to increase its stability and durability. The wire mesh can be galvanized and coated with PVC if used under highly corrosive conditions. The wire baskets can be constructed into various geometric shapes. For example, a hexagonal configuration is designed to conform firmly to uneven surfaces yet still maintain its integrity structurally.

The use of gabions and mattresses as natural building blocks and erosion control has a number of advantages. The strength and flexibility of the steel wire mesh allows the rock-filled basket to change shape without failure due to unstable ground or scour from moving water. Gabions and mattresses are permeable and therefore eliminate the problems due to the hydraulic lift forces. Also they permit plant growth for added stability and trapping efficiency. Climate has no measureable effect on the performance and longevity of gabions and mattresses. Finally, gabions and mattresses are economical to implement and provide a cost effective means of stabilization and erosion control.

Gabions and mattresses are supplied to the job site as folded mesh and tied in pairs. They are unfolded, placed in position like brick, tied together, and filled with durable rock. The mesh containers can also be filled first and placed by hand or by a crane to areas difficult to access, eg., underwater.

Major applications of gabions and mattresses include the following: revetments to protect river embankments against erosion; stabilization of bridge abutments; groins to deflect and "train" river currents; irrigation and ship canal linings; check dams, weirs, and drop structures; culvert protec-

tion; protective works to dissipate wave action along coastal and lake shores and boat launching ramps. Gabions are also utilized for constructing retaining walls on steep unstable slopes, check dams, weirs and drop structures.

Due to the variety of gabion applications, studies of gabion performance have necessarily encompassed many areas. General applications and specific uses are discussed below to illustrate the versatility of this structure. Following this, results of experiments and tests focusing on different aspects of gabion behavior are given. Data are included where available.

## 2.2 Applications

Gabions have been studied and used to serve a variety of purposes in the past. Many projects and studies have been done which describe their applications and utility as discussed below.

First, Roth (1977), Velut et al., (1977), Schuster (1974), Stephenson (1979), Forest Service (1979), and Burroughs (1979) reviewed applications, general designs, general implementation and case studies of gabion structures. Stephenson emphasized that their properties are suitable in energy dissipation works particularly in hydraulic engineering. The Forest Service (1979) has published a report based on a workshop which included general geotechnical investigations of gabions.

Secondly, gabions are used to stabilize low volume economical roads (Transportation Research Board, 1979). Details of a method for using gabions on low water crossings for primitive or secondary forest roads are given by Leydecker (1973) and discussed in the next section.

Gabions have been included in the development of an innovative substructural system for short span highway bridges. GangaRao (1978) found that gabions were one of the structures best suited for substructures on the bridge design from the industrialized construction viewpoint. Ten different systems were analyzed in detail with a view toward ease of erection, economy, maintenance, longevity, efficiency, versatility, etc. Reinforced earth, gabions, segmental plank, cellular box, steel bent, driven steel pile bent, concrete bent, stub system, concrete and timber cribbing were considered to be reasonable structures for short-span bridge abutments. Depending upon the merits and demerits, gabions, concrete bent, cellular box, segmental plank and timber cribbing appeared to be best suited from the industrialized construction viewpoint.

Webster and Watkins (1977) investigated the feasibility of commercial wire gabions, among other techniques, for constructing bridge approach roads across soft ground. The test section was on a soft-clay subgrade and traffic loads were on 5-ton trucks. The 1-foot gabions were filled with 3 to 7 inch rock and covered with 2 inches of crushed stone. The performance of this structure was considered to be extremely good.

One of the approaches to solving highway landslide problems in Tennessee was to use gabions. Royster (1975) discusses various geotechniques used in combination with gabions to mitigate stability problems in the Smokey Mountains. The steel-mesh wire baskets filled with heavy rock are the key elements in repairing massive slides and are used in place of sheet piling, masonry construction or concrete cribbing.

Streambank stabilization and river training are some of the more common applications of gabions and mattresses, e.g., Gotz (1978) in Germany, Keown et al., (1977) in the United States, Pernier (1977) and Michel (1977) in France, and a study in Columbia ("Checking River Erosion in Columbia," 1973). In addition, it is considered to be a natural and relatively unobtrusive technique for stabilizing streambeds in new town developments (Holeman and Sauer, 1969).

Gabions and mattresses have also been used extensively for reveting canals and canalised water courses, e.g., irrigation. Oswalt, et al. (1975) compared the effectiveness of utilizing riprap and mattresses for bank protection of the Fourmile Run local flood-control project. Agostini and Papetti (1978) described the dimensions of trapezoidal channel sections and applied linings formed with gabions and mattresses.

The use of gabions as sediment detention devices has been studied by Tan and Thirumurthi (1978) in Canada and by Poche and Sherwood (1976). These studies indicate that the filtering capacity of gabions is limited to bedload material. Poche and Sherwood determined the sediment trapping efficiency of straw filter barriers and gabions. A flume was designed and built for the laboratory portion of the study and 21 bales were tested. Trapping efficiencies varied from 46 to 88 percent; the overall average was 68 percent. No significant differences were noted in the efficiencies of straw and hay, and the bulk density and porosity of the bales correlated poorly with the trapping efficiencies. Field observations of contractor-placed bale barriers showed a high percentage of failures. Most failures were due to undercutting, end

flow, and washouts. Experimental field barriers with numbers and positions based on the universal soil loss equation were installed in place of the unmodified barriers. To minimize barrier failures, loose straw was wedged under and between the bales making up the barrier; the barrier length was extended so that the bottoms of the end bales were higher than the top of the lowest middle bale; and loose straw was scattered behind each barrier. Trapping efficiencies approximating laboratory efficiencies were obtained with the experimental barriers. Gabions filled with crushed stone yielded significantly lower trapping efficiencies than that of straw and hay bales. However, a layer of straw at the bottom of the gabion increased the efficiency to levels comparable to those of straw bales.

Coastal engineering has utilized gabions and mattresses in designs of shore protection structures. An annotated bibliography of the development of groynes, including gabion construction is given in Balsillie and Bruno (1972). Chishom (1976) described the use of gabions as secondary protection along the sea coast of New Zealand.

A similar application was implemented on the Lake Huron shore (Quigley, et al., 1974). A system of three gabion groynes were set up to protect a 122 m long section of coast already subject to severe earth movements. In the absence of adequate design information, the design was based on preliminary wind data and field observations of beach characteristics, sand availability and probable wave heights. The groynes were spaced about 36 m apart and extended off-shore from the cliff toe for a distance of about 18 m. The ends of the groynes, therefore, extended to the plunge point of 1.2 m high waves generated by strong trade winds and about 60 percent of the distance to the estimated location of the plunge point of severe storms. The beach height at the cliff toe has built itself up to 1.8 m above present water levels and provides a beach berm just adequate to stabilize the lower portions of the failing cliff behind it during the wet spring conditions of 1974. The installation has been very successful, and the groynes have rapidly filled with sand and gravel.

Another practical use of gabions and mattresses is for stabilizing lake shores and storm water catchments in urban areas. A project described in Ground Engineering Magazine (1976) regarded that in the United Kingdom, banks of a lake were stabilized by the use of gabions placed over 0.5 mm thick Fibertex filter sheet (a non-woven material of 95 percent polypropylene). A one meter square gabion was sunk onto the bottom of the lake to form a

buttress from behind which Fibertex was anchored. The Fibertex was then rolled up onto the profile of the bank and covered with a 170 mm deep gabion mattress filled with 50-102 mm limestone rubble.

Gabion installations have been used in experiments to improve, enhance, and modify stream fisheries and rehabilitate channelized streams. Their relative effectiveness and impact on the biology and chemistry of a stream has been variable according to studies by Maughan and Nelson (1980), Cooper and Wesche (1976) Bradt and Wieland (1978) and Barton and Winger (1973). An example of an effective use which provided a means of preventing young salmon from migrating to the sea was described by McSwain and Schmidt (1976). The gabions which were made of heavy triple twisted wire were shipped flat, filled with 6" minimum size cobbles, and tied on the job site. In addition to the gabions, a perforated steel pipe, a metal slide gate with concrete headwall, an emergency flow weir box, and natural stream gravel and cobbles were used to develop 6 different diversion structures. Their construction is described below.

A gabion dam is constructed as near the canal head as is practical. Perforated pipe (36") encased or surrounded by river run gravel is placed through the dam and extended upstream in the river bed at an elevation where it can be covered with about 7" of gravel. Thus all the water to the canal comes through the gravel pipe perforations and the gabion dam. As an emergency water supply feature, a weir box with removable flash boards is installed in the dam so that the gravel, perforations or dam interstices do not clog. A few feet downstream, a metal slide gate on a concrete headwall is provided for positive flow regulation.

Gabion structures were included in a study of barriers which reduce noise levels. Harmelink and Hajek (1973) conducted field evaluation of five barrier types: earth embankment, normal density and lightweight pre-cast concrete panel walls, aluminum walls, plywood walls and a gabion wall. Results indicated that they are relatively ineffective in reducing freeway traffic sound levels. For example, the barriers, located midway between the houses and the pavement or at the highway shoulder, 60 ft. - 140 ft. (18m-43m) from the nearest houses, provided only 2-6 dba reduction at the first row of houses, 4 ft. (1.2m) above ground. Immediately behind the barriers, where the reductions are of little real benefit, reductions of 8 dba - 14 dba were achieved.

### 2.3 Behavior and Design

A variety of studies have been conducted to test the behavior of gabion structures and develop design methods. Several experimental studies and design procedures are reviewed below.

Lavagnino (1974) described the construction of modified revetment of monolithic gabions which proved to be an effective solution to bank erosion at a river in northern California which was frequently washed out by floods. The \$1 million federally funded emergency repair program minimized erosion on an economically important forest lumber road. Eleven-gauge galvanized steel wire mesh baskets were constructed and design elements included keying bottom gabion baskets into rock or suitable foundation to minimize scouring below the bottom basket. A problem encountered was significant differential settling of gabions due to restricted drainage in the backfill. Free draining backfill and the use of counterforts to add structural stability were recommended to remedy this situation. Leydecker (1973) devised a method using gabions on low water crossings for secondary roads which proved to be both economical and aesthetic. Basically, the road at the water crossing is designed to give good line and grade through the stream. The final elevation of the low point of the parabolic grade line is usually 6" to 12" above the stream bed elevation at the downstream edge of the road. Gabions 6'-6" x 3'-3" are placed at the final grade line with the upstream edge of the gabion alongside the downstream edge of the road. The gabions are backfilled and stream gravel is pushed up behind the gabions to form the running surface. Essentially, the gabions form a 6" to 12" high porous dam which retains the stream gravel.

Stephenson (1980) devised charts for placing gabion weirs on sloping and horizontal surfaces. The charts and equations were verified experimentally to determine structural stability against sliding and overturning.

Gerodetti (1981) reviewed hydraulic studies which were conducted for a proposed rockfill cofferdam for the El Cajon hydroelectric project in Honduras. The cofferdam had a steel sheetpile sealing wall and its downstream surface was protected with armoured gabions.

Oswalt, et al. (1975) conducted a 1:30 hydraulic model investigation to evaluate bank protection requirement for the Fourmile Run local flood-control project. They found that in several reaches of the channel, the flow conditions resulted in failure of the 36-inch riprap, while the mattresses with proper toe protection reduced the scour considerably and provided the

necessary protection. Mattresses ranging from one foot to three feet thick were investigated in the model. Although no precise design rules were established for determining thickness of mattresses required for stability against flow, there were several areas in the model in which 36-inch thick riprap and 12-inch thick mattresses were stable. This indicated that the required mattress thickness is no more than one-third the required riprap thickness.

Oswald and Maynard (1978) conducted a series of tests at the U.S. Army Engineer Waterways Experiment Station (WES) to evaluate the effectiveness of several schemes using gabions for bank protection. Specifically, efforts were directed at evaluating the use of gabions for hard points or toe protection similar to the way riprap is used for hard points or toe protection at several prototype sites in the Vicksburg District. No results were specified.

Brown (1979) investigated various theoretical, experimental and prototype aspects of the use of gabion-type revetments. His theoretical analysis considers the momentum flux of the impacting wave jet and the destabilizing effects of this upon an element of the revetment. Laboratory wave tests were made for slopes of 1:4 to 1:1-1/2 for a variety of waves. Different modes of failure were encountered, including downslope sliding predominantly on steep slopes and uplift/buckling on flatter slopes. Thin mattresses showed a pronounced tendency to buckle. Two experimental panels were constructed to assess material behavior and toe stability. Two prototype revetments were designed and constructed in accordance with the proposed design rules.

Modeling studies include work by Posey (1957, 1969). Tests of erosion protection in model channels were conducted in an apparatus designed to permit comparisons under severe erosion exposure. Comparison with field installations shows that successive layers meeting the specifications for reverse filters will give complete protection to the finest, most erodible soils (Posey, 1969). According to Posey, accurate prediction of the sizes necessary to prevent the topmost layer from being washed away cannot be made, and this must be determined by trial. If large enough stones are not available, smaller stones will also resist erosion bound with mesh tubing.

Posey (1957) also recommended the use of "rock sausages" or gabions when designing and constructing highway fills. The size of the sausages required for various exposures was not determined, but full-scale tests showed that a

minimum practicable size would be ample to protect highway fills under the most severe conditions (high velocity flows) likely to be encountered.

Six different outlet modification designs for overbank control structures were evaluated by Copeland (1978). Model tests were conducted on five of the designs and design variations. A 1:24 scale section model was used to simulate discharges up to 550,000 cfs. Type 5 outlet modification design, utilizing gabions placed parallel to the flow on a 1V on 10H slope, was deemed the best of the six designs tested.

During the process of reconsidering the requirements of a revetment/breakwater layer on a coast in Australia, a specification for a structurally flexible, cohesive, massive and porous 'blanket' was evolved by Brown (1978). This specification finds an obvious expression in Reno Mattresses, and a series of model tests were carried out using stone filled mesh bags to represent the mattresses.

Saunders and Grace (1981) described model tests of channel structures constructed of concrete and gabions. Tests were conducted at an undistorted scale ratio of 1:12 to determine the discharge characteristics of the structures, size and extent of riprap required to prevent scour downstream of the structures, effects of ice flowing over the structures, and stability of the gabion structures.

Shorelines are commonly protected by stone revetments, rubble mound groins or breakwaters. When the erosive forces of waves are larger, large stones or concrete blocks of special interlocking shapes are placed on the surface over underlayers of stones of smaller size. Pillai and Verma (1978) tested in the laboratory protective surfaces of stones enclosed in nets underlain by a gravel filter. The size of stones needed within the enclosing net was relatively small and the volume of stones was reduced considerably as compared to that in the case of loose stones. They concluded that the development of strong and durable synthetic fibers provides for effective use of stones enclosed in nets to protect the higher part of beaches.

Nasser and McCorquodale (1974) studied unsteady non-Darcy flow in rectangular rock-fill embankments with impervious cores by subjecting the embankments to nonlinear, shallow water waves. Crushed rock and quartz were utilized, in sizes ranging from 0.7 cm to 4.4 cm, to build experimental embankments of various widths. The waves in all experiments were nonbreaking. The embankments were tested for several wave conditions. Empirical formulas

are presented for transmission, reflection, runup, and rushdown, and all give good correlations. An upward shift of the mean water level in the embankments was detected during the experiments. It was found that transmission decreased with decreasing conductivity and increasing wave steepness and embankment width, and that reflection decreased with increasing conductivity and width of embankment.

Experimental work on monitoring structural deformation of gabion walls has been done by Veress and Hatzopoulos (1979). During the course of the project (Veress, et al., 1977), practical tests of the theoretical developments were done on an in-place gabion wall. The monitoring consisted of photographing the structure from three camera stations. The camera was modified to a plate camera to provide the maximum accuracy. The methodology consisted of the geodetic determination of the camera location and the orientation and photogrammetric determination of targets (natural and artificial) on the structure. During the course of this project more than 100 target locations were determined by three dimensional coordinates. The maximum error was found to be plus 3/4 inch; the average, 1/2 inch. This represents a relative accuracy of 1/58,000 to 1/120,000 of the photographic distance. Using the actual construction site for research permitted immediate implementation. The instrumentation as well as the methodology along with the computer program was transmitted to the Washington State Highway Department and their Photogrammetric Branch was assisted in the implementation.

After review of the available literature, it was found that very little information regarding the design of mattresses for protecting river channels and canals existed. Most of the model studies for designing mattresses was for protecting the coastal or shoal line against wave attacking and was quite site specific. Agostini and Papetti (1978) recommended a thickness of Reno Mattress related to flow velocities (see Table 2.1) and presented hydraulic tables for various roughness coefficients and channel geometries. They found by comparing the use of mattresses with the use of riprap that a saving of 25 to 30 percent could be obtained by using the mattresses. Additionally, a savings of at least 50 percent in reduced wastage could be obtained by using mattresses for underwater installation as compared to using the riprap under water.

Table 2.1. Thickness of Reno Mattress Related to Water Velocity.

Water Velocity m/sec	Mattress Thickness m
0.9 - 1.8	0.15
1.8 - 3.6	0.15 - 0.25
3.6 - 4.5	0.25 - 0.30
4.5 - 5.4	0.30 - 0.50 and greater

Considering the available information, it is clear that very limited information is available regarding the performance of mattresses under high flow conditions. Additional study is required to answer the following questions:

1. What are the permissible design flow conditions for various types of mattresses?
2. What will be the changes in mattress performance when the flow conditions are higher than the critical (incipient motion) conditions?
3. What is the requirement of filter under high flow conditions?

The study results presented in this report will address these questions.

### III. MATTRESS TEST PROGRAM

#### 3.1 Introduction

Testing ofrevet mattresses under a range of hydraulic conditions representative of actual field conditions would require discharges in excess of those available in most laboratories. Furthermore, the costs associated with such tests would be prohibitively high. To adequately evaluate mattress performance over a range of conditions, a two-section test scheme involving full-scale tests complemented by scale-model tests was developed. In developing the test methodology, velocity was assumed to be the major factor controlling mattress stability. Data obtained from full-scale testing at the required velocity but reduced depth, were supplemented with scale-model testing in order to determine the effect of depth on mattress stability.

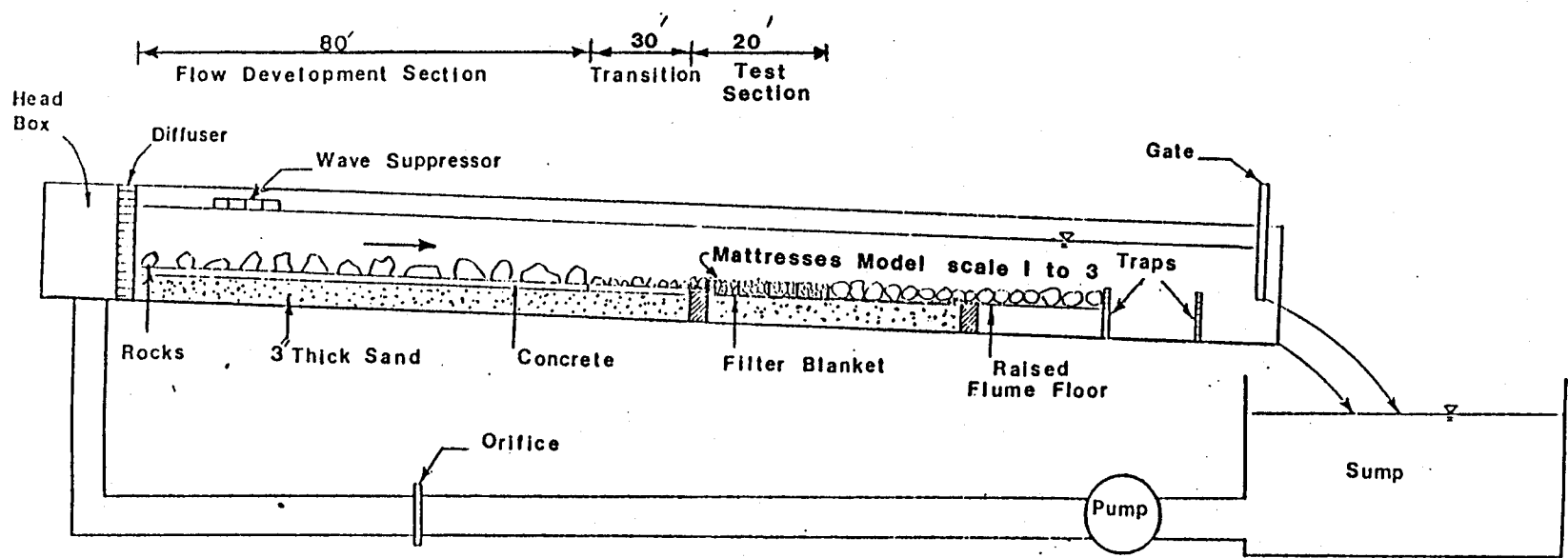
#### 3.2 Scale-Model Mattress Test Program

##### 3.2.1 Test Facilities and Test Scales

Hydraulic tests of scale-model mattresses were conducted using the eight-foot wide indoor flume located in the Hydraulics Laboratory at the Colorado State University Engineering Research Center. This flume is eight feet wide, four feet deep and two hundred feet long, and can be raised or lowered to produce slopes ranging from zero to about two percent. A maximum flow rate of approximately 100 cfs can be achieved. Valves and orifices are utilized to respectively control and measure discharges. Figure 3.1 shows the experimental setup for scale-model testing in the eight-foot indoor flume.

Two series of scale-model mattress tests were conducted: one utilized the original eight-foot flume and the other utilized the reduced four-foot flume which was fabricated by installing a 100-foot long partition wall at the center of the eight-foot indoor flume. The main reason for this width reduction was to test scale-model mattresses under increased unit-width discharge, velocity and depth conditions.

Indoor testing entailed construction of scale-model wire mesh mattresses geometrically similar to the prototype Maccaferri mattresses reduced by a scale ratio of 1:3. Table 3.1 provides model-to-prototype scaling ratios for various hydraulic variables. Table 3.2 shows the dimensions of model-scale mattresses made of commercially available hexagonal mesh screening. The mattresses tested in the study include 6-inch, 9-inch, 12-inch and 18-inch thick mattresses. Because available mesh screen for making model-scale



3.2

Figure 3.1. Scale-model experimental setup.

Table 3.1. Model-to-Prototype Scaling Ratios.

Variable	Model-to-Prototype Scaling Ratios
Length	1:3
Rock Size	1:3
Velocity	1: $\sqrt{3}$
Discharge	1:3 <sup>2.5</sup>
Shear Stress	1:3
Pressure	1:3
Force	1:3 <sup>3</sup>

Table 3.2. Dimensions of Model-Scale and Full-Scale Mattresses Tested.

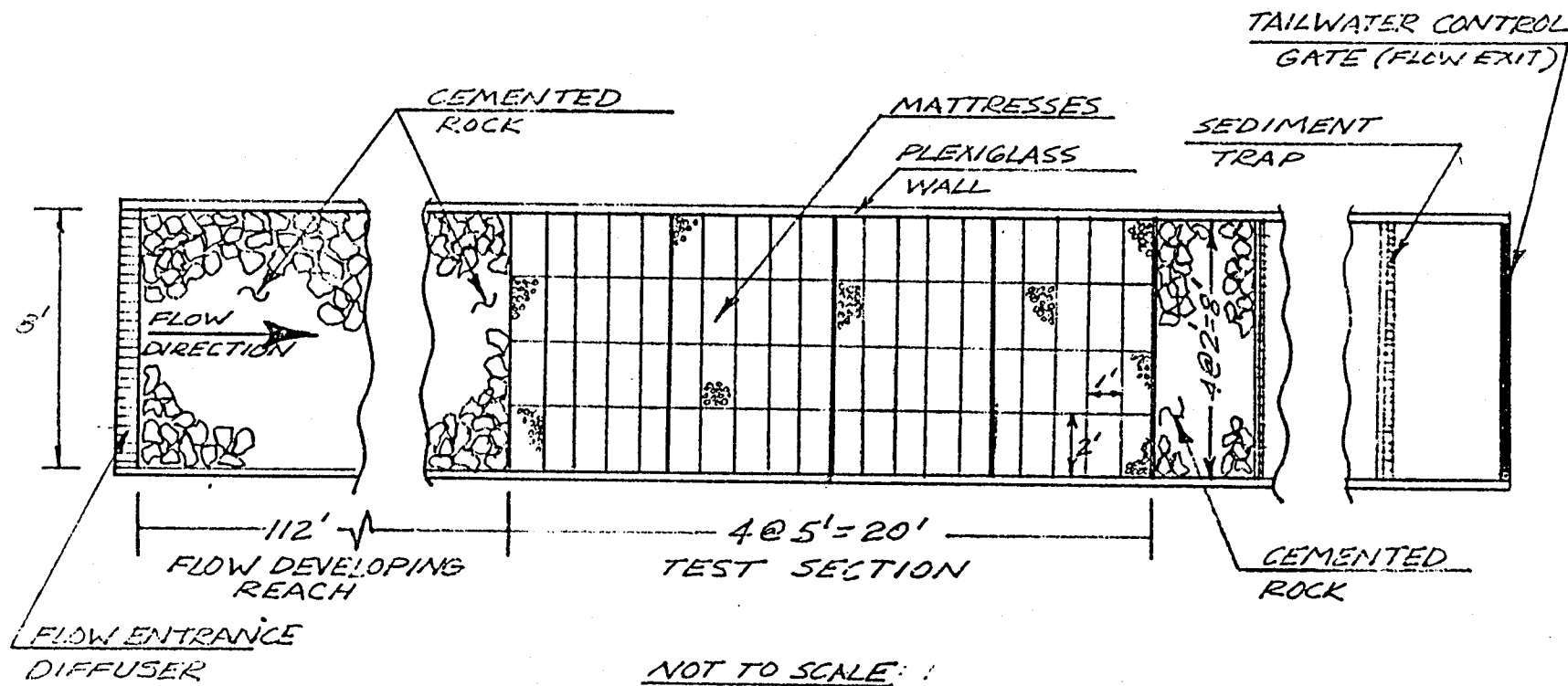
Test	Prototype				Model			
	Thickness (inches)	Mesh Type (cm)	Wire Dia. (mm)	Filling Rock (inches)	Thickness (inches)	Mesh Type (inches)	Wire Dia. (mm)	Filling Rock (inches)
<u>Four-Foot Flume</u>								
A	6	6 x 8	2 - 2.2	3 - 6	2	3/4 x 5/4	0.6 - 0.7	1 - 2
B	9	6 x 8	2 - 2.2	3 - 6	3	3/4 x 5/4	0.6 - 0.7	1 - 2
C	12	6 x 8	2 - 2.2	4 - 6	4	3/4 x 5/4	0.6 - 0.7	1.5 - 2
D	18	8 x 10	2.4-2.7	4 - 8	6	1 x 3/2	0.8 - 0.9	1.5 - 2.5
E	6	6 x 8	2 - 2.2	3 - 6	2	3/4 x 5/4	0.6 - 0.7	1 - 2 (grouted)
<u>Eight-Foot Flume</u>								
	9	8 x 10	2.4-2.7	3 - 6	3	1 x 3/2	0.8 - 0.9	1.5 - 2
<u>Outdoor Prototype</u>								
6"	6	6 x 8	2	3 - 6	-	---	---	---
9"	9	6 x 8	2	3 - 6	-	---	---	---

mattresses was limited, it was difficult to achieve dynamic similarity between the model mesh and prototype mesh. Tensile tests conducted by Maccaferri Gabions and by the Colorado Test Center indicated that the model-scale mesh utilized for the model tests in the four-foot flume was more flexible compared to full-scale ones. The results obtained from these model tests would guarantee a safety coefficient. However, comparison between model and prototype test results indicates that their results are convertible as will be discussed in the next chapter.

The construction procedures used to make the model mattresses were similar to the procedures set forth in Maccaferri literature covering construction of reno mattresses. The base, sides and ends of each mattress section were made from a single panel of wire mesh. Seventeen-gage salvage wires were woven into the external edges to help stiffen and strengthen the mattress section. Each five-foot mattress section was then divided into compartments by adding diaphragm sections at one-foot intervals. Diaphragms were secured to both the sides and base with 19-gage wire. Following assembly of the individual sections, the 16 mattress units were placed in position in the flume and laced together to form a single monolithic revetment layer eight feet wide and 20 feet long. A schematic view of the mattress test section in the 8-foot flume is shown in Figure 3.2. For the mattress testing in the 4-foot flume, eight mattress units were placed in position as shown in Figure 3.3. All adjoining edges were tied together using 19-gage wire which was passed through each mesh opening in turn using a double turn of wire at alternate mesh openings.

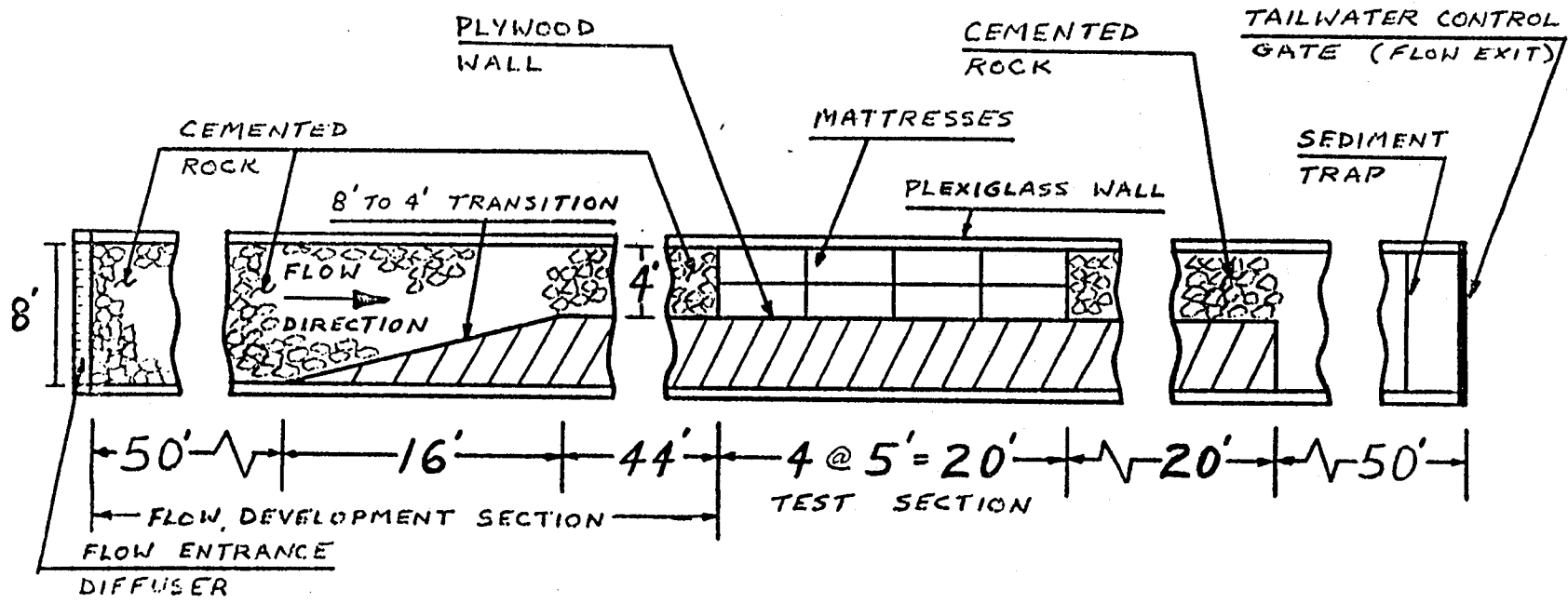
Fill materials were obtained from an aggregate supplier and contained gravel and crushed rocks that had been screened to sizes of 1 to 1-1/2 inches, 1-1/2 to 2 inches, and 2 to 2-1/2 inches. These different sizes of rocks were utilized to fill different types of model-scale mattresses as given in Table 3.2, according to a 1:3 scaling ratio of the specified rock ranges required for the full-scale mattresses.

Following filling of the mattress units, lids were wired down to the top edges of all sides as well as to the internal diaphragms. The wire lacing method used to attach the lids was as previously described with a double turn of wire made at every second mesh.



MATTRESS MODEL SETUP  
IN THE  
8' TILTING FLUME

Figure 3.2. Plan view of scale model mattress configuration.



NOT TO SCALE

MATTRESS MODEL SETUP  
IN THE  
4' TILTING FLUME

Figure 3.3. Plan view of scale-model mattress configuration in the 4-foot flume.

The reno mattresses were placed over a sand/filter cloth base layer. The base layer consisted of a 0.5 mm sand layer overlain by DuPont Typar Style 3401 nonwoven filter fabric. This fabric have the following specifications: weight = 4.0 oz/yd<sup>2</sup>; thickness = 15 mils; permeability = 0.03 cm/sec; and equivalent opening size = 70 to 100 U.S. Std. Sieve. The base sand was wetted and compacted with a roller prior to installation of the filter fabric. Edges of the fabric were secured to nailing strips on the flume sidewalls. If a seam was required, this seam was made by overlapping the upstream piece of fabric approximately 1.5 feet on the lower piece. Cement was used to bond the overlapped fabric pieces together.

To provide some indication of rock movement within mattress diaphragms, the surface layer of rock in alternative mattress diaphragm sections were painted with red spray paint (see Figures 3.4 and 3.5). This procedure provided a means whereby rock stability could be inspected and qualitatively assessed prior to and following test runs. A 35 mm camera fitted with a wide-angle lens was utilized to take photographs of the entire mattress following tests where rock movement was visible.

As indicated in Table 3.2, Test E conducted in the four-foot flume was designed for evaluating the effects of sand asphalt mastic grouting on stability of reno mattresses. Because of the scale reduction, it was necessary to prepare a suitable mix of the sand asphalt mastic to grout the reno mattress models different from that used for those in full scale. This special mix was said to have characteristics corresponding to those obtained in full scale both as regard to the purability and consolidation. The mixtures for the models and for the prototype were:

	<u>Model</u>	<u>Prototype</u>
Sand	50%	66-73%
Filler	29%	12-16%
Bitumen	21%	15-18%

The following laboratory analyses were conducted to evaluate the properties of the sand asphalt mastic mixture:

A. Sand sieve analysis:

<u>ASTM Sieve No.</u>	<u>Percent Finer</u>
10 (2 mm)	100
40 (0.42 mm)	86

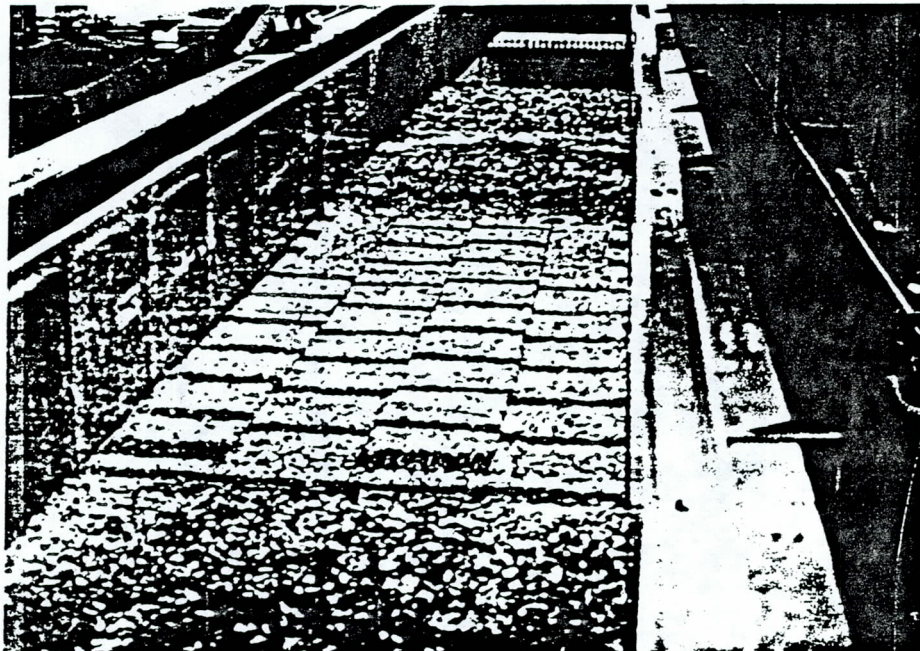


Figure 3.4. Overview of 8-foot tilting flume test setup.

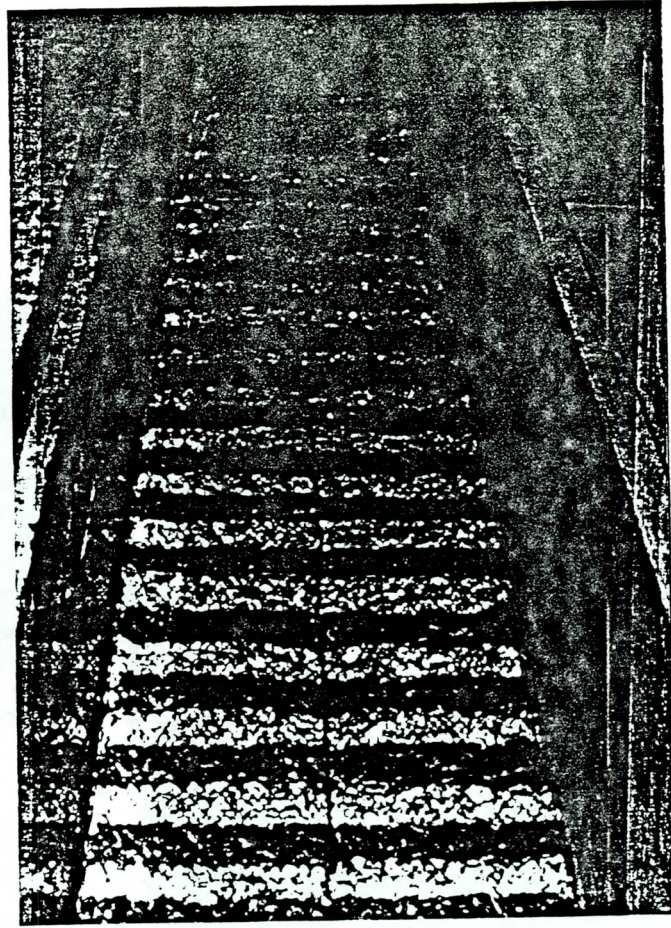


Figure 3.5. Overview of the 4-foot tilting flume test setup.

	3.11	
80 (0.177 mm)		6
200 (0.074 mm)		1

B. Filler Sieve analysis:

<u>ASTM Sieve No.</u>	<u>Percent Finer</u>
80 (0.177 mm)	100
200 (0.074 mm)	96

C. Flow stability on 1:3 inclined plane:

After four hours at 30°C, down flow 3 mm.

After four hours at 40°C, down flow 4 mm.

D. Flow stability on 1:15 inclined plane:

After one hour at 70°C, down flow 43 mm.

After three hours at 70°C, down flow 100 mm.

E. Bitumen penetration test:

The Dow penetration at 25°C was 82 pen.

Further information regarding the mastic grouted gabions and reno mattresses can be obtained from Maccaferri Gabions (see references).

For Test E, the Model-scale mattresses were prepared and installed using the procedures described earlier. The mix of the sand asphalt mastic was poured at a temperature of 175°C in such a quantity as to fill 70 percent of the voids of the mattress. The voids were 40 to 45 percent of the total mattress volume. This operation was referred to as "surface grouting." Figure 3.6 shows the model-scale reno mattresses grouted with the sand asphalt mastic mixture. Another type of grouting was called "complete penetration" which needs a quantity of mastic to fill the voids to about one to two cm above rock surface.

To provide a smooth transition of flow to and from the mattress test section, stabilized sections were constructed both upstream and downstream of the test section. Transition sections were constructed by grouting gravel and rock in place. These stabilized sections extended for a distance of approximately 30 feet above and below the model test section (see Figure 3.1). Anchoring of the upstream edge of the model mattress sections was accomplished securing a 1/4 x 3 inch steel plate to the floor perpendicular to the axis of the flume. The upstream edge of the first mattress sections were then wired to this plate.

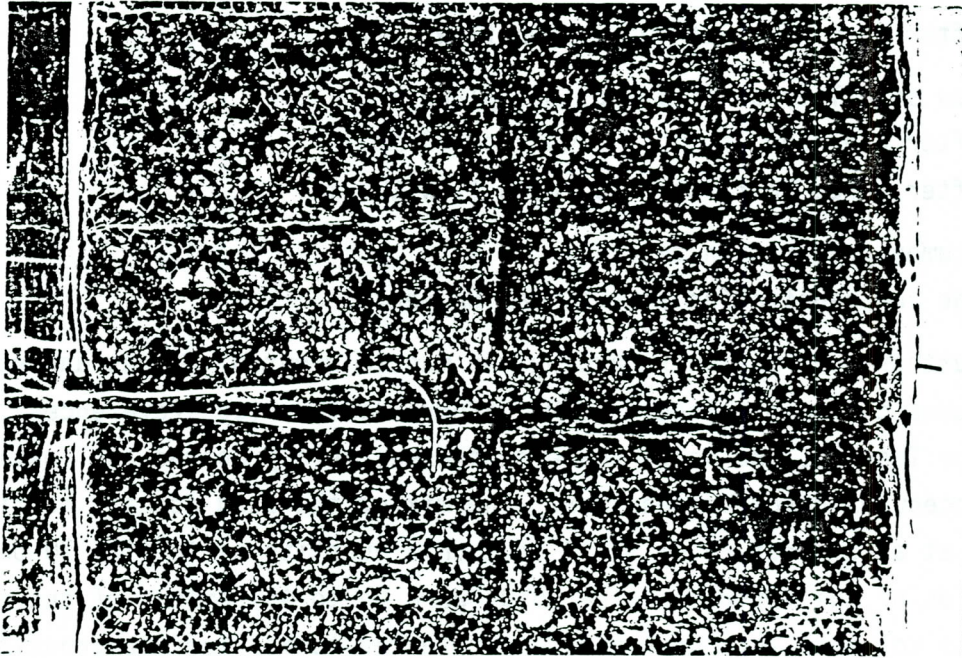


Figure 3.6. Model - scale reno mattresses grouted with the sand asphalt mastic.

### 3.2.2 Instrumentation

#### Adjustment and Measurement of Discharge

The three available pumps were used either singly or in combination to produce the required flow rate for each test condition. Rates of flow provided by each pump to the flume headbox were evaluated from derived relationships for discharge as a function of head differential,  $\Delta h$ , across orifice plates located in the supply lines on all pumps. Manometers were utilized to determine the head differentials, which were then input to the following discharge relationships:

$$\text{Pump \#1} \quad Q = 18.0 (\Delta h)^{1/2} \quad (3.1)$$

$$\text{Pump \#2} \quad Q = 12.8 (\Delta h)^{1/2}$$

$$\text{Pump \#3} \quad W = 5.17 (\Delta h)^{1/2}$$

where  $\Delta h$  is in feet of water. Pump discharge rates were regulated by adjusting in-line butterfly valves until the desired total flow rate was achieved.

#### Regulation of Depth and Measurement of Elevation and Velocity

Depth of flow under subcritical flow condition ( $F < 1$ ) was adjusted by means of a sluice gate located at the downstream end of the flume. For supercritical flow conditions ( $F > 1$ ) depth of flow was determined by the discharge, slope, and bed roughness, the downstream sluice gate being used to regulate flow into the flume tailbox.

At the beginning of each test run, the tailwater gate was operated in a manner that produced a depth of flow well above the uniform flow depth for the given conditions. By adjusting the tailwater gate, depth was then reduced to the point where the desired uniform flow depth occurred within the test section. This operation insured that no rock movement would be precipitated by nonuniform flow conditions during startup.

A point gage was utilized to measure water and bed surface elevations. Velocity was measured using an Ott propeller-type velocity meter.

### Pressure Instrumentation

Measurement of vertical pressure fluctuations associated with turbulence in a moving fluid can be accurately determined using pressure transducers. For testing of scale-modelrevet mattress sections, a differential pressure transducer with a 1.0 psi diaphragm was used. A Pace model CD-25 signal conditioner and a Thermo Time Systems (TSI) model 1076 true root-mean square (RMS) voltmeter comprised the readout device.

Calibration of the pressure transducer was accomplished with a differential manometer. The calibration procedure consisted of applying varying amounts of differential head,  $\Delta h$ , to the transducer and then recording the voltage produced by the deflected diaphragm. A curve fit using the least squares technique on a programmable calculator provided a linear equation relating  $\Delta h$  to voltage in the form

$$V = A (\Delta h)$$

where  $V$  is the voltage produced by the deflected transducer diaphragm,  $\Delta h$  is the differential head causing the deflection, and  $A$  is the calibration constant. Figure 3.7 gives the calibration curve for the 1.0 psi transducer diaphragm.

After the pressure transducer calibration had been completed, it was mounted on the flume wall and set up to measure the pressure fluctuations within the gabion mattress section. One side of the transducer was connected via a valve manifold to three lengths of 0.25 inch diameter copper tubing. These lengths of tubing were placed along the center line of the mattress section and wired down when the mattress lids were installed during mattress construction. Prior to installation, the end of each piece of tubing was sealed and numerous holes were drilled through the tubing sidewalls. This operation was necessary so the tubing would transmit a pressure intensity associated with fluctuations in the static head, excluding stagnation pressure intensity associated with the flow velocity. The tubing was terminated at five-foot intervals, making it possible to obtain pressure readings at the midpoint of the mattress section and at points five feet from the upstream and downstream ends.

The other side of the pressure transducer was connected, again via a valve manifold network, to three pressure taps drilled in the plexiglass flume sidewalls. Locations of the sidewall taps corresponded to terminus locations of the copper tubing within the flume. A stilling well was placed in line

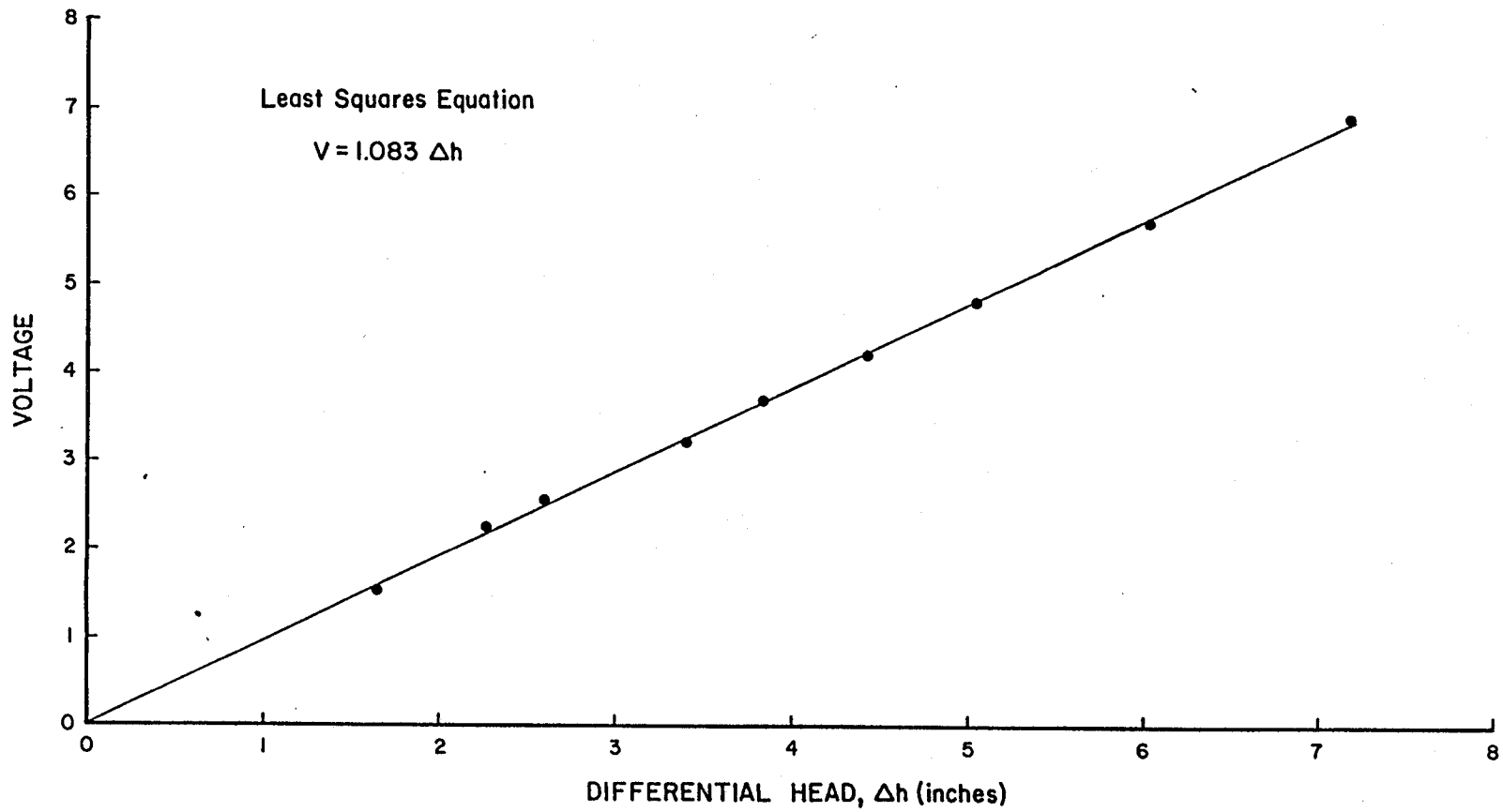


Figure 3.7. Pressure transducer calibration relationship.

with the copper tubing from the sidewall taps to damp out any fluctuating component of pressure. In this manner, the transducer provided an indication of the turbulence relative to the mean depth of flow. Figure 3.8 is a schematic view of the valve manifold network for connecting the transducer.

### 3.2.3 Test Procedure

Tasks associated with preparation for each test run consisted of setting the slope of the flume, balancing or zeroing instrumentation, defining pre-run conditions through observations and/or photographs, and establishing the desired flow conditions in the flume. Figure 3.9 shows a view of the 4-foot flume run for  $Q=50$  cfs and Figure 3.10 shows a view of the eight-foot flume run for  $Q=95$  cfs.

Once the desired flow conditions or terms of discharge, depth and velocity had been established, data collection was undertaken. Depth and velocity data were collected at three cross sections in the scale-model mattress test section. The location of these cross sections corresponded with the positions of the pressure taps. Depth of flow was determined using a steel point gage. This quantity (depth) was then used to establish vertical placement of the current meter in order to obtain an average flow velocity. For depths of flow greater than one foot, velocity readings were taken at 0.2 and 0.8 times the depth with an Ott propeller-type current meter. Velocity measurements were taken at 0.6 times the depth when total depth was one foot or less. At each cross section velocity was measured at the centerline.

Collection of pressure data consisted of adjusting the manifold network to isolate the pressure tap at one cross section, and then recording the RMS voltage signal resulting from deflection of the transducer diaphragm.

After completion of the data collection, the pumps were shut down and the flume was allowed to drain. Mattress sections were scrutinized to identify any significant rock movement. Photographs were taken to document the occurrence of any appreciable shifting of rock within the model mattresses.

In summary, sequential steps occurring prior to, during, and after a test run included the following:

#### Pre-Run

1. Set flume slope
2. Establish pre-run conditions via observations and/or photographs.

# INSTRUMENTATION SCHEMATIC FOR 8' TILTING FLUME TESTS

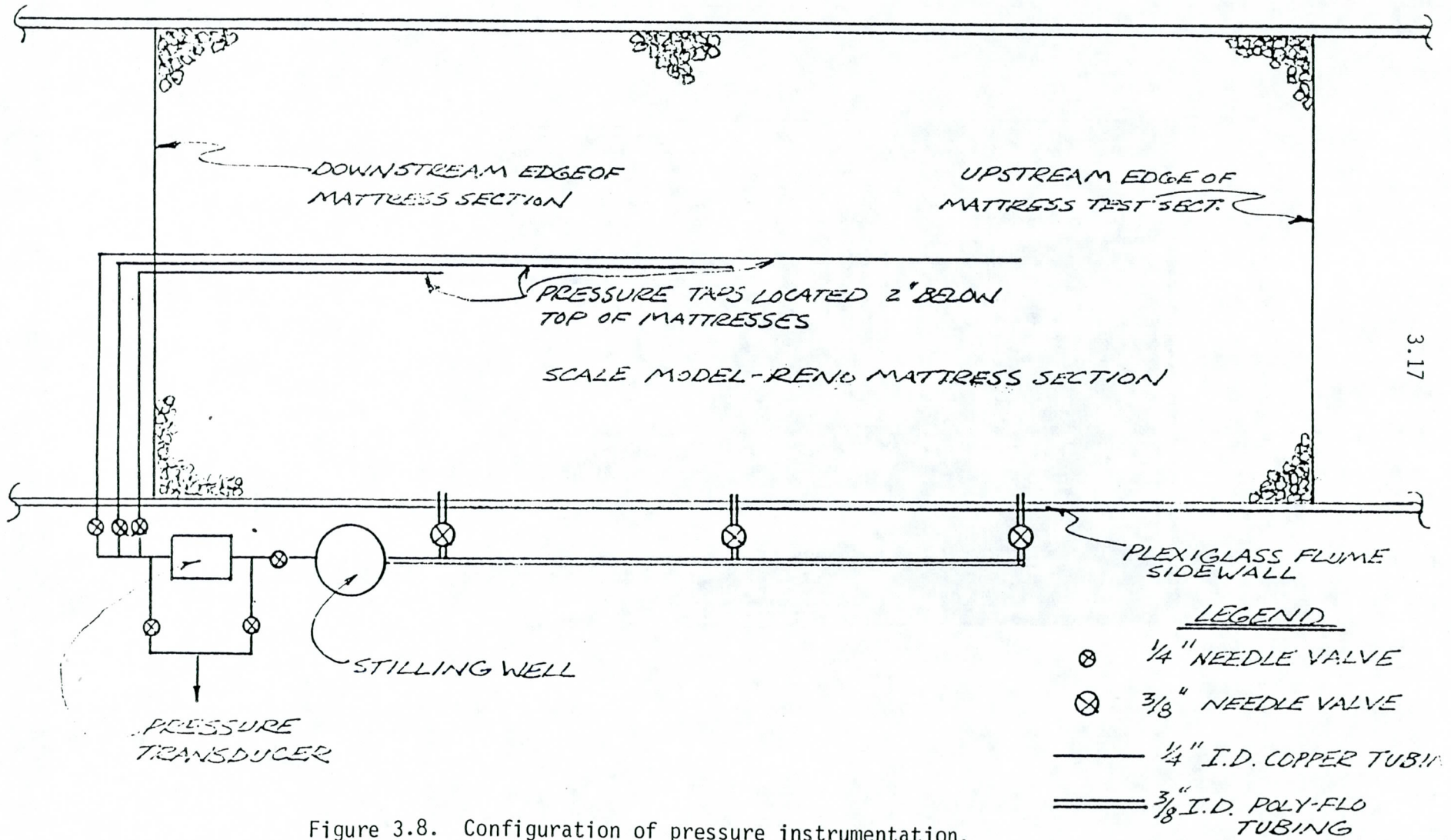


Figure 3.8. Configuration of pressure instrumentation.

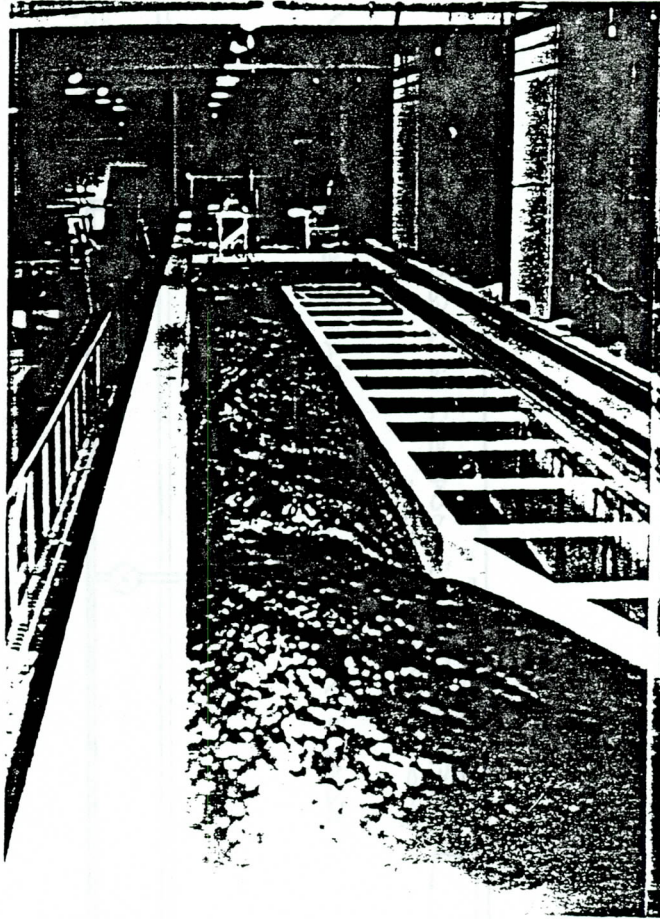


Figure 3.9. A view of 4-foot flume run for  $Q = 50$  cfs.

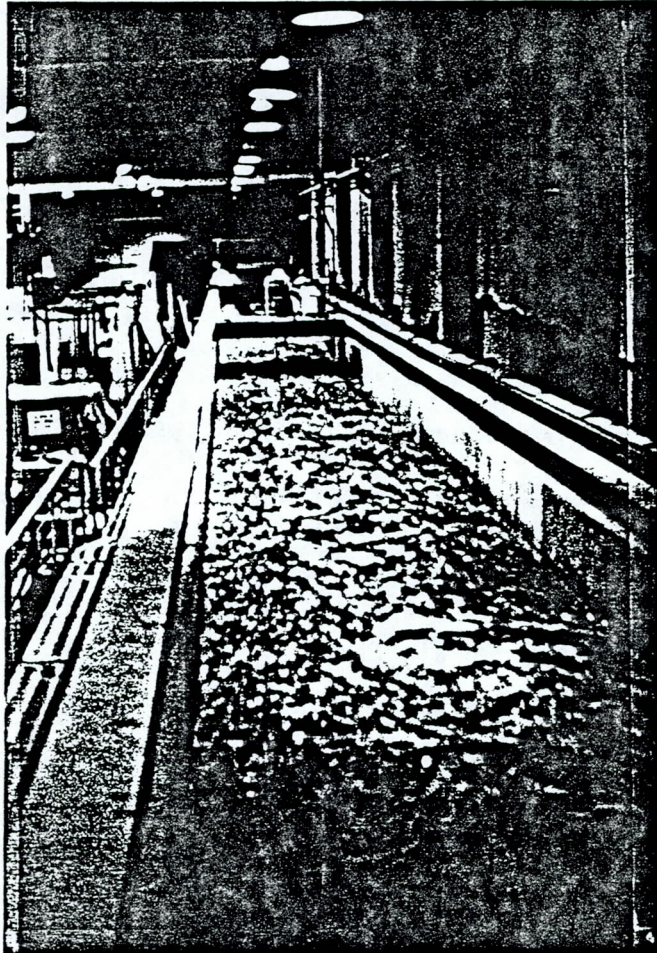


Figure 3.10. A view of 8-foot run.

3. Balance pressure transducer, zero chart recorder.

#### Run

1. Attain desired flow conditions, discharge and depth, through adjustment of pumps.
  - a. Determine total discharge from differential manometer readings using known pump discharge relationships.
  - b. Measure water-surface elevations on the mattress test section using a point gage to determine water-surface slope, water depth and uniformity of flow conditions.
2. Measure average velocity using a Ott current meter at the flume center-line. Take measurements at three cross sections located five feet from the upstream and downstream ends, and in the center of the mattress test section.
3. Collect transducer DC voltage signal data.
4. Measure transducer RMS voltage signal using TSI true RMS meter.
5. Plot transducer voltage signal output using single-channel chart recorder.

#### Post-Run

1. Shut down pump system and drain flume.
2. Scrutinize mattresses for rock movement, deformation of wire baskets, or any other changes resulting from the completed test run.
3. Take photographs to document any significant changes observed in the modelrevet mattresses.
4. Prepare for next run.

#### 3.2.4 Test Conditions and Data Collected in the 8-Foot Flume

Table 3.3 indicates the range of hydraulic conditions in the 8-foot flume to which scale modelrevet mattresses were subjected. Only the scaled 9-inch mattresses were tested in the 8-foot flume. The characteristics of these mattress units are described in Table 3.2. Station numbers in Table 3.3 indicate the longitudinal position within the mattress test section where data were collected. Station 1 was located five feet above the downstream end of the test section, Station 2 coincided with the midpoint, and Station 3 was located five feet from the upstream end. These locations coincided with locations of pressure taps placed within the mattress rock fill.

Table 3.3. Scale-Model Mattress Test Data  
in the 8-Foot Flume.

Run No.	Station	Flow Rate (cfs)	Depth (ft)	Flume Slope	Velocity (fps)	Froude Number	RMS Pressure $\sqrt{p \cdot 2}$ (psf)
1	1	20.8	0.86	0.0172	3.30	0.62	1.53
	2	20.8	0.70		3.65	0.77	
	3	20.8	0.49		5.28	1.33	
2	1	37.8	1.20	0.0069	4.10	0.66	1.06
	2		1.15		4.24	0.70	
	3		1.11		4.29	0.72	
3	1	56.7	1.58	0.0040	4.45	0.62	1.35
	2		1.59		4.43	0.62	
	3		1.60		4.35	0.61	
4	1	75.4	2.19	0.0015	4.77	0.57	3.03
	2		2.23		4.74	0.56	
	3		2.26		4.76	0.56	
5	1	91.0	2.17	0.0040	5.80	0.69	4.37
	2		2.24		5.68	0.67	
	3		2.26		5.62	0.66	
6	1	68.3	1.78	0.0059	5.59	0.74	4.02
	2		1.83		5.52	0.72	
	3		1.82		5.61	0.73	
7	1	46.5	1.12	0.0102	5.34	0.89	2.88
	2		1.09		5.58	0.94	
	3		1.00		6.23	1.10	
8	1	27.6	0.60	0.0201	5.15	1.17	2.55
	2		0.60		5.38	1.22	
	3		0.62		5.80	1.30	
9	1	80.1	1.82	0.0079	6.31	0.82	2.90
	2		1.83		6.47	0.84	
	3		1.83		6.71	0.87	
10	1	53.2	1.04	0.0135	6.83	1.18	2.65
	2		0.99		7.22	1.28	
	3		1.01		7.27	1.27	

Table 3.3. continued

Run No.	Station	Flow Rate (cfs)	Depth (ft)	Flume Slope	Velocity (fps)	Froude Number	RMS Pressure $\sqrt{p \cdot 2}$ (psf)
11	1	93.1	1.60	0.0118	8.05	1.12	3.18
	2		1.52		8.50	1.21	
	3		1.56		8.63	1.22	
12	1	65.2	1.14	0.0203	9.13	1.51	4.07
	2		1.14		9.00	1.49	
	3		1.16		8.95	1.46	
13	1	94.1	1.45	0.0159	8.54	1.25	5.76
	2		1.46		8.67	1.26	
	3		1.46		8.77	1.28	
14	1	94.6	1.39	0.0199	9.86	1.47	5.97
	2		1.39		9.73	1.45	
	3		1.41		9.86	1.46	

The analysis of data was performed utilizing the following equations and methods. Froude number is calculated from Equation 3.2 introduced previously.

$$F = \frac{V}{\sqrt{gD}} \quad (3.2)$$

where  $V$  is the mean velocity,  $D$  is the depth and  $g$  is the gravitational acceleration. Computed values of the Froude number are included in Table 3.3.

The Manning equation is a commonly used relationship to approximate the average velocity in open channels. In English units the equation is

$$V = \frac{1.49}{n} R^{2/3} S^{1/2} \quad (3.3)$$

where  $V$  is the average velocity,  $R$  is the hydraulic radius,  $S$  is the slope, and  $n$  is defined as the Manning roughness coefficient with the dimension  $L^{1/6}$ . To calculate Manning's roughness factor,  $n$ , the difference between the smooth flume walls and the rough bed should be considered. The following evaluation of resistance to flow in the eight-foot tilting flume at CSU is obtained from Fiuzat, Chen and Simons (1982). The flow cross-sectional area in this case is divided into two parts,  $A_b$  and  $A_w$  where resistance to flow is caused by the bed and the walls, respectively. It is assumed that the mean velocity and energy gradient are the same for  $A_b$  and  $A_w$  and Manning's equation can be applied to each part of the cross section as well as to the whole, i.e.,

$$\frac{V^2}{S} = \left(\frac{1.49}{n} R^{2/3}\right)^2 = \left(\frac{1.49}{n_b} R_b^{2/3}\right)^2 = \left(\frac{1.49}{n_w} R_w^{2/3}\right)^2 \quad (3.4)$$

where the subscripts  $b$  and  $w$  stand for bed and wall, respectively. Equation 3.4 can be simplified to

$$\frac{R}{n^{3/2}} = \frac{R_b}{n_b^{3/2}} = \frac{R_w}{n_w^{3/2}} \quad (3.5)$$

Using  $R = A/P$ , where  $A$  is area and  $P$  denotes wetted perimeter, Equation 3.5 becomes

$$\frac{A}{n^{3/2} P} = \frac{A_b}{n_b^{3/2} P_b} = \frac{A_w}{n_w^{3/2} P_w} \quad (3.6)$$

or

$$A_b (n_w^{3/2} P_w) = A_w (n_b^{3/2} P_b) \quad (3.7)$$

It is known that  $A = A_b + A_w$ , or  $A_b = A - A_w$ , so

$$(A - A_w) (n_w^{3/2} P_w) = A_w (n_b^{3/2} P_b)$$

$$A (n_w^{3/2} P_w) - A_w (n_w^{3/2} P_w) = A_w (n_b^{3/2} P_b)$$

$$A (n_w^{3/2} P_w) = A_w (n_w^{3/2} P_w + n_b^{3/2} P_b)$$

$$A \frac{n_w^{3/2} P_w}{A_w} = n_w^{3/2} P_w + n_b^{3/2} P_b \quad (3.8)$$

Equations 3.6 indicate that

$$\frac{n_w^{3/2} P_w}{A_w} A = n^{3/2} P \quad (3.9)$$

Substituting Equation 3.9 into Equation 3.8,

$$n^{3/2} P = n_w^{3/2} P_w + n_b^{3/2} P_b \quad (3.10)$$

In Equation 3.10,  $n$  and  $P$  are the overall Manning's  $n$  and wetted perimeter of the flume, that represent the combined effect of both the walls and the bed. For a flume width  $W$  and flow depth  $D$ ,

$$P = W + 2D \quad (3.11)$$

$$n = \frac{1.49}{V} \left( \frac{WD}{W + 2D} \right)^{2/3} S^{1/2} \quad (3.12)$$

and

$$P_w = 2D \quad (3.13)$$

$$P_b = W \quad (3.14)$$

Knowing that the flume is built out of smooth painted metal and Plexiglas, (Chow, 1959, pp. 110-111)

$$n_w = 0.012 \quad (3.15)$$

The flume width is 8.0 ft. Substituting these values and using Equations 3.13 and 3.14, in Equation 3.10

$$n^{3/2} P = (0.012)^{3/2} (2D) + n_b^{3/2} (8) \quad (8)$$

and solving for  $n_b$

$$n_b = \left[ \frac{n^{3/2} P - (0.012)^{3/2} (2D)}{8} \right]^{2/3} \quad (3.16)$$

where  $n$  and  $P$  are determined by Equations 3.11 and 3.12, or

$$P = 8 + 2D \quad (3.17)$$

$$n = \frac{1.49}{V} \left( \frac{8D}{8 + 2D} \right)^{2/3} S^{1/2} \quad (3.18)$$

Using average values of velocity, depth, and slope for each test run, Equation 3.18 was used to compute overall Manning roughness coefficient,  $n$ , values. Computed values are shown in Table 3.4. The average value of  $n$  for all the test runs is 0.022. Equation 3.16 was then used to calculate Manning roughness factors,  $n_b$ , for the model mattress surface. These values are also included in Table 3.4. The average value of  $n_b$  is 0.025.

Turbulence pressure data obtained from the pressure taps situated within therevet mattress layer were used to compute the degree or intensity of turbulence pressure defined as

$$\frac{\sqrt{P_i^2}}{\bar{P}} \quad (3.19)$$

where the numerator is the root-mean-square (RMS) pressure intensity from Table 3.3. RMS is a measure of the magnitude of turbulence pressure. The quantity  $P$  is the mean pressure intensity related to the depth of flow. Computed values for the turbulent pressure intensity are included in Table 3.4. Figure 3.11 shows the relationship between the degree of turbulence pressure and Froude number.

Table 3.4. Manning's Roughness Coefficient for the Model-Scale Mattresses Tests Conducted in the 8-Foot Flume.

Run	Manning's Roughness Coefficients		$\sqrt{\frac{p \cdot Z}{\bar{p}}}$
	Overall $\bar{n}$	Bed $\bar{n}_b$	
1	0.021	0.023	0.032
2	0.021	0.024	0.013
3	0.023	0.025	0.013
4	0.015	0.027	0.021
5	0.021	0.027	0.030
6	0.024	0.026	0.033
7	0.023	0.024	0.038
8	0.025	0.023	0.056
9	0.024	0.026	0.024
10	0.021	0.024	0.037
11	0.021	0.025	0.030
12	0.022	0.024	0.051
13	0.023	0.025	0.058
14	0.022	0.025	0.063
	$\bar{n} = 0.022$	$\bar{n}_b = 0.025$	

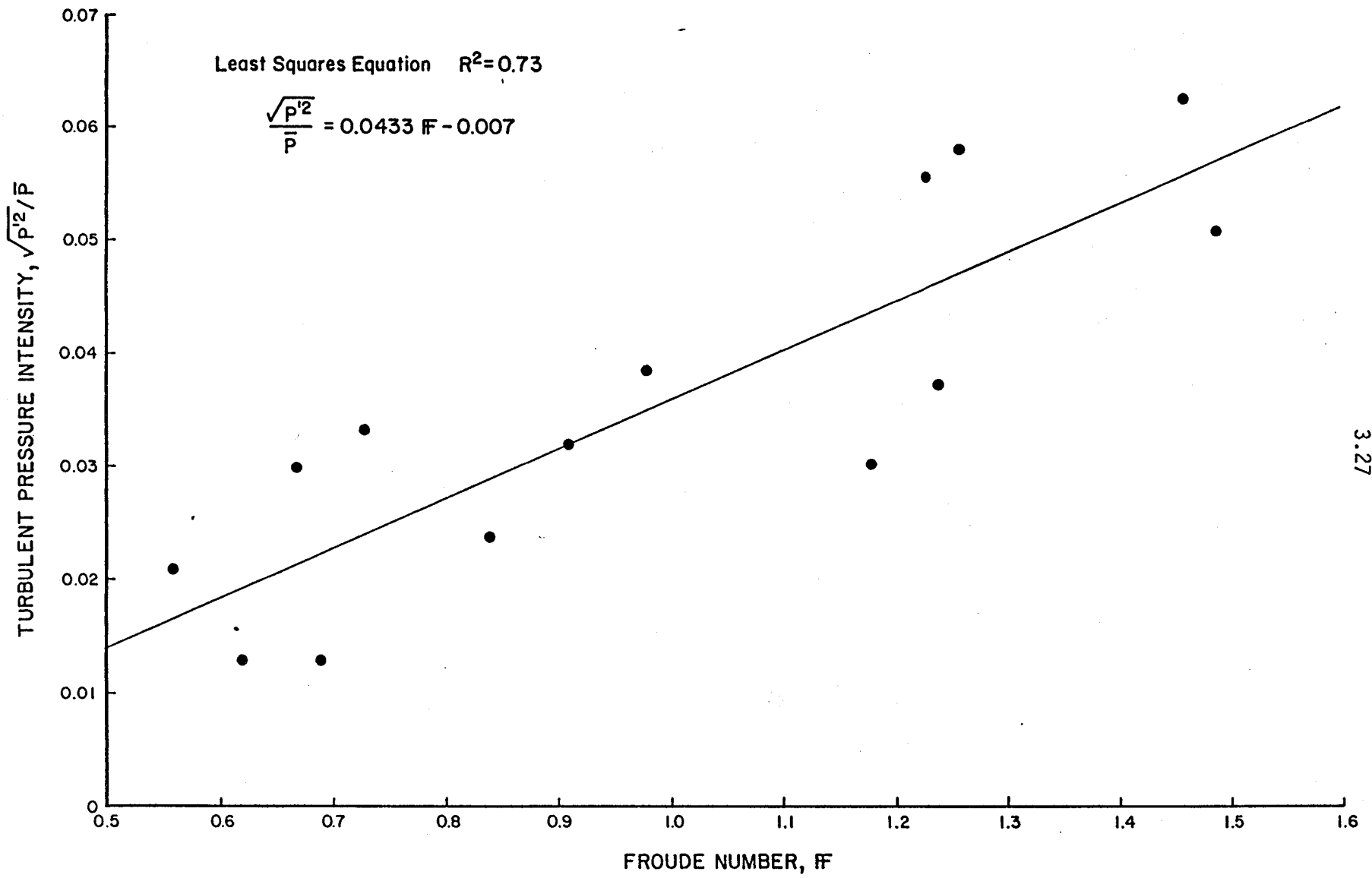


Figure 3.11. Turbulent Pressure Intensity versus Froude Number.

### 3.2.5 Test Conditions and Data Collected in the 4-Foot Flume

Table 3.5 indicates the range of hydraulic conditions in the 4-foot flume to which scale modelrevet mattresses were subjected. The characteristics of the various mattresses tested are described in Table 3.2. In Table 3.5, the shear stress  $\tau$  is computed by

$$\tau = \gamma R_b S \quad (3.20)$$

where  $\gamma$  is the unit weight of water,  $R_b$  is the hydraulic radius due to bed roughness determined using Equation 3.5 and  $S$  is the friction slope which is assumed equal to the flume slope. The Shields parameter is computed by

$$C_* = \frac{\tau}{(\gamma_s - \gamma) d_m} \quad (3.21)$$

where  $\gamma_s$  is the unit weight of rocks and  $d_m$  is the median size of rocks given in Table 3.2. The bed roughness coefficient  $n_b$  is computed using the same method described in the previous section except that the top width  $W=4$  ft. The resulting equation for computing  $n_b$  is then

$$n_b = \left[ \frac{n^{3/2} P - (0.012)^{3/2} (2D)}{4} \right]^{2/3} \quad (3.22)$$

where  $P = 4 + 2D$ .

## 3.3 Full-Size Mattress Test Program

### 3.3.1 Test Facilities

Figure 3.12 shows the experimental setup used to test prototype mattresses. The test facilities consist of a flume seven feet wide, four feet high, and 75 feet long situated on a 13 percent slope. This flume was reduced to six-feet wide for testing the nine-inch thick mattresses. Water is supplied to the flume from Horsetooth Reservoir via a 36-inch diameter pipe. The discharge capacity is about 100 cfs. A nozzle was designed and fabricated to discharge water to the flume directly from the 36-inch supply pipe. The bottom edge of the nozzle coincides with the upper edge of a concrete transition section. This testing system could generate velocities in excess of 20 fps within the test section. Regulation of the discharge was accomplished through operation of a valve located at the head of the flume. A annubar located in the supply line is utilized to measure the flow rate. Two-way radios help coordinate flow regulation and data collection efforts.

Table 3.5a. Run Sequence for Test A  
6-Inch Mattress.

Total Discharge Q, cfs	Depth D, ft	Flume Slope S, ft/ft	Velocity V, fps	Shear Stress $\tau$ , psf	Shields Parameter $C_*$	Froude Number F	Bed Roughness $n_b$
53	2.15	0.004	7.10	0.532	0.044	0.86	--
70	2.59	0.004	7.37	0.646	0.053	0.81	--
55*	1.82	0.01	8.67	1.136	0.094	1.13	0.0199
72	2.10	0.01	9.02	1.310	0.108	1.10	0.0208
85	2.43	0.01	9.72	1.516	0.125	1.10	0.0205
71	1.86	0.02	10.84	2.321	0.192	1.40	0.0243
91	2.14	0.02	11.49	2.671	0.221	1.38	0.0247

\*Flow condition at which movement of filling rocks was first observed.

Table 3.5b. Run Sequence for Test B  
9-Inch Mattress.

Total Discharge Q, cfs	Depth D, ft	Flume Slope S, ft/ft	Velocity V, fps	Shear Stress $\tau$ , psf	Shields Parameter $C_*$	Froude Number F	Bed Roughness $n_b$
50	2.06	0.004	6.27	0.514	0.042	0.77	--
70	2.61	0.004	7.51	0.651	0.054	0.82	--
56*	1.89	0.01	8.58	1.179	0.097	1.10	0.0204
71	2.18	0.01	8.82	1.360	0.112	1.05	0.0215
82	2.29	0.01	9.58	1.429	0.118	1.12	0.0200
86	2.16	0.015	10.65	2.022	0.167	1.28	0.0219
74	1.86	0.02	11.66	2.321	0.192	1.51	0.0226
92	2.18	0.02	11.75	2.721	0.225	1.40	0.0235

\*Flow condition at which movement of filling rocks was first observed.

Table 3.5c. Run Sequence for Test C  
12-Inch Mattress.

Total Discharge Q, cfs	Depth D, ft	Flume Slope S, ft/ft	Velocity V, fps	Shear Stress $\tau$ , psf	Shields Parameter $C_*$	Froude Number F	Bed Roughness $n_b$
50	2.1	0.004	5.92	0.524	0.035	0.72	--
67	2.6	0.004	8.1	0.65	0.044	0.89	--
51	1.75	0.01	7.9	1.09	0.074	1.05	0.0218
62	2.0	0.01	8.5	1.25	0.084	1.06	0.0217
81*	2.3	0.01	9.9	1.50	0.101	1.13	0.0205
20	0.85	0.02	7.3	1.06	0.072	1.40	0.0234
66	1.9	0.02	11.3	2.25	0.152	1.48	0.0227
92	2.15	0.02	12.4	2.75	0.186	1.47	0.0223

\*Flow condition at which movement of filling rocks was first observed.

Table 3.5d. Run Sequence for Test D  
18-Inch Mattress.

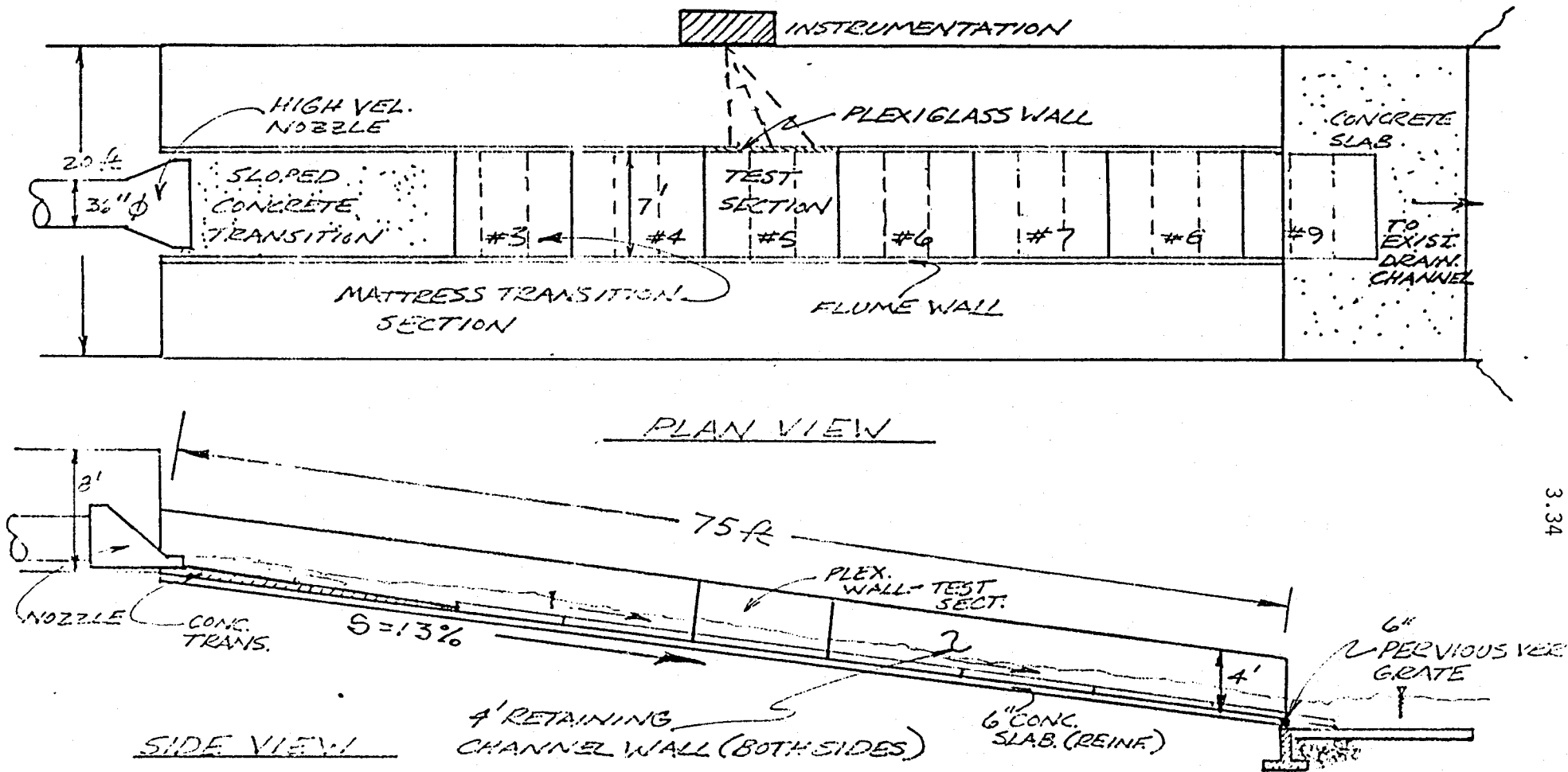
Total Discharge Q, cfs	Depth D, ft	Flume Slope S, ft/ft	Velocity V, fps	Shear Stress $\tau$ , psf	Shields Parameter $C_*$	Froude Number F	Bed Roughness $n_b$
72	2.65	0.004	7.12	0.661	0.041	0.77	--
56	1.94	0.01	7.77	1.21	0.075	0.98	0.0227
84*	2.35	0.01	9.56	1.466	0.091	1.10	0.0206
88	2.19	0.015	10.88	2.050	1.27	1.30	0.0215
93	2.10	0.02	11.99	2.621	0.163	1.46	0.0226

\*Flow condition at which movement of filling rocks was first observed.

Table 3.5e. Run Sequence for Test E 6-Inch  
Mattress With Mastic.

Total Discharge Q, cfs	Depth D, ft	Flume Slope S, ft/ft	Velocity V, fps	Shear Stress $\tau$ , psf	Shields Parameter $C_*$	Froude Number F	Bed Roughness $n_b$
55	2.16	0.004	6.71	0.539	0.045	0.80	--
85	2.36	0.01	9.23	1.473	0.122	1.06	0.0215
93	2.21	0.02	11.80	2.758	0.228	1.40	0.0239

NOTE: No movement of rocks within the grouted mattresses was observed.



3.34

EXPERIMENTAL SETUP FOR  
MACCAFERRI MATTRESS TESTS

Figure 3.12. Experimental setup for prototype Maccaferri mattress tests.

Prototype mattress testing entailed construction of full-scale wire mattresses supplied by Maccaferri Gabion. Characteristics of the 6-inch and 9-inch mattresses which were tested in the flume are given in Table 3.2.

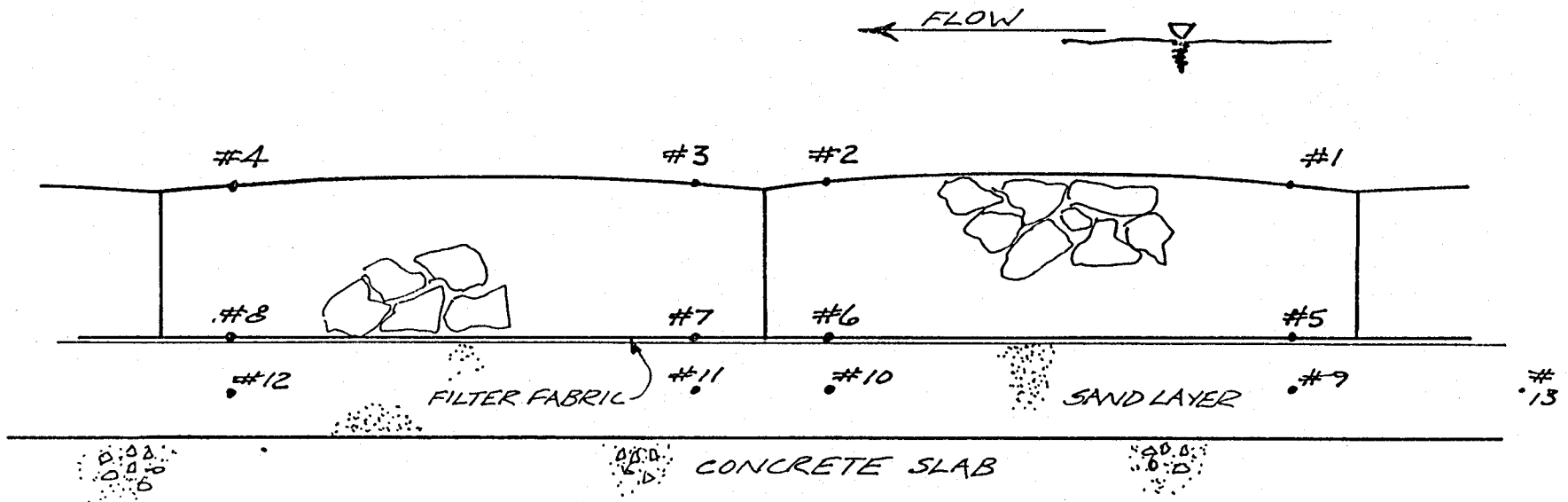
These mattresses were constructed by SLA crews utilizing normal procedures, as outlined in Maccaferri literature covering construction practices for Reno Mattresses. Following assembly of the individual units, mattresses were placed the entire length of the outdoor flume (75 ft) and all adjoining edges were attached as specified.

Fill material was supplied by a local quarry. This fill rock was composed of a combination of limestone and dolomite. Rock was angular to semiangular in shape and specified by the supplier as three to six inches (7.6-15.2 cm) in diameter. Upon filling the mattresses, however, it was noted that approximately 15 percent of the rock was of a size which fell below this three inch diameter minimum. The SLA crew made attempts to place this smaller rock in the lower portions of the mattress and fill the remaining area with larger rock. The filling of the mattresses was accomplished with the aid of a crane which placed rock within the mattresses. The SLA crew then hand-placed this rock as noted previously to the Maccaferri specifications of one to two inches (2.5-5.1 cm) above the average mattress height. This slight over-filling allows the mattress lids (which are fabricated slightly longer than the mattress length) to fit properly and mattress material to be more tightly packed. Upon placement of the fill material, the lids were securely wired as specified. The revet mattresses were placed over a sand/filter base layer. The base layer was installed according to the procedure previously described.

### 3.3.2 Instrumentation

The instrumentation for full-scale revet mattress testing was set up so that similarity between prototype data and model data would be maintained insofar as possible. This procedure would facilitate extrapolation of the scale-model test results to prototype mattress behavior. Figure 3.13 shows the configuration of pressure probes for measuring pressure head plus velocity head during the 9-inch mattress testing. Thirteen pressure lines were initially placed in the revet mattresses and the sand layer as indicated. These lines were connected to piezometric tubes which were backed by scalar paper.

PRESSURE TAP LOCATION DIAGRAM



NOTE: UPON SAND WASH-OUT, TAPS 9-13 WERE DISCONNECTED. FURTHER TESTS WERE PERFORMED ON THE RIGID BED.

Figure 3.13. Pressure tap location diagram for the 9-inch full-scale mattress tests.

A pitot tube was utilized to measure velocity in the outdoor prototype flume. A differential mercury manometer connected to the pitot tube was used to measure the velocity head,  $V^2/2g$ , from which flow velocity was determined. Discharge was measured using a calibrated orifice. Stage and bed elevation were measured by using point gages. Velocities immediately above and below mattresses were determined from the piezometric tube readings less the hydrostatic pressures.

### 3.3.3 Test Conditions

Mattresses were placed over a sand/filter cloth base layer. The 6-inch layer of sand base was overlain by a woven polypropylene filter fabric. The base sand was wetted and compacted prior to the installation of the fabric, which was then attached to nailing strips on the flume side walls. Tabel 3.6 shows the test conditions over the six-inch thick mattresses. Tables 3.7 and 3.8 show the test sequence for testing of the 9-inch units and the subsequent flow depths and velocities resulting from each test discharge. The discharge within the mattress was computed by assuming that velocity through rock voids was two-thirds the velocity immediately below the mattress, and that the porosity of the rock was 0.45. Figure 3.14 shows an overall view of the outdoor flume during a test run.

### 3.3.4 Problems Pertaining to Full-Scale Mattress Tests

Because of extreme high velocity and turbulence (e.g., see Figure 3.15), several problems were encountered during the full-scale mattress tests:

1. Flow entering the flume through the nozzle exerted considerable impact forces on the rock. This caused a shift of filling rock and exposed the underlying filter fabric of the mattress unit immediately downstream of the nozzle at a velocity of about 20 fps. This impact force is considerably larger than shear force to which mattresses are normally subjected. Special design considerations should be given when the impact force is significant to alleviate the problems associated with the impact zone below the nozzle.
2. The combination of high velocity and relatively steep slope (13%) caused piping of sand underneath the filter fabric even though the protective mattresses remained stable. A similar situation may be encountered in the field.
3. Because of the extreme turbulence flow, the water depth in the flume could only be approximated and checked using a continuity equation. The measuring error could be on the order of  $\pm 10$  percent of actual values.

Table 3.6. Test Run Sequence - Discharge, Depth, Velocity Measurements for the 6-Inch Full-Scale Mattress Tests.

Total Discharge $Q_T$ , cfs	Velocity $V_1$ , fps	Depth $D_1$ , ft	Velocity $V_2$ , fps	Depth $D_2$ , ft
18	7.1	0.30	7.1	0.30
56	15.2	0.47	12.0	0.57
92	19.2	0.60	14.6	0.87
96	20.0	0.60	14.9	0.90

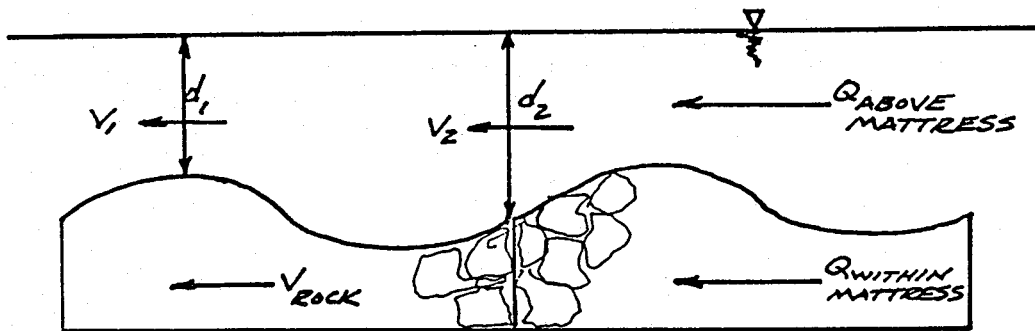


Table 3.7. Test Run Sequence - Discharge, Depth, Velocity Measurements for the 9-Inch Full-Scale Mattress Tests.

Total Discharge $Q_T$ , cfs	Velocity $V_1$ , fps	Depth $D_1$ , ft	Velocity $V_2$ , fps	Depth $D_2$ , ft	Discharge	
					$Q_{\text{Above Mattress}}$ cfs	$Q_{\text{Within Mattress}}$ cfs
18	6.8	0.33	6.8	0.33	13.5	4.5
30	10.8	0.38	10.1	0.43	26.0	4.0
40	12.4	0.42	10.6	0.56	35.6	4.4
60	16.4	0.50	14.2	0.65	55.4	4.6
80	17.4	0.57	13.4	0.94	75.6	4.4
90	19.4	0.57	14.6	0.98	85.8	4.2

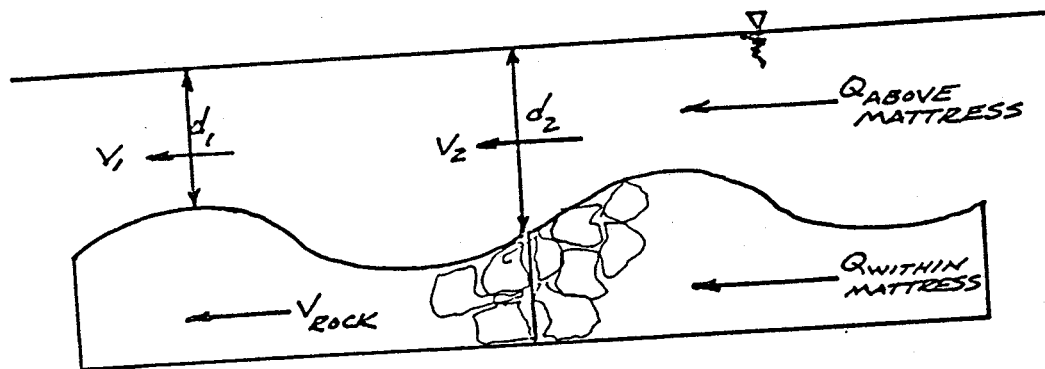


Table 3.8. Determination of 9-Inch Mattress Properties, Roughness Coefficient,  $n_b$  - Bed Shear Stress,  $\tau_b$ .

Total Discharge $Q_{\text{Total}}$ cfs	Discharge $Q_{\text{Above}}$ Mattress cfs	Average Velocity $V$ fps	Average Depth $D$ ft	Hydraulic Radius $R$ ft	Total Roughness Coeff. $n$	Bed Roughness Coeff. $n_b$	Bed Hydraulic Radius $R_b$ ft	Bed Shear Stress $\tau_b$ psf
30	26	10.5	0.41	0.361	0.026	0.028	0.403	3.27
40	35.6	11.5	0.52	0.421	0.026	0.028	0.471	3.82
60	55.4	15.3	0.60	0.486	0.022	0.024	0.554	4.49
80	75.6	15.4	0.82	0.606	0.025	0.028	0.719	5.83
90	85.8	17.0	0.84	0.615	0.023	0.026	0.739	5.99

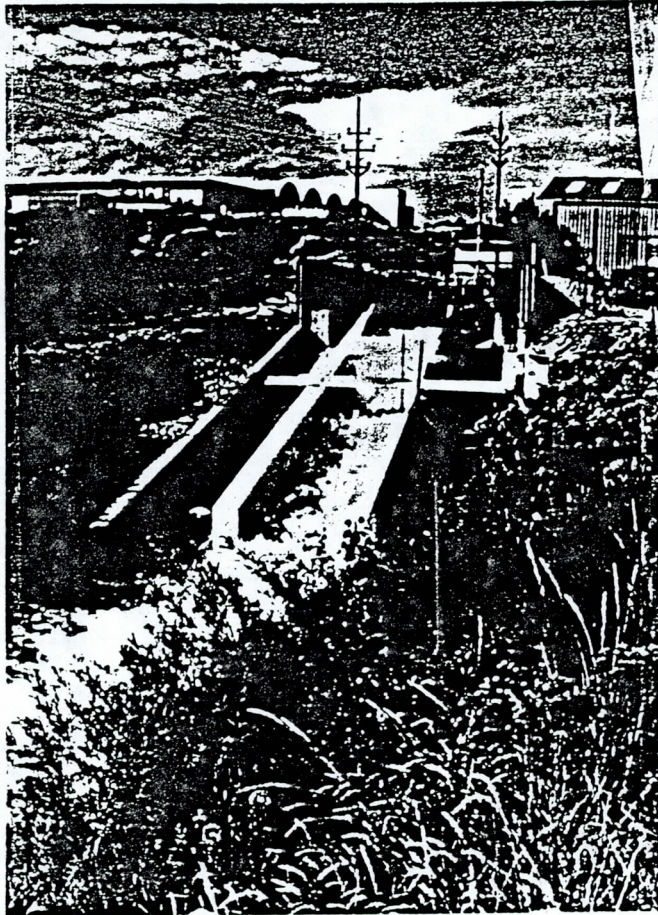


Figure 3.14. Overall view of outdoor flume setup.  $Q = 80$  cfs.

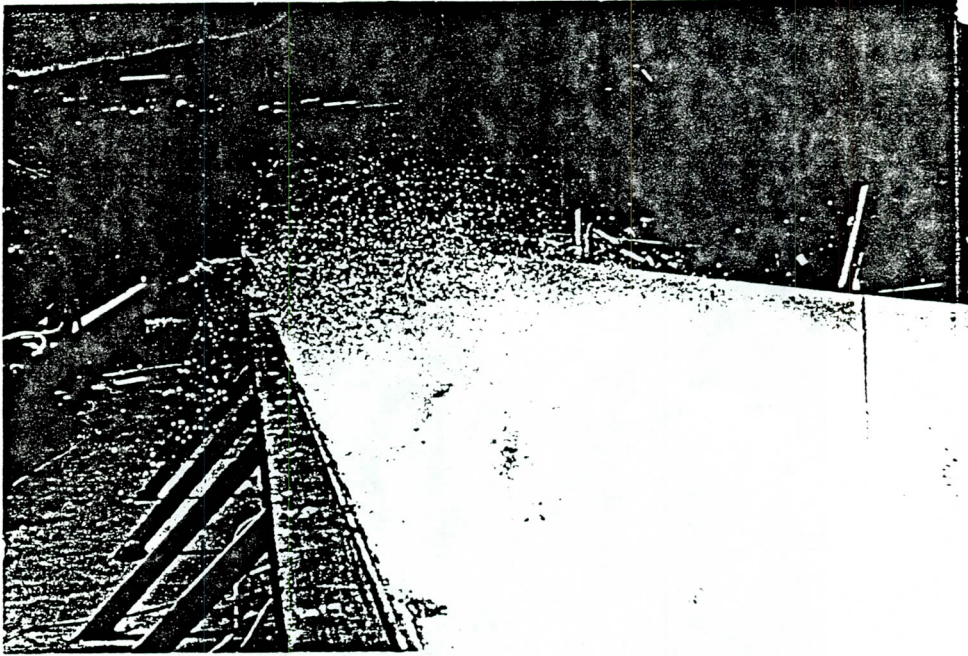


Figure 3.13. View of flume in vicinity below nozzle for  $Q = 56$  cfs.

#### IV. ANALYSIS OF RESULTS

##### 4.1 Introduction

The data collected in the model-scale mattress and full-scale mattress tests were analyzed to determine:

1. Hydraulics of channels protected by mattresses.
2. Incipient motion conditions.
3. Deformation of mattresses under high flow condition.

Whenever appropriate, model and prototype testing data were plotted together to evaluate the similarity of model and prototype results. It should be pointed out that the hydraulic conditions of mattress tests are limited to nearly normal flow over mattress beds. Additional tests should be conducted for mattress protection over banks with bend effects. The results of these additional tests can then be combined with the present study to formulate a more thorough design criteria.

##### 4.2 Hydraulic of Mattress Channels

The hydraulic variables considered in the analysis include:

1. Roughness coefficients
2. Velocity distribution
3. Relation between shear stress and velocities
4. Velocity at the mattress and filter interface.
5. Velocity at the filter and soil interface.
6. Pressure variation

###### 4.2.1 Roughness Coefficients

Manning's roughness coefficients were computed for all the test conditions using Equations 3.3 and 3.16 and were tabulated in Tables 3.4, 3.5 and 3.8. According to Meyer-Peter and Muller, the surface roughness of a sand-gravel bed can be related to a particular size of which 90 percent of particles is finer by weight,  $d_{90}$  (in meters), i.e.,

$$n_b = \frac{d_{90}^{1/6}}{26} \quad (4.1)$$

Figure 4.1 shows the comparison between the measured data and the computed values from Equation 4.1. The good agreement indicates that Equation 4.1 can be utilized to compute Manning's  $n$  for the mattress.

For the 3- to 6-inch filling rock utilized in the 6-inch and 9-inch mattresses,  $D_{90} \approx 5.5$  inches. Then according to Equation 4.1,  $n \approx 0.0275$ . This agrees well with the measured data. For the 18-inch mattresses, the filling rocks would be 4- to 8-inch size with a  $D_{90} \approx 7.5$  inches. The corresponding Manning's  $n$  computed from Equation 4.1 would be 0.0292.

With the increase in flow velocities, rocks within the mattresses would be moved downstream to cause a bed wave formation. This would slightly increase Manning's  $n$ . For example, if the bed elevation difference between the highest and lowest points within a diaphragm of a mattress unit was equal to the median size of the filling rock, the Manning's  $n$  would be increased by about 5 percent.

#### 4.2.2 Velocity Distribution

The measured velocity distribution for model scale mattress tests agree reasonably well with the log velocity distribution. According to Einstein (Simons and Senturk, 1977), for hydraulic rough boundary, the vertical velocity distribution can be determined by

$$\frac{u}{V_*} = 5.75 \log \left( 12.25 \frac{d}{K_s} \right) \quad (4.2)$$

where  $u$  is the time-averaged velocity at a depth  $d$ ,  $V_*$  is the shear velocity obtained by  $\sqrt{\tau_b/\rho}$ ,  $K_s$  is the representative bed roughness approximated by the median size of filling rock. Figure 4.2 shows the comparison of some measured velocity distribution with that computed from Equation 4.2.

For average velocity,

$$\frac{V}{V_*} = 5.75 \log \left( 12.25 \frac{R_b}{K_s} \right) \quad (4.3)$$

Figure 4.3 compares the measured average velocity for model scale mattress tests with the values computed from Equation 4.3. The agreement is reasonable. The results of the Manning's  $n$  and velocity distribution analyses indicate that hydraulic theories for gravel bed open channels are applicable for the mattress channels.

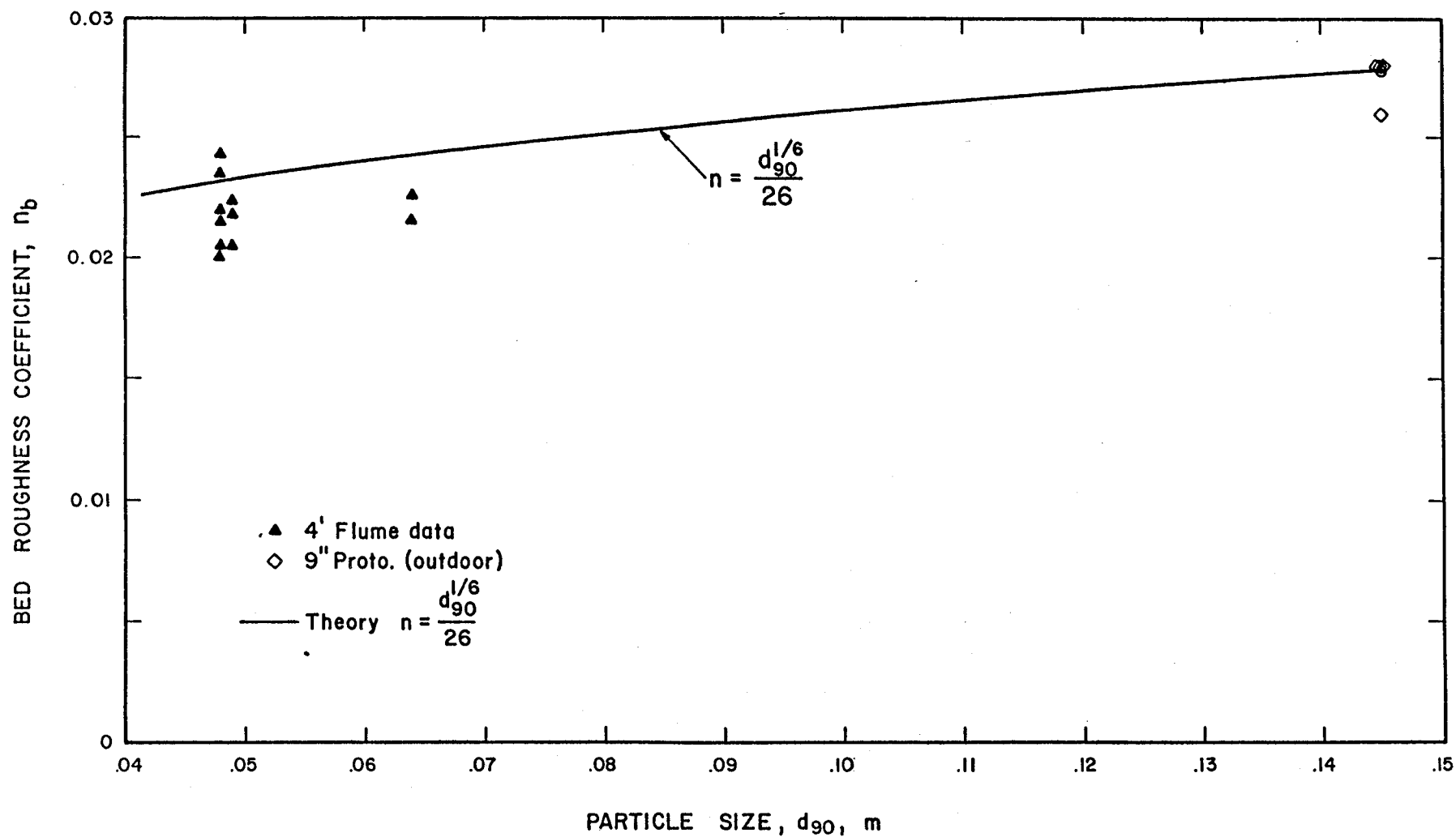


Figure 4.1. Comparison between the measured and computed Manning's roughness coefficient.

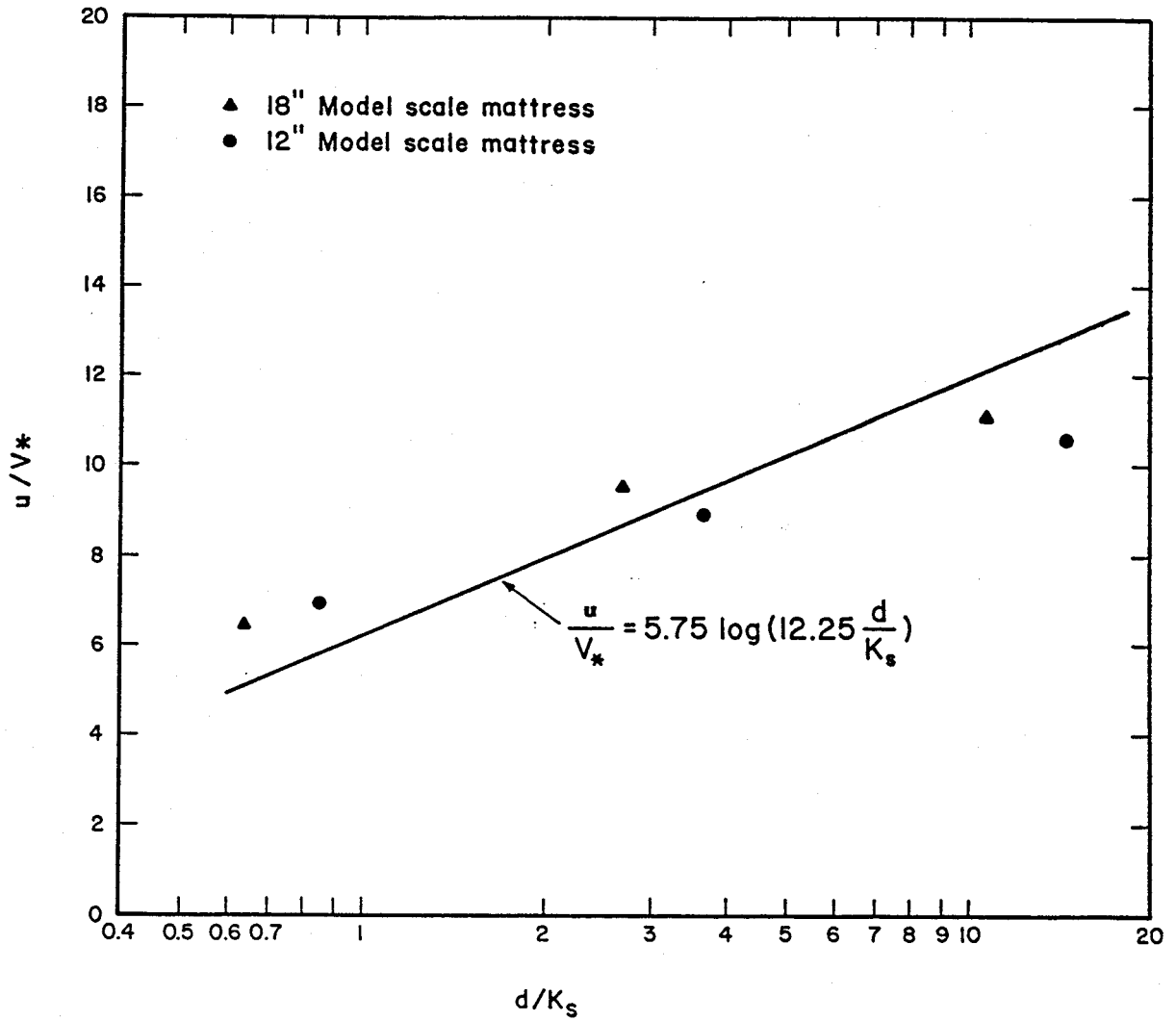


Figure 4.2. Velocity distribution for selected model-scale mattress tests in the 4-foot flume.

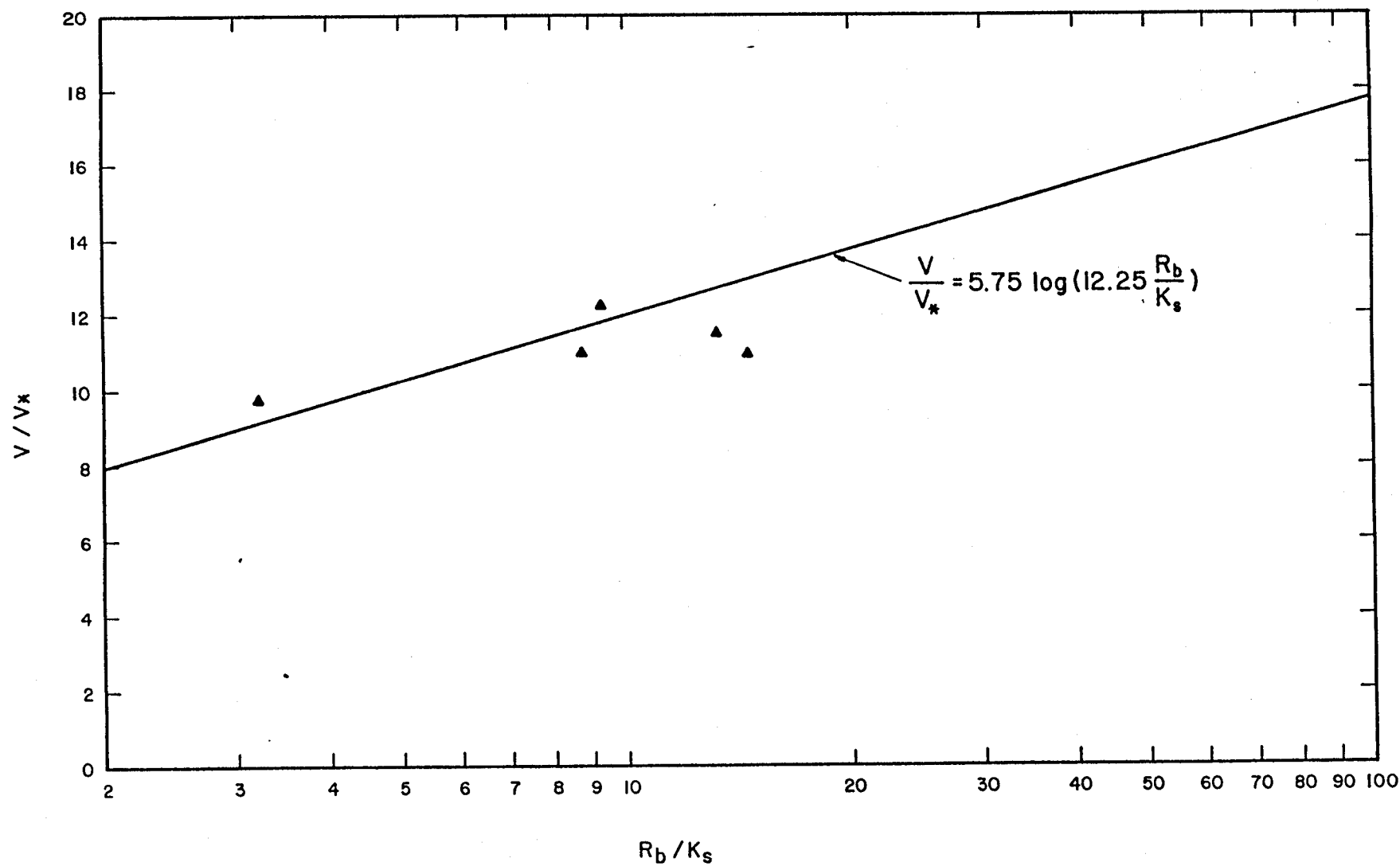


Figure 4.3. Average velocity for selected model-scale mattress tests in the 4-foot flume.

### 4.2.3 Relation Between Shear Stress and Velocities

Applying Manning's equation, a relation between the bed shear, velocity and hydraulic radius can be developed:

$$\tau = \frac{\gamma n_b^2}{2.21} \frac{V^2}{R_b^{1/3}} \quad (4.4)$$

Figure 4.4 shows some results obtained from the model-scale mattress tests in the 4-foot flume. The line shown on the figure was determined by assuming  $n_b = 0.025$ . A good agreement indicates the applicability of Equation 4.4. This equation indicates that for the same velocity, shear stress increases with decrease in hydraulic radius or depth. Also shear stress strongly dependent on velocity and weakly dependent on depth. Because shear stress is the major factor that controls the stability of mattress and riprap, for a given velocity, as depth is increased, stability will be increased due to the reduction in shear stress.

A similar conclusion was obtained based on riprap tests conducted by Fiuzat, et al. (1982). Figure 4.5 shows a derived relationship between the median rock size ( $d_{50}$ ), flow depth (D) and the Froude Number F for incipient motion runs. The best-fit equation to  $d_{50}/D$  and  $F^3$  is:

$$\frac{d_{50}}{D} = 0.222F^3 \quad (4.5)$$

which is the equation of the line in Figure 4.4. Equation 4.5 can be rewritten as:

$$d_{50} D^{1/2} = 0.222 \frac{V^3}{g^{3/2}} \quad (4.6)$$

Equation 4.6 shows that for a given velocity, as depth is decreased, mean rock size must increase for stability to be maintained. Conversely, increasing depth of flow allows smaller rock to be utilized while still maintaining stability. The stable size of rock is inversely proportional to  $D^{1/2}$  while it is proportional to  $V^3$ .

Overall, the research of Fiuzat, Chen and Simons (1982) indicates that for a given flow velocity, riprap stability increases with increasing depth and decreases with decreasing depth. Also, velocity was found to be a major controlling factor related to riprap stability while depth was found to have a

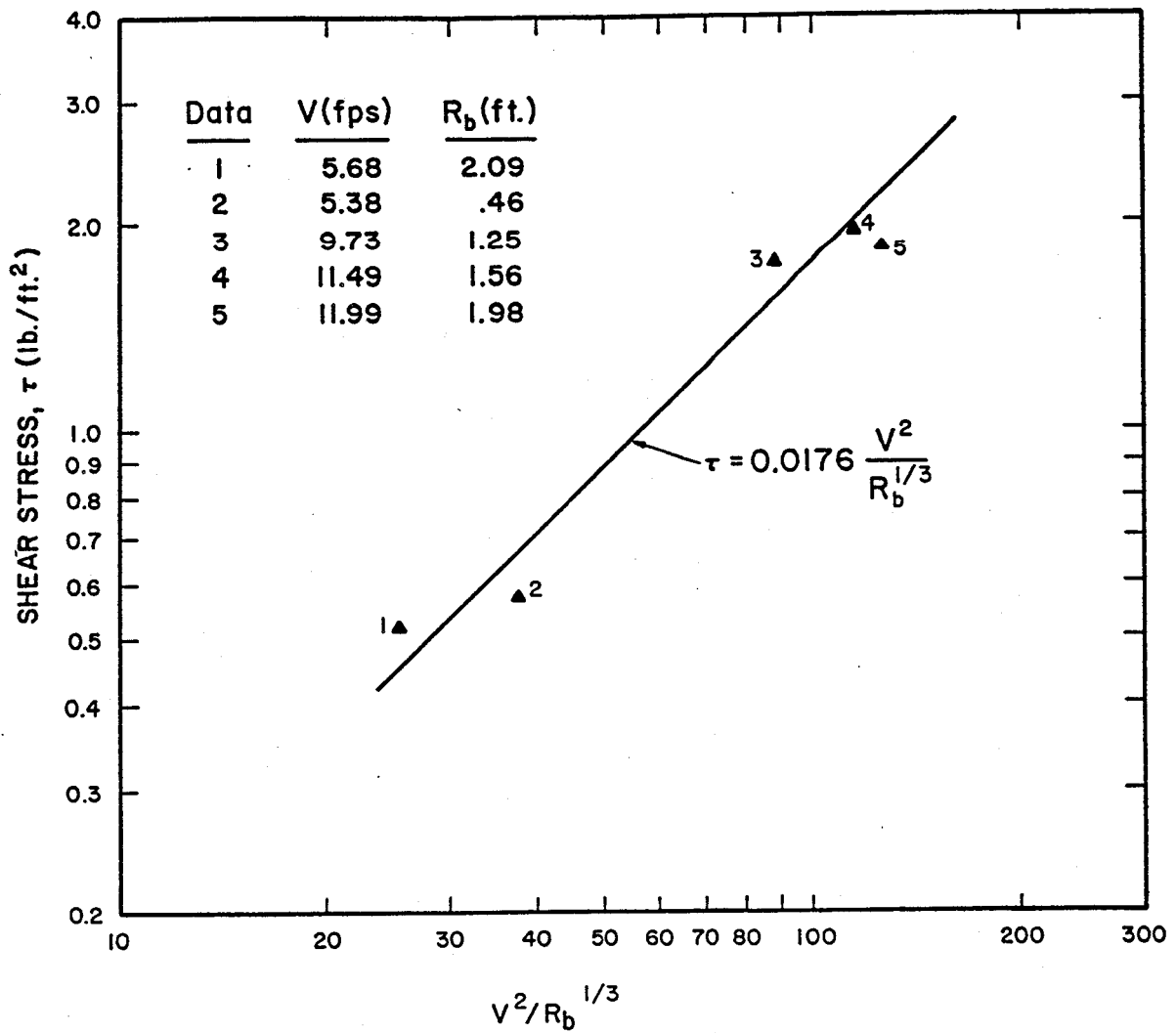


Figure 4.4. Relationship between shear stress, velocity and hydraulic radius.

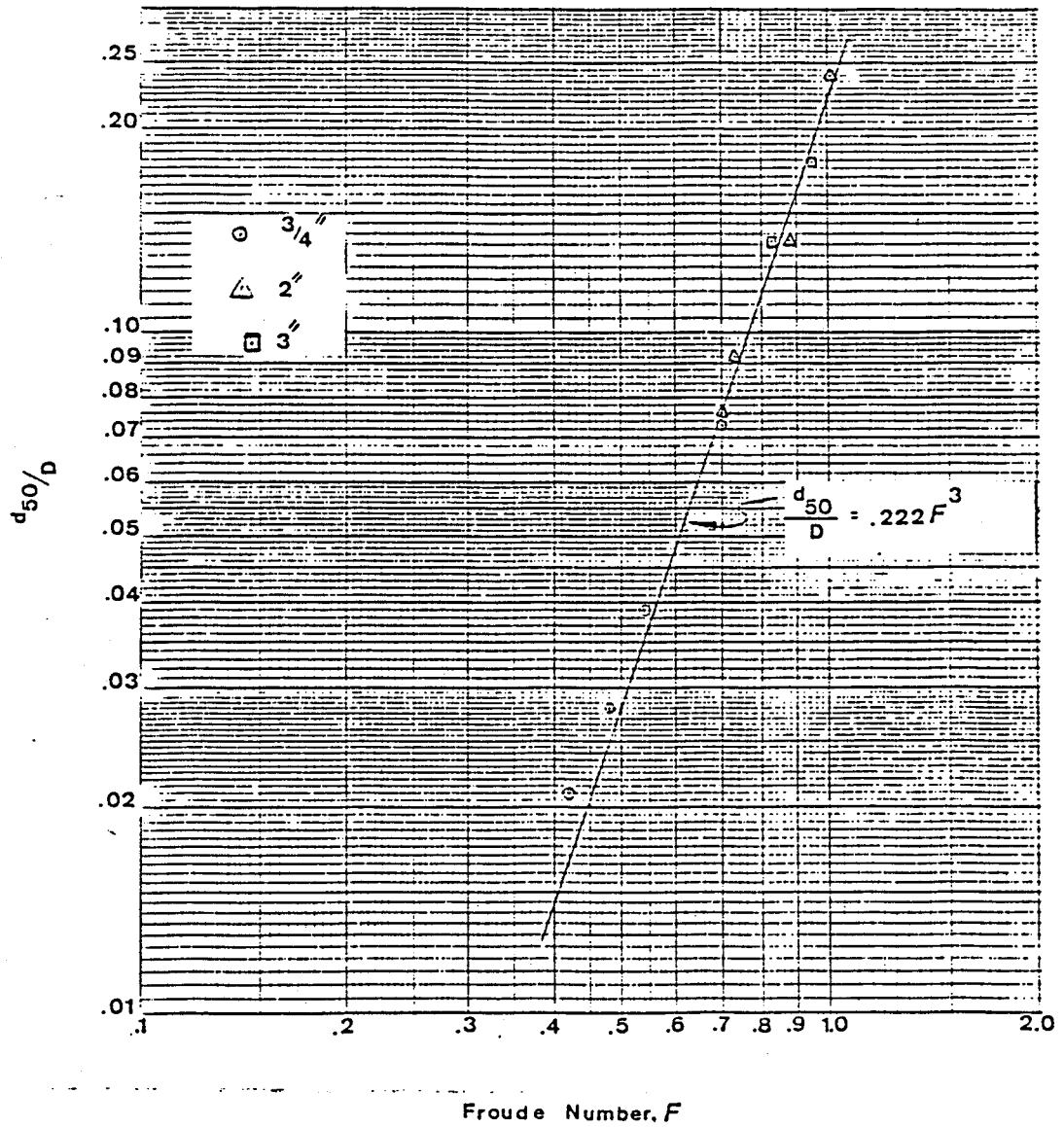


Figure 4.5.  $\frac{d_{50}}{D}$  vs. Froude number (from Fiuzat, et al. 1982).

lesser influence. Assuming that mattress stability follows the same general pattern, testing of prototyperevet mattresses under conditions of high velocity and relatively shallow depth would create a more critical condition than would testing at greater depths. Additional discussion on stability of mattresses will be presented in the section on "Incipient Motion Conditions."

#### 4.2.4 Velocity at the Mattress and Filter Interface and at the Filter and Soil Interface

In riprap and Reno mattress linings, the thickness and rock sizes are dictated by two factors, the ability to prevent erosion of the base materials and the ability to resist movement by the current.

The former, in effect, requires the velocity of the water passing through the rock layer to be nil (or sufficiently low to avoid moving soil particles) at the rock/soil interface. A thin layer can achieve this if the rocks and therefore the voids between them are small, and if the channel slope is small. With large rocks, the voids are large, and to obtain the necessary reduction in water velocity, the layer must be proportionally thicker. However, for a relatively steep channel, the water velocity at the mattress/filter interface would be mainly dependent on the channel slope and opening size of the interface, because the voids between mattress rocks are sufficiently large to allow significant flow passing through.

Based on the model-scale mattress tests in the 4-foot flume, it was found that the velocity immediately underneath the mattresses remained somewhat unchanged regardless of the flow conditions above the mattresses and the thickness of mattresses. This situation is only true when the major flow direction is parallel to the mattress surface. Therefore, it was assumed that Manning's equation was applicable to determine the velocity in the mattress filter interface:

$$V_b = \frac{1.486}{n_f} \left(\frac{d_m}{2}\right)^{2/3} S^{1/2} \quad (4.7)$$

where  $V_b$  is the velocity in the mattress/filter interface,  $n_f$  is the averaged Manning's roughness coefficient, and  $d_m$  is the median size of filling rocks. It was assumed that the hydraulic radius approximately equalled one-half of the median rock size.

Assuming that  $n_f \approx 0.02$ , the computed results were plotted on Figure 4.6, comparing with measured data from model-scale mattress tests. The reasonable agreement indicates that Equation 4.7 is applicable to determine the flow velocity in the mattress and filter interface for a parallel flow condition. However, if the major flow direction approached the mattress surface with a significant angle, then the value of  $V_b$  would be larger than that computed from Equation 4.7 because of additional dynamic flow force acting on the mattress. This additional force may significantly affect the stability of base material underneath the filter fabric.

According to the full-scale 9-inch mattress tests, the velocity underneath the filter fabric at the filter and soil interface,  $V_f$ , depends upon the velocity immediately above the Tyvar filter fabric in an order of about  $1/4 - 1/2$  of  $V_b$ . For other filter fabrics commonly utilized for channel stabilization, this velocity range is also about right. Our earlier study (Chen, et al. 1981) regarding performance of various filter fabrics indicates that permeabilities of these filters are not sufficiently different to affect velocity through filters unless they are clogged. For steep channels,  $V_b$  could be on the order of 4 fps. Then,  $V_f$  could be on the order of 2 fps. This velocity could be sufficiently large to move base material even though the mattress structures remained stable. In this case, a gravel filter layer that can effectively damp velocity may be a better way to protect the base material.

#### 4.2.5 Pressure Variation

Results from measurement of turbulence pressure plotted in Figure 3.11 for all of the test runs indicate that the value of  $\sqrt{p'^2} / \bar{P}$  (Equation 3.19) never exceeds 0.08. In other words, turbulence pressure represented by the RMS value is never greater than eight percent of the total static pressure intensity ( $\bar{P}$ ). This reveals that pressures associated with turbulence probably did not have significant destabilizing effects within the scale-model mattresses for the range of hydraulic conditions tested. In addition, Figure 3.11 shows that the turbulent pressure intensity decreases with a decrease in Froude number. This indicates that for the same velocity the turbulent pressure intensity decreases with increase in depth, and therefore the mattress is more stable with greater depth. In general the velocity gradient

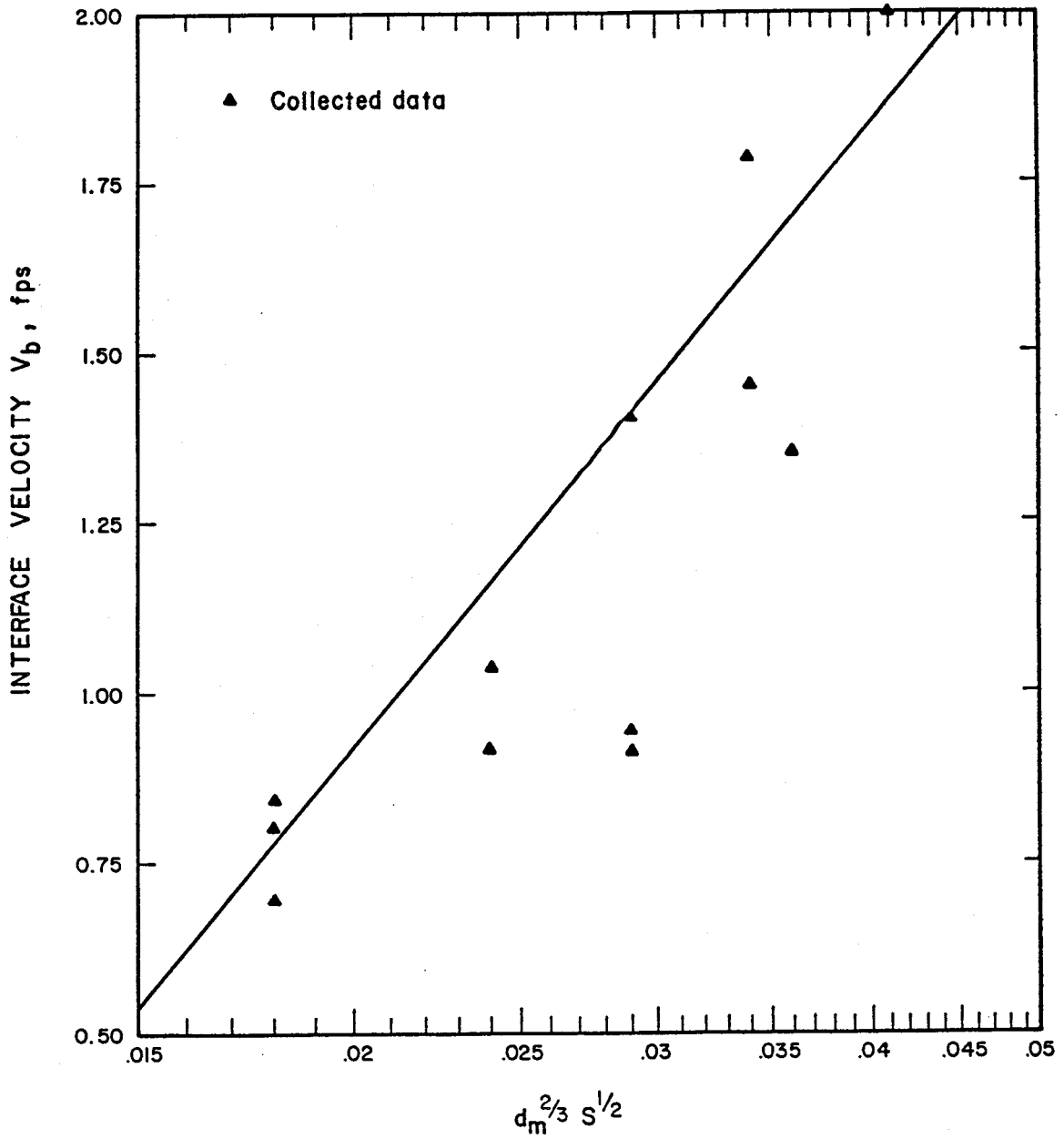


Figure 4.6. Comparison between the measured and computed velocity in the mattress and filter interface.

near the bottom is larger for shallow depth. Because shear stress is proportional to the velocity gradient, flow drag acting on the mattress is larger for shallower depth with the same average velocity. It is therefore concluded that for a given flow velocity, mattress stability increases with increasing depth and decreases with decreasing depth. Also velocity is a major controlling factor related to mattress stability while depth has a lesser influence. Based on Fiuzat, Chen and Simons (1982), the effect of velocity on the riprap stability to that of depth is on the order of six to one.

For the full-scale mattress tests, the sum of hydrostatic pressure head and velocity head was measured at locations shown on Figure 3.13. Figures 4.7 and 4.8 show these specific heads varying with discharge. It was found that specific heads under a severely deformed mattress remained fairly constant. If this was true, the deformed 9-inch mattresses with the thicknesses of rock layer reduced from 9 to 10 inches to 6 inches would remain useful for protecting the base materials from being eroded by flow due to pressure differences. It should be pointed out that the sand base material was washed out at the beginning of the test. The mattress and the pressure lines were then placed directly on the rigid flume bed. This could interfere with the actual pressure distribution during deformation of mattresses. Further tests with more stable underneath base materials are required to evaluate the effects of mattress deformation on base material protection.

#### 4.3 Incipient Motion Conditions

The usefulness of riprap and Reno mattresses for channel protection depends on the ability of riprap/mattress to prevent erosion of the soil and the ability to resist movement by the current. As stated earlier, the velocity of the water at the mattress/filter (or soil) interface is dependent on rock voids, the channel slope and the spacing size of the interface. For the ungrouted mattresses tested in this study which had large voids, the latter two factors were found to be predominant factors affecting the velocity at the interface. If this velocity (or channel bed slope) is small, a geotextile filter is recommended because it is easier to install. However, if the interface velocity is high due to steep channel slope or oblique flow directions, a gravel filter with sufficient thickness is recommended because it is more efficient to dissipate the velocity.

SPECIFIC ENERGY VERSUS  
TOTAL DISCHARGE

TAP LOCATION → #

- 2    △
- 3    ○
- 4    □

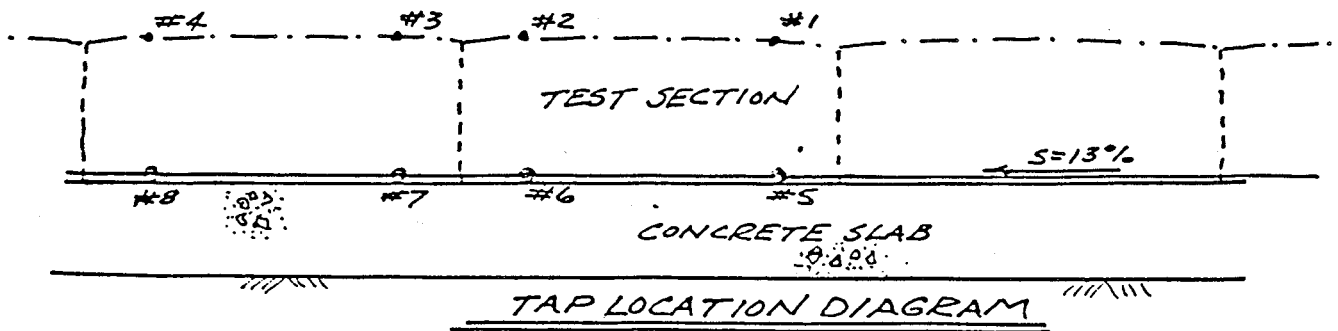
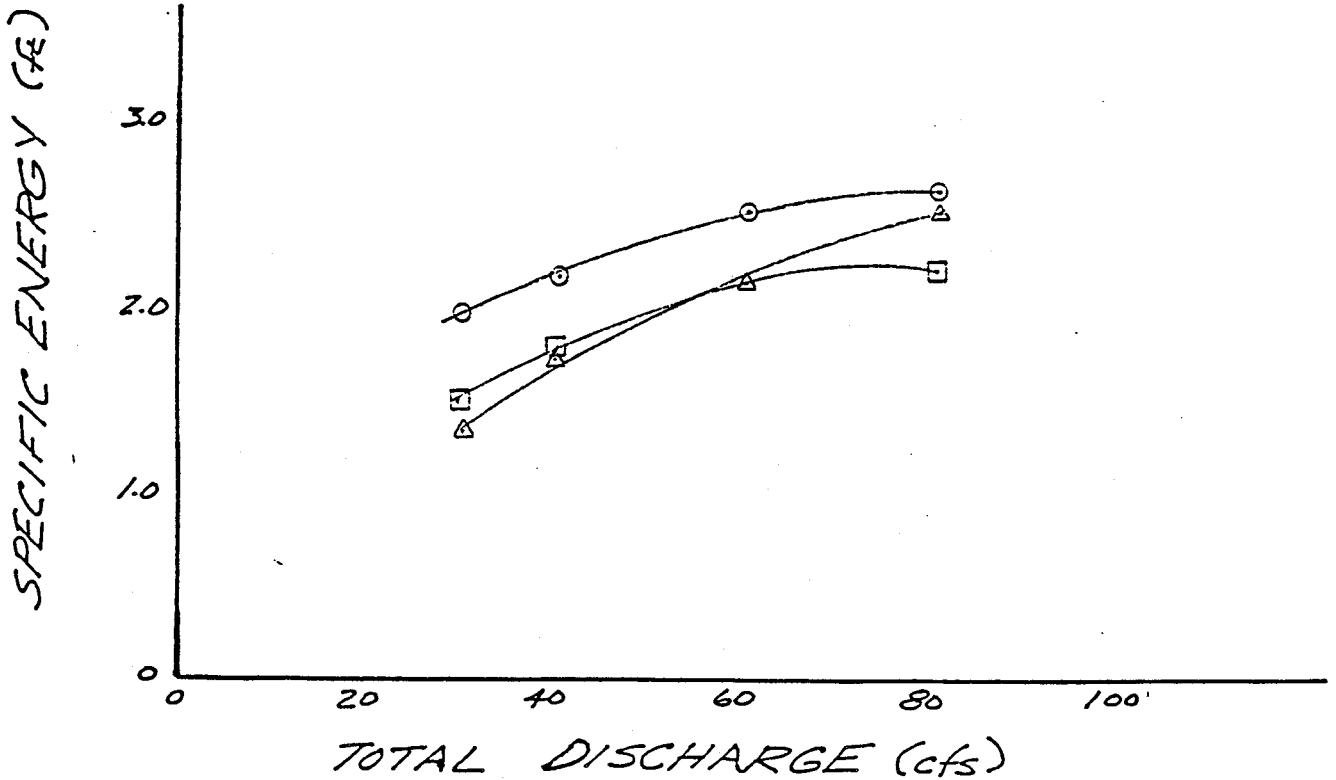


Figure 4.7. Variation of specific head immediately above the full-scale mattresses.

SPECIFIC ENERGY VERSUS  
TOTAL DISCHARGE

TAP LOCATION → #

- 6 Δ
- 7 ○
- 8 □

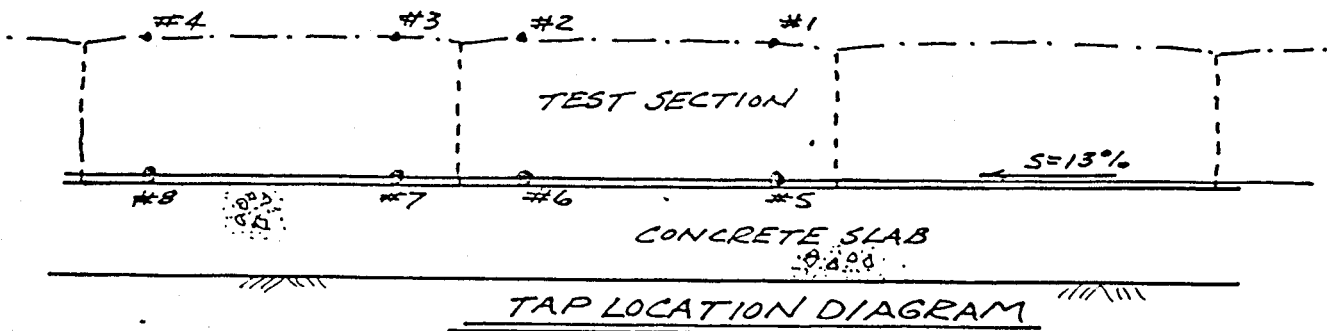
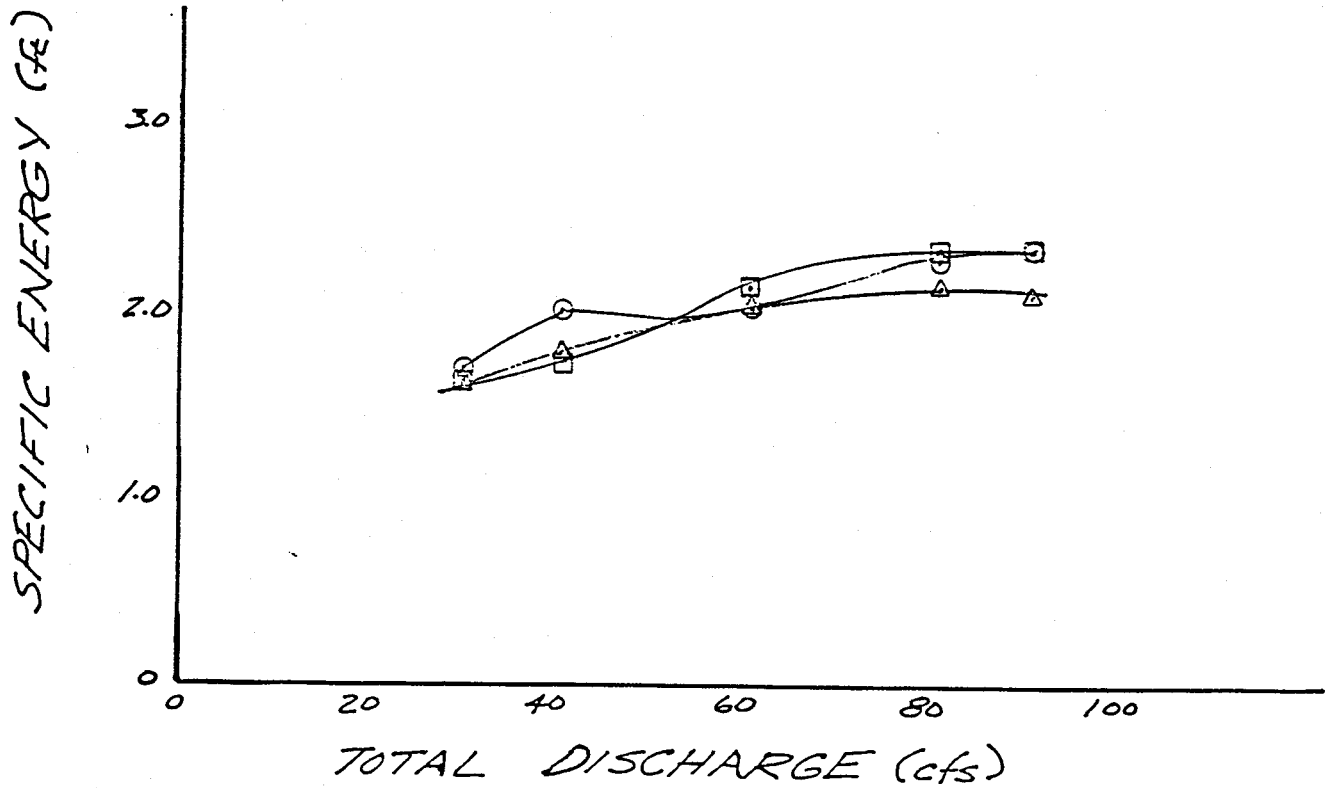


Figure 4.8. Variation of specific head immediately below the full-scale mattresses.

The ability of the mattress to resist movement by the current relies on its monolithic continuity to resist displacement and not its mass. The rocks inside the mattress are retained by the wire netting. In general, when the velocity and shear stress reach a critical magnitude, the rocks inside the mattress start to move in the main direction of flow. To determine this critical velocity and shear stress which initiate the rock movement, the tests of a mattress unit began with low flow rates and progressed to higher values. The conditions which initiate the movement of rocks within the mattress were determined.

Figures 4.9 and 4.10 show the critical velocity versus median particle size and versus mattress thickness, respectively. The critical velocities for median particle size larger than six inches and mattress thickness larger than 18 inches are extrapolated values. Further verification is required. All the model-scale mattress data tested in the 4-foot flume had a Froude number less than 1.5 and the full-scale mattress tested in the outdoor steep flume had a Froude number larger than 3.0. As described earlier for the same velocity, the size of mattresses should be increased for a shallower depth condition to obtain the same degree of stability in a deeper channel. Figure 4.10 shows that an 18-inch mattress unit should be utilized for a highly supercritical flow ( $F > 3$ ) to obtain the same degree of stability as a 9-inch mattress for a nearly critical or subcritical flow ( $F < 1.5$ ). Critical velocity for incipient motion of riprap which was determined based on  $C_* = 0.047$  was also plotted on Figure 4.9. This figure indicates that mattress mesh improves the stability of filling rocks by tightening rocks as a unit. Figure 4.9 shows that 4-inch rocks tightened in mattress meshes can sustain 12 to 14 fps velocity, while the same velocity can cause movement of 6- to 8-inch rocks.

The critical velocities for various mattress thicknesses determined from this study were compared with the velocities suggested by Agostini and Papetti (1978) as follows:

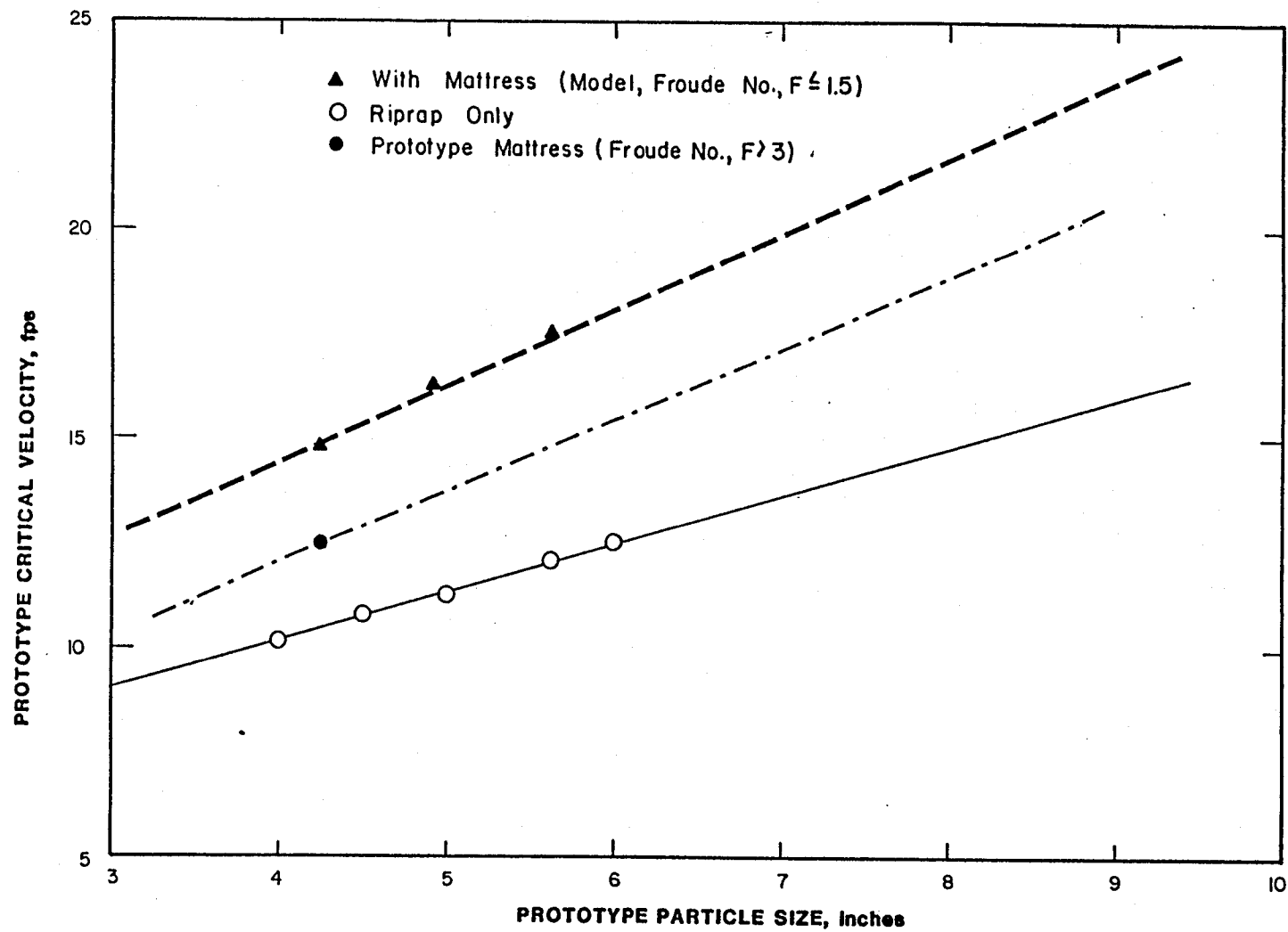


Figure 4.9. Critical velocity that initiates rock movement as a function of rock size.

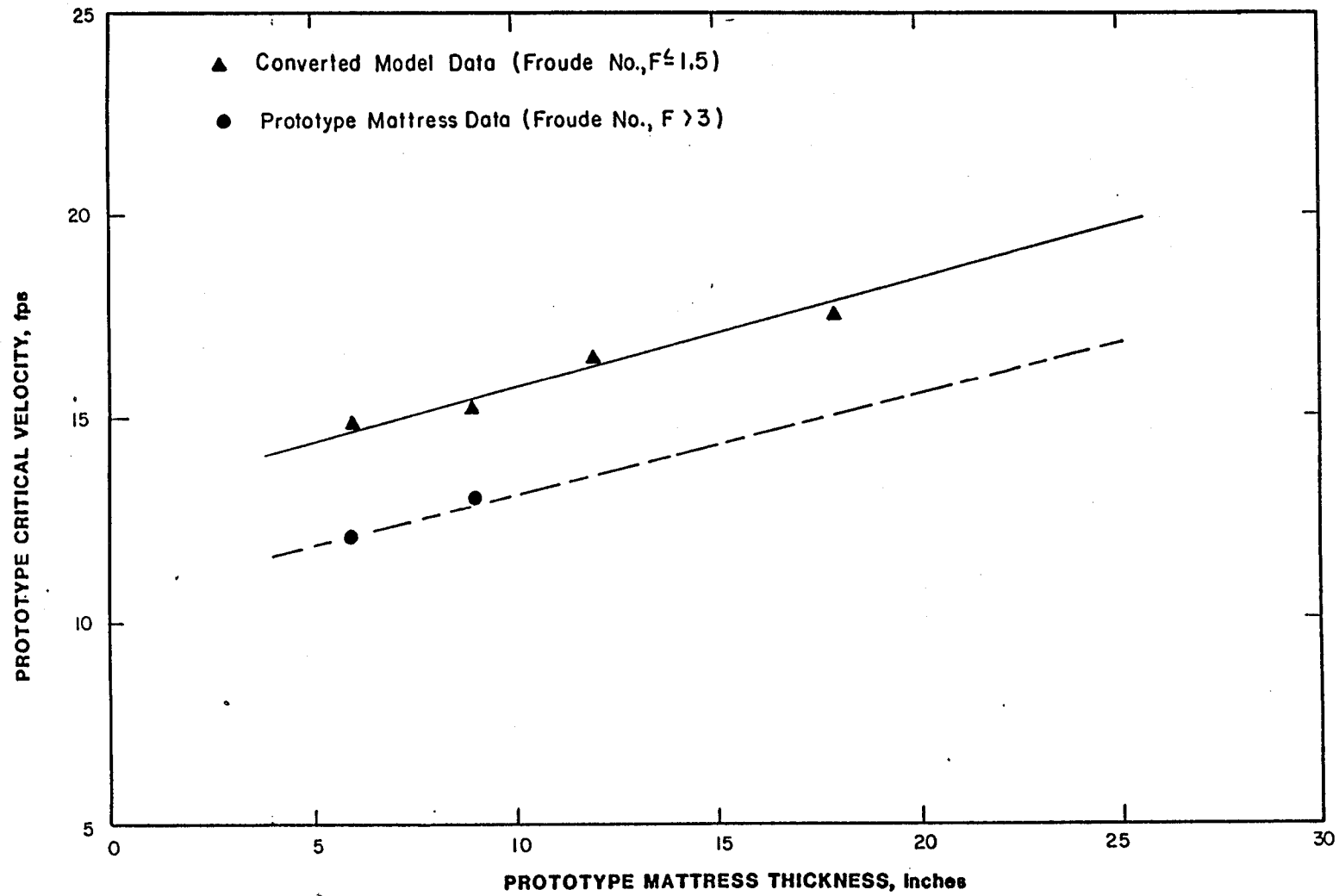


Figure 4.10. Critical velocity that initiates rock movement as a function of mattress thickness.

Mattress Thickness (inches)	Critical Velocity Determined From This Study (fps)		Velocity Suggested by Agostini, and Papetti (fps)
	<u>F &lt; 1.5</u>	<u>F &gt; 3</u>	
6	14.5	12.1	5.9
9	15.4	13.0	11.8
12	16.4	13.8	14.8
18	18.3	15.6	17.7

It was found that the permissible velocities suggested by Agostini and Papetti were all lower than the critical velocities determined from this study for  $F < 1.5$ , particularly for 6-inch and 9-inch thick mattresses. This indicated that mattress linings designed by using Agostini and Papetti's criteria were thicker than that actually required. Significant savings can be obtained by using the new criteria obtained from this study.

Critical shear stress which initiated the movement of tested mattresses was plotted against the filling rock sizes and mattress thicknesses. Figure 4.11 shows the measured critical shear stress versus rock sizes within and without mattress. This figure shows that the critical shear stress converted from the model-scale and that measured from the full-scale mattresses are comparable. Also mattress mesh would enhance stability of filling rock by doubling the critical shear stress comparing to that for the riprap along. Figure 4.12 shows the Shield parameter  $C_*$  versus the shear Reynolds number  $R_*$ . This figure shows that  $C_* \approx 0.10$  for the mattress while  $C_* \approx 0.047$  for the riprap.

The thickness of a riprap protection structural can be determined using the following steps:

1. Determine the median size of riprap to protect channel bed against a shear stress  $\tau$ .

$$d_m = \frac{\tau}{0.047(\gamma_s - \gamma)}$$

2. Determine the thickness of riprap, which is about  $2d_m$ .

The following table presents a comparison between the required thickness of riprap and that of mattresses for several values of shear stress:

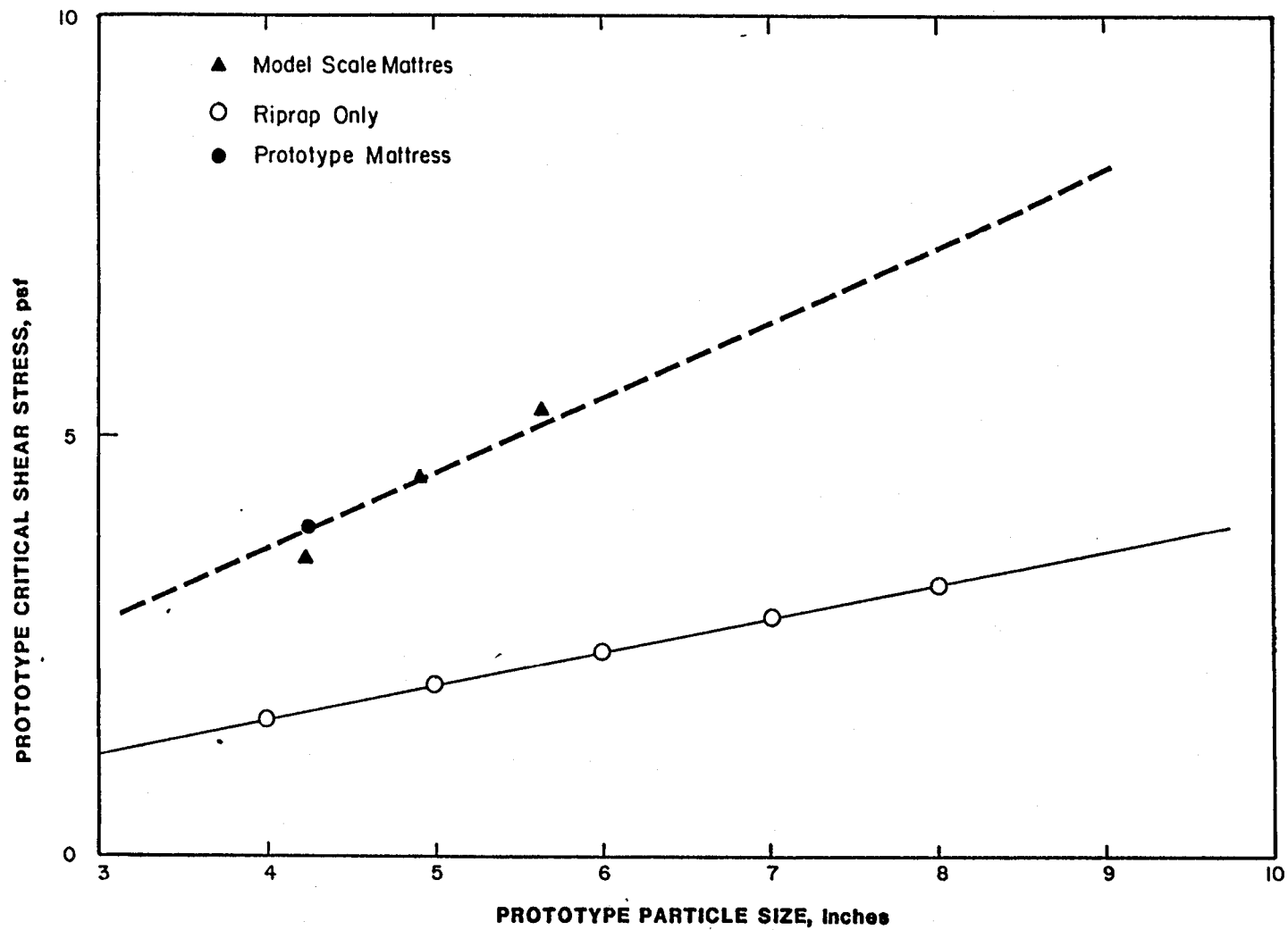


Figure 4.11. Critical shear stress versus rock sizes for the with and without mattress cases.

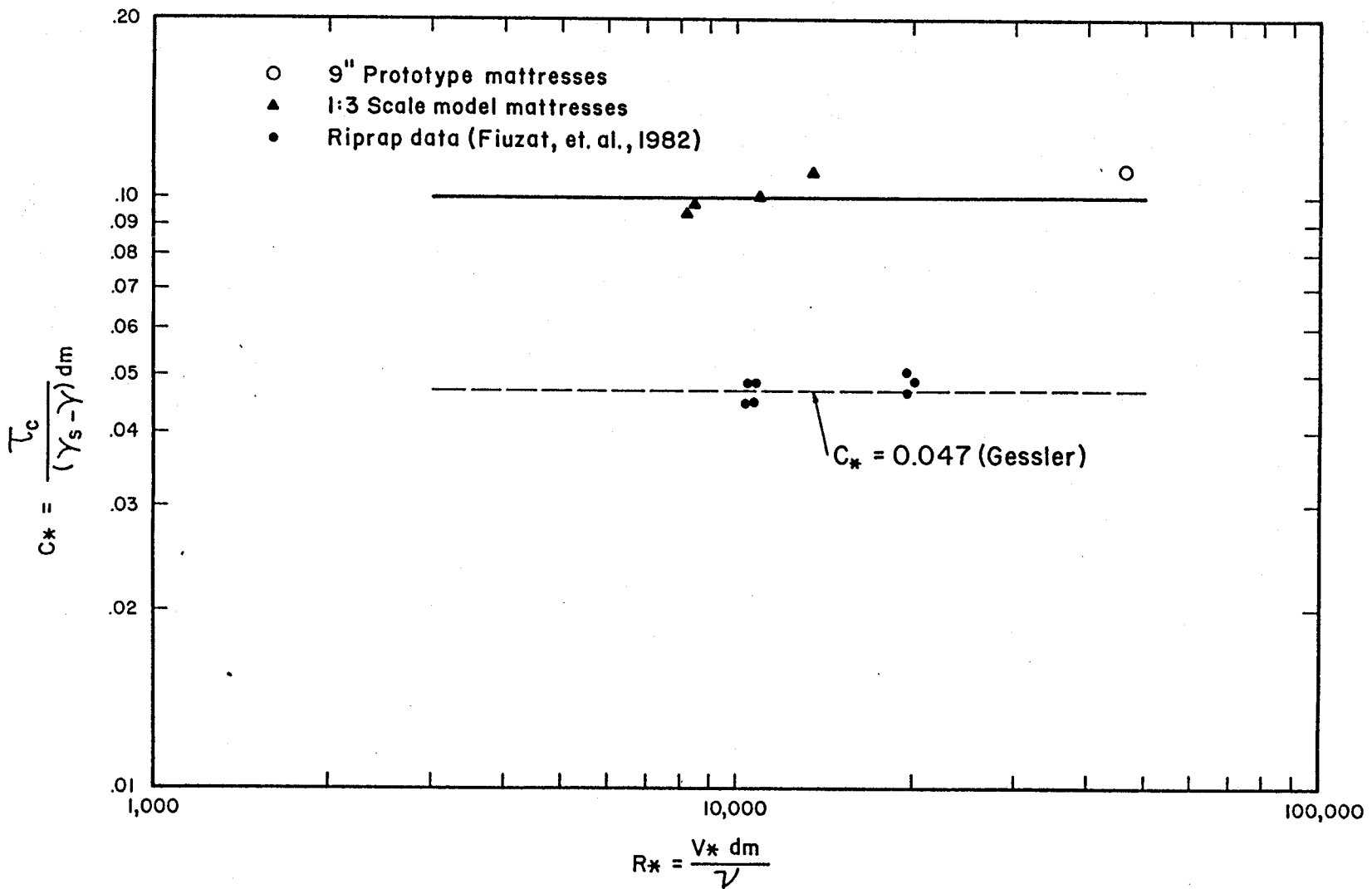


Figure 4.12. Shields parameter as a function of the shear Reynolds number for with and without mattress cases.

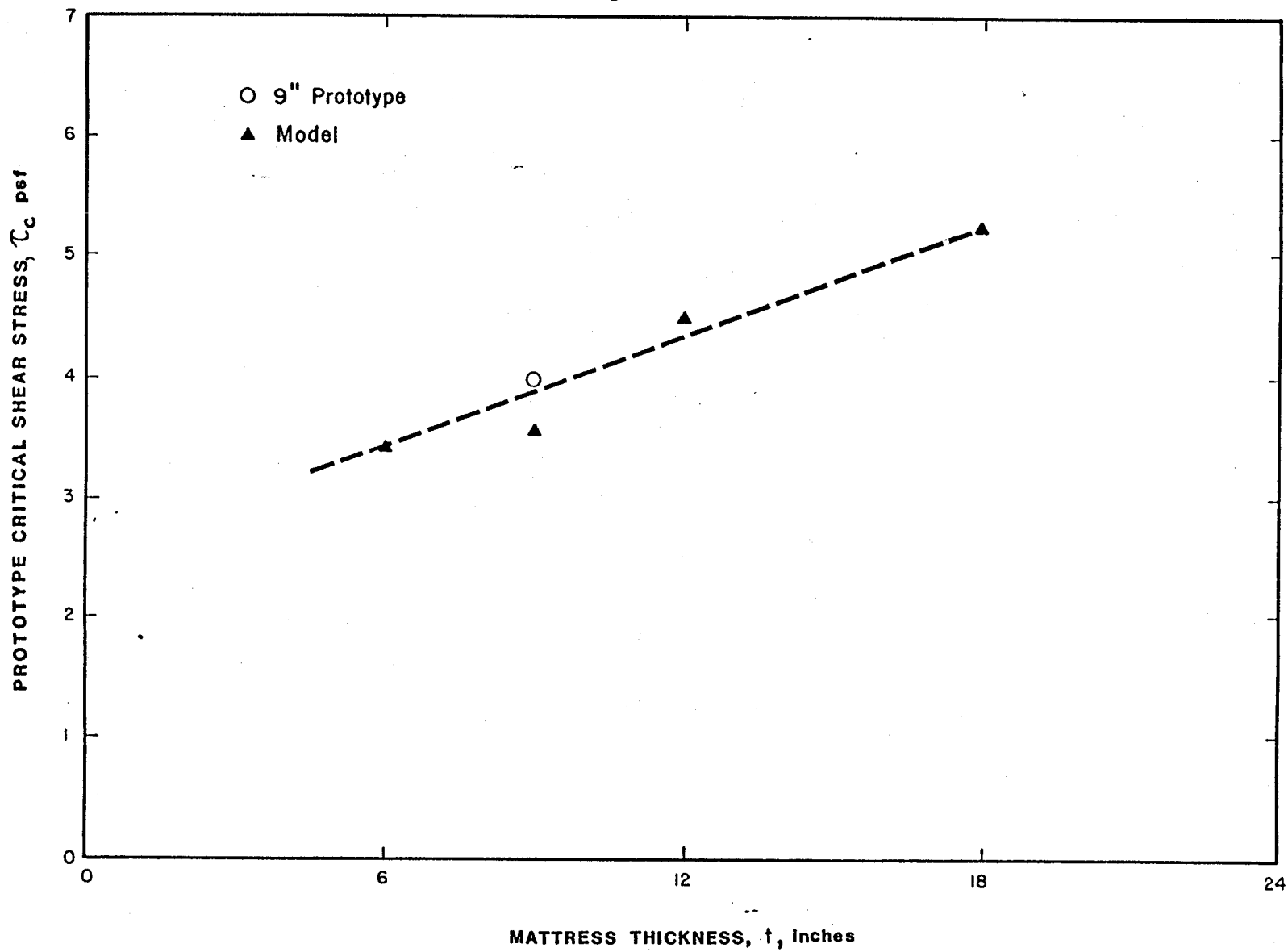
<u>Shear Stress</u> (lbs/ft <sup>2</sup> )	<u>Thickness (inches)</u>	
	<u>Mattress</u>	<u>Riprap</u>
3.5	6	17
4.0	9	20
4.6	12	23
5.5	18	28

The required mattress thickness given above was determined from the laboratory tests and is shown in Figure 4.13. This comparison shows that in practical flow range, the required thickness of riprap could be 1.5 to three times of mattress thickness.

It should be pointed out that the model-scale mattresses tested in the eight-foot flume were made of stronger wire mesh than the mattresses tested in the four-foot flume. No significant movement was observed when the converted prototype velocity reached 17 fps, while there was significant rock movement for mattresses made of thinner wire under the same velocity. This indicates that the wire mesh strength is a major factor controlling stability of mattresses. For model-scale mattress test E which was grouted by mastic asphalt, there was not observed movement of rock within the mattresses when subjected to velocity up to 20 fps. This indicates that grouting of mattresses using sand asphalt mastic can significantly increase the stability of mattresses.

#### 4.4 Deformation of the Mattress

With further increase in flow velocity and shear stress beyond the critical values, a significant amount of rocks would move from the upstream portions of a mattress compartment to the downstream portion of the compartment. Figure 4.14 shows the typical sequence of rock movement and resultant deformation of mattress compartments observed. It should be noted that for each flow velocity, the reno mattresses appeared to reach a condition of relative stability fairly rapidly. In other words, although increasing the flow velocity resulted in additional rock movement within the mattress, movement did not occur throughout the test. As a result, the flow duration for a given velocity appeared to have only a minor influence on rock movement within the mattress.



4.22

Figure 4.13. Critical shear stress versus mattress thickness.

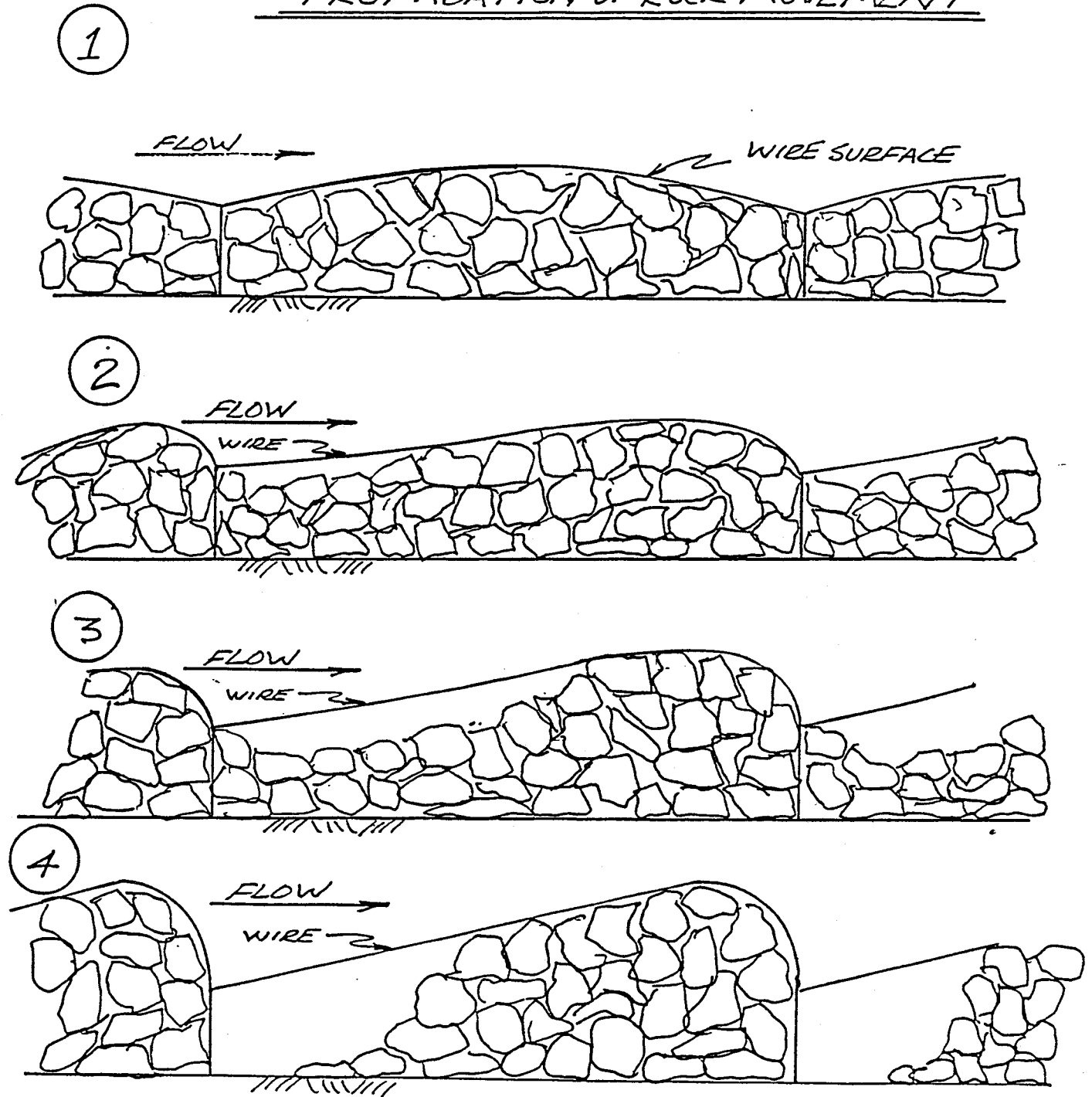
PROPAGATION OF ROCK MOVEMENT

Figure 4.14. General pattern of rock movement within a mattress compartment.

It was observed that the surface deformation conformed to the same general shape and movement was propagated in the same manner as for model-scale and full-scale mattresses. Figure 4.15 and 4.16 illustrate these comparisons for full-scale mattresses under similar flow velocities. Evidence of the rippling effect of the deformation of mattress compartment is presented in Figures 4.17 and 4.18 for nine-inch full-scale mattresses, Figure 4.19 for six-inch full-scale mattresses, and Figure 4.20 for model scale 12-inch mattresses.

As previously stated, the mattress deformation would not significantly affect the specific head variation underneath the mattress unless the extent of rock movement within the mattress was such that the filter or base materials were exposed. This indicates that the mattress even after deformation provided a similar degree of protection to that provided by an undeformed mattress if the reduced rock thickness section was more than one median size thick. Both the model-scale and full-scale mattress tests show similar phenomena.

To evaluate the degree of deformation, a parameter  $\Delta z/d_m$  was utilized, where  $\Delta z$  is the height difference between the lowest and highest rock surface within a mattress compartment and  $d_m$  is the median size of the filling rock. The maximum values of  $\Delta z/d_m$  were plotted against the effective

Shields parameter,  $C_*' = \frac{\tau - \tau_c}{(\gamma_s - \gamma)d_m}$  in Figure 4.21. An increase in  $C_*'$

resulted in an increase in  $\Delta z/d_m$ . Based on the observation of mattress deformation, the reduction in the filling rock thickness was about  $\Delta z/2$ . Therefore, to insure that the soil protected by mattresses would not be exposed, the value of  $\Delta z/d_m$  should be less than  $2(t/d_m - 1)$  where  $t$  is the thickness of the mattress. Based on this relation and Figure 4.21, soil protected by mattresses with a thickness larger than or equal to nine inches and a compartment length of three feet would not be exposed to direct flow attack under a velocity up to 20 fps.

In summary, mattresses would maintain effectiveness to protect base materials even subjected to flow current stronger than the incipient motion condition. Mattresses with a thickness equal to or larger than nine inches would still be effective in protecting base materials in a mild slope channel bed under a velocity up to 20 fps. However, gravel filters or a combined

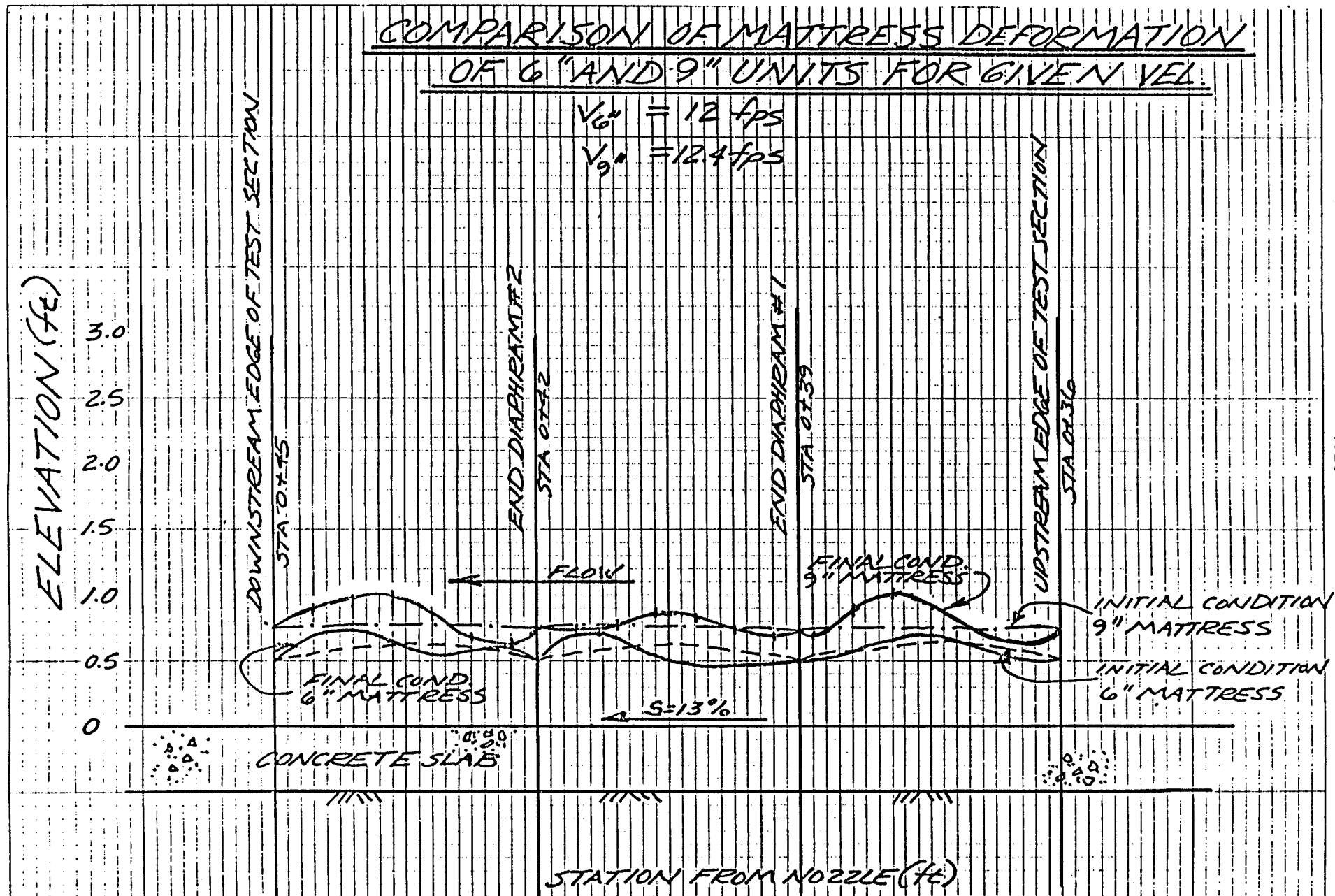


Figure 4.15. Comparison of deformation of 6-inch and 9-inch full-scale mattress units for a velocity of 12 fps.

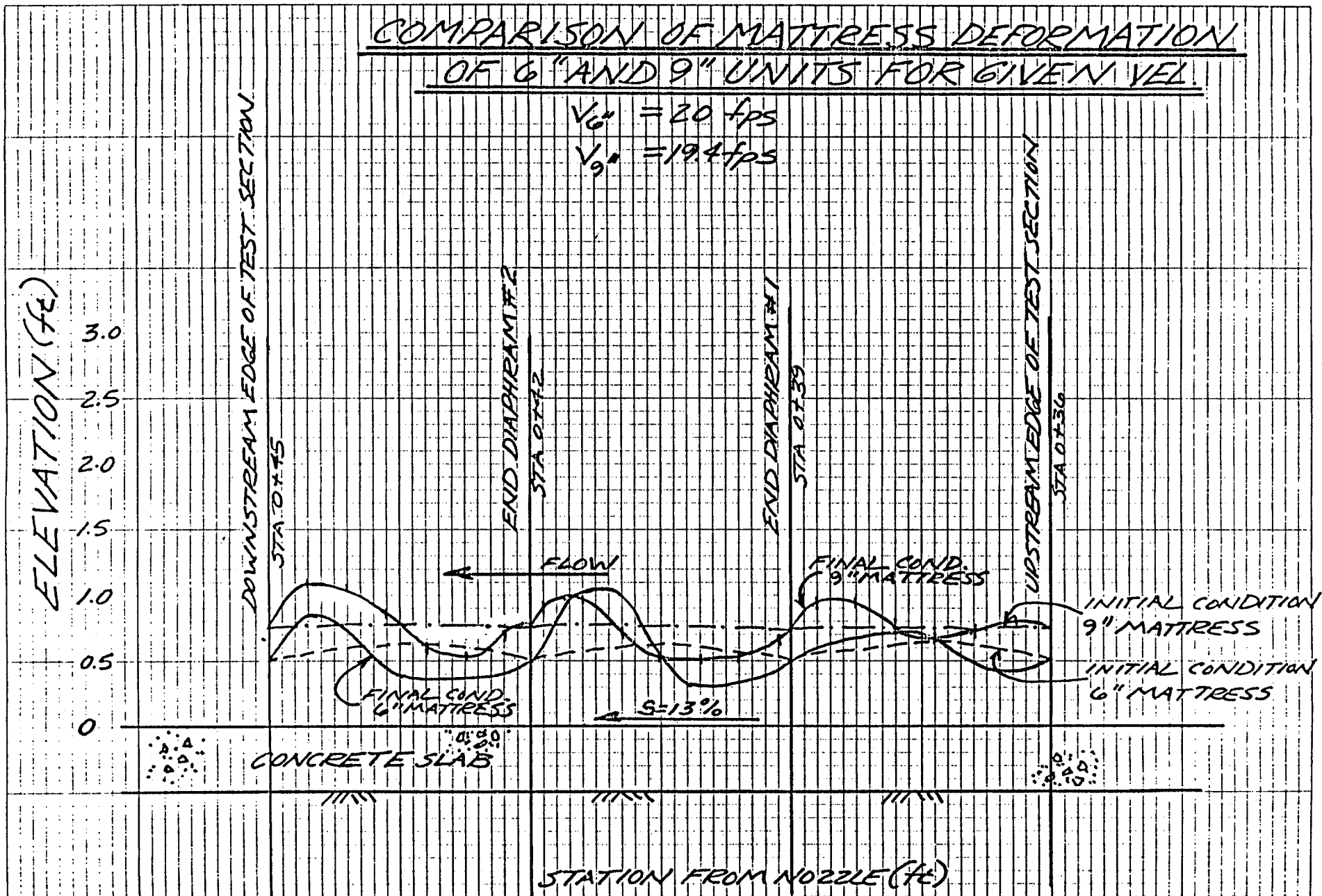


Figure 4.16. Comparison of deformation of 6-inch and 9-inch full-scale mattress units for a velocity of 20 fps.

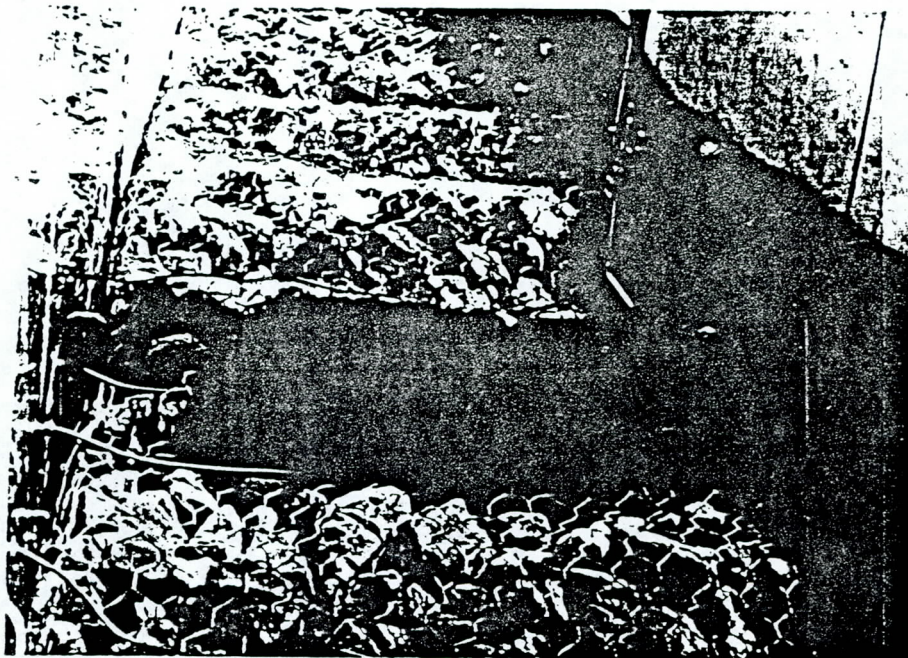


Figure 4.17. Deformation of mattresses (9") due to rock movement (looking downstream).  $V = 16.4$  fps.

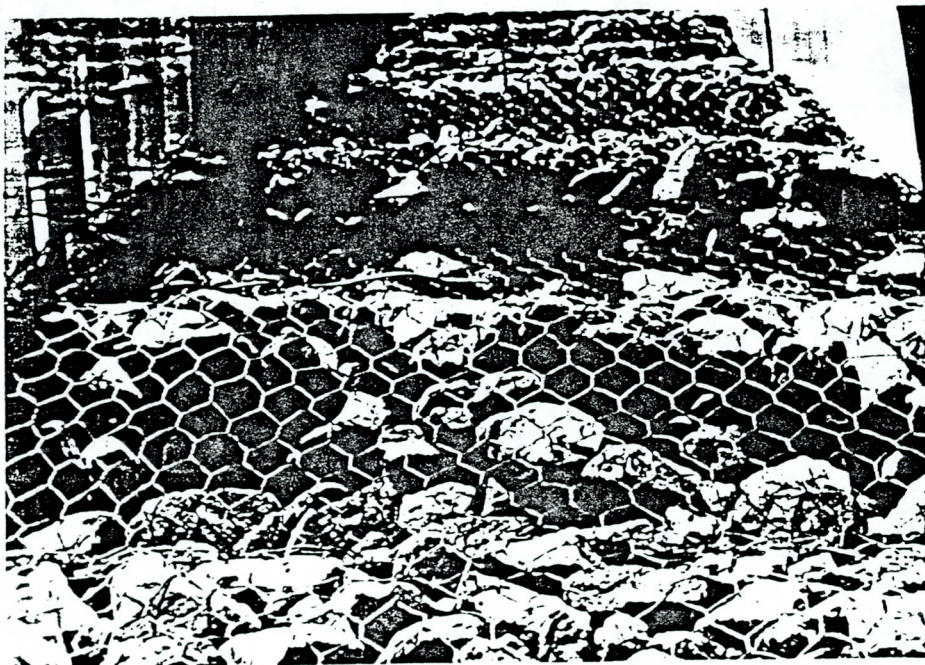


Figure 4.18. Deformation of mattresses (9") due to rock movement (looking downstream).  $V = 17.6$  fps.

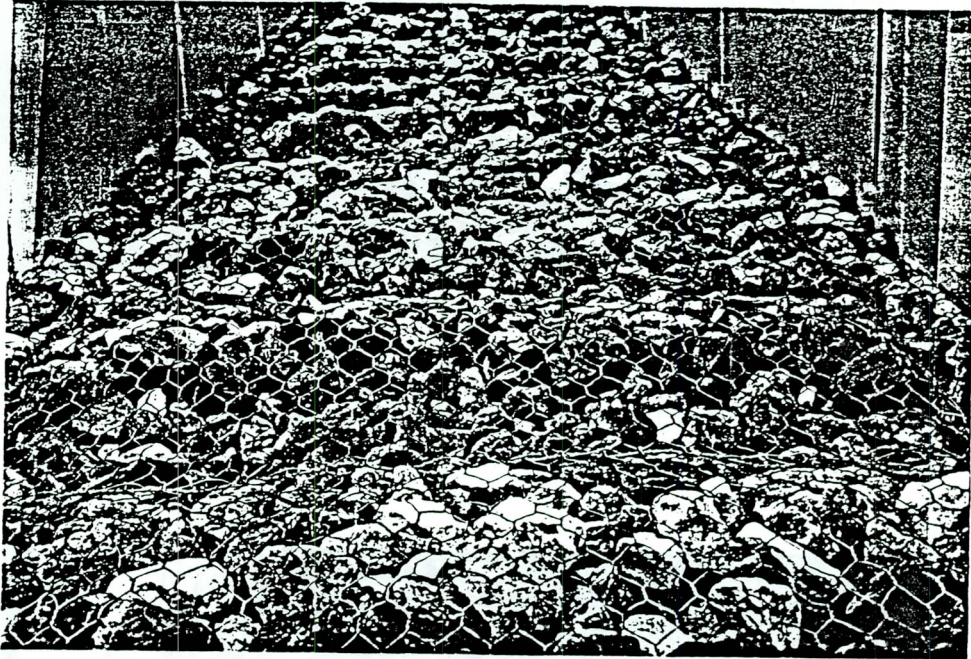


Figure 4.19. Deformation of 6" full-scale mattresses due to rock movement.  $V = 19.2$  fps.

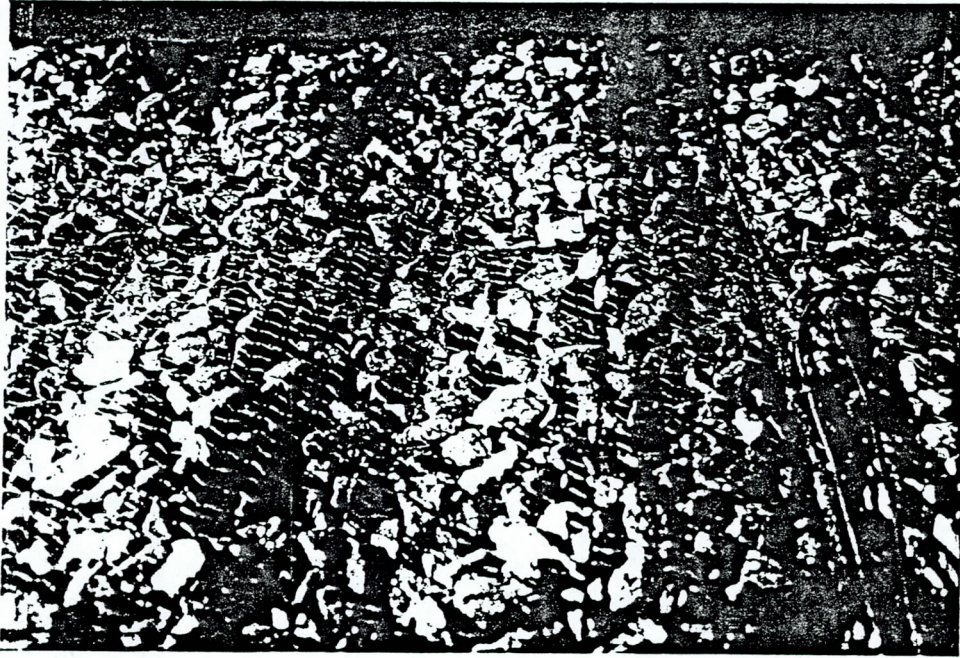


Figure 4.29: Deformation of 6" model-scale mattresses (corresponding to 18" full-scale mattress).  $V_m = 12.0$  fps (corresponding to  $V_p = 20.8$  fps).

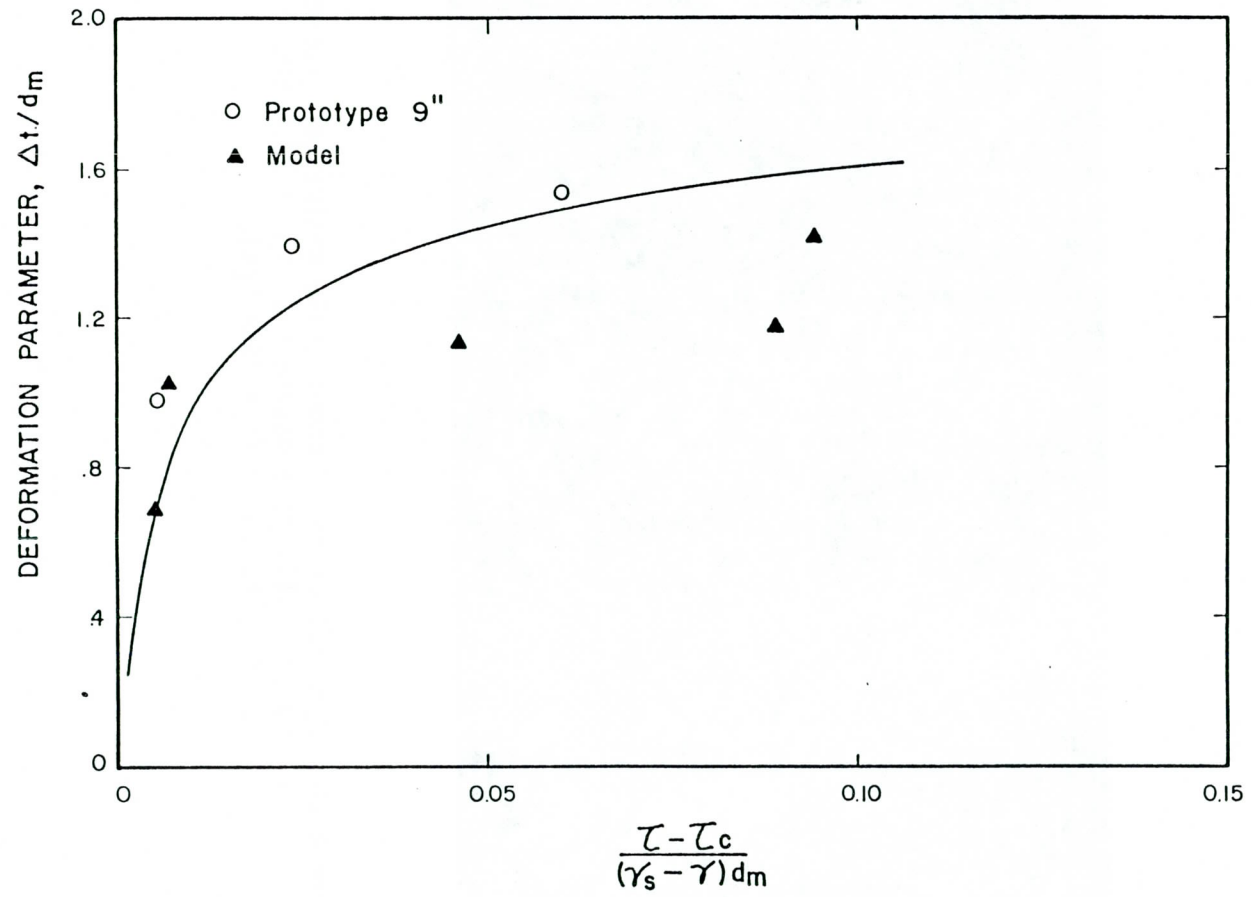


Figure 4.21. Relationship between the deformation factor and effective Shields parameter.

geotextile/gravel filter should be utilized to reduce the water velocity at the mattress/filter interface that attacks the base materials. Another alternative would be to grout the mattresses using sand mastic asphalt. This would consolidate the mattresses and essentially eliminate velocity that attacks the base materials. Additional studies should be conducted to evaluate the effectiveness of various filter designs to improve the ability of mattresses to stabilize channels under extremely high flow conditions.

## V. DEVELOPMENT OF DESIGN CRITERIA

### 5.1 Development Approach

As described earlier, the effectiveness of mattress protection works is indicated by two factors; the ability to prevent erosion of the base materials and the ability to resist movement by the current. The following steps are proposed to design the mattress protection works:

1. Determine the hydraulic conditions in the mattress channel for a given design discharge.
2. Determine the mattress requirement based on incipient motion criteria.
3. Determine the velocity at the mattress/filter (or base soils) interface.
4. Determine filter requirement to safely protect base materials.
5. Determine potential deformation of mattress when flow discharge is larger than the design discharge.

Detailed descriptions of each major design step are presented in the following sections. Design examples are given in the Appendix. It should be noted that all the mattress tests were conducted on flume beds. The developed criteria for protecting banks were based on theories and some empirical equations and should be verified whenever possible. No bend effects were evaluated during the study. Also the recommendation on filter requirement was based principally on engineering judgment. Additional study of the requirement of filter to enhance structure stability should be conducted.

### 5.2 Determination of Hydraulic Conditions

The major hydraulic variables to be determined in a channel to be protected byrevet mattresses include: roughness coefficient, velocity, depth and shear stress. The Manning's roughness coefficient can be determined from Equation 5.1:

$$n_b = \frac{d_{90}^{1/6}}{26} \quad (5.1)$$

where  $d_{90}$  is in meters. The normal velocity, depth and hydraulic radius can then be determined from Manning's equation for given discharges. The corresponding bed shear stress can be determined from:

$$\tau = \gamma DS \quad (5.2)$$

where  $\gamma$  is the unit weight,  $D$  is the water depth, and  $S$  is the friction slope which can be approximated by the average channel bed slope.

### 5.3 Determination of Mattress Requirement Based on Incipient Motion Criteria

The flow condition that causes the incipient motion of the filling rock within mattresses on channel bed can be determined by Figures 4.9 through 4.13, or by the following relation:

$$\frac{\tau_c}{(\gamma_s - \gamma)d_m} = 0.1 \quad (5.3)$$

The proposed steps include:

1. From Figure 4.10 or 4.13, determine the required thickness of mattresses and the corresponding filling rock sizes for the given design bed shear stress.
2. Assuming that Equation 5.3 can be also applied to banks, determine the permissible shear stress on the bank,  $\tau_s$ , based on Equation 5.3 and tractive force theory from the following equation:

$$\tau_s = \sqrt{1 - \frac{\sin^2 \theta}{\sin^2 \phi}} \tau_c \quad (5.4)$$

where  $\theta$  is the bank slope,  $\phi$  is the angle of repose of filling rocks equal to about 41 degrees for the Reno mattresses, and  $\tau_c$  is the critical shear stress for the bed computed from Equation 5.3.

3. Determine the maximum shear stress acting on the bank,  $\tau_m$  for the given design condition. For a trapezoidal channel section:

$$\tau_m = 0.75 \gamma DS \quad (5.5)$$

where  $D$  is the water depth and  $S$  is the bed slope.

4. Compare  $\tau_s$  with  $\tau_m$ . If the  $\tau_s$  is larger then the design mattress is adequate. If the  $\tau_m$  is larger but not more than 20 percent larger, then there may be some deformation of mattresses on banks. However, the mattress protection will remain effective if the filter design is adequate.
5. In case of very high velocity (15 to 25 fps), it may be desirable to grout the reno mattress with sand asphalt mastic than to use a larger reno mattress thickness. This has been verified by our experiments and practical experiences.

The steps described above for bank protection, were based on the tractive force theory which may or may not be applicable to mattress protection works. Additional data should be obtained to verify the applicability of the tractive force theory to design mattresses.

#### 5.4 Determination of Velocity at the Mattress/Filter (or Base Soil) Interface

The velocity at the mattress/filter interface can be determined by:

$$V_b = \frac{1.486}{n_f} \left(\frac{d_m}{2}\right)^{2/3} S^{1/2} \quad (5.6)$$

in which  $n_f = 0.02$ . Equation 5.6 has been verified using model-scale mattress test data. The velocity immediately underneath the filter fabric was found to be about 1/4 to 1/2 of  $V_b$ . This velocity strongly affects the stability of base soils. The magnitude of  $V_b$  can be significantly reduced by properly grouting and installing the mattresses.

If a gravel filter is utilized, then  $V_b$  can also be determined from Equation 5.6 by assuming that  $n_f = 0.025$ . The velocity at the interface of gravel filter and base soil decreases with increase in the gravel filter thickness. No relation is available to determine this interface velocity. It is assumed that the velocity drop through the gravel filter layer is proportional to the head loss of flow through the gravel voids, namely:

$$h_f = f \frac{L}{d_v} \frac{V_b^2}{2g} = \frac{V_b^2}{2g} - \frac{V_f^2}{2g} \quad (5.7)$$

where  $f$  is Darcy-Weisbach friction coefficient, assumed equal to 0.05,  $L$  is the thickness of gravel filter,  $d_v$  is the equivalent diameter of voids which is approximately equal to 1/5 of median gravel size, and  $V_f$  is the velocity at the filter and soil interface. Therefore, the thickness of gravel required to reduce the interface velocity from  $V_b$  at the mattress/filter interface to  $V_f$  at the filter/soil interface can be determined from:

$$L = \frac{d_v}{f} \left[ 1 - \left(\frac{V_f}{V_b}\right)^2 \right] \quad (5.8)$$

Additional study is required to evaluate the effects of the filter on the stability of base soil, particularly under the high flow current and impact force condition.

### 5.5 Determination of Filter Requirement

Because geotextile filter is easy to install and has been proven to be effective as an integral part of protection work, this type of filter is recommended when the interface velocity is small. Otherwise, a gravel filter is recommended. Proposed design steps follow:

1. Compute the velocity  $V_b$  at the mattress/filter interface using Equation 5.6.
2. Determine  $V_f = 0.5 V_b$ .
3. Compare  $V_f$  with the erosion velocity  $V_e$  that causes erosion of base soil.

For noncohesive soil,

$$V_e = 1.67 d^{1/2} \quad (5.9)$$

where  $d$  is particle size in mm. Equation 5.9 is developed using Shields parameter equal to 0.05, specific gravity of particle equal to 2.65 and Darcy-Weisbach friction factor equal to 0.025.

For cohesive soil,

$$V_e = \sqrt{\frac{8\tau}{f\rho}} \quad (5.10)$$

where  $\tau$  can be determined from Figure 5.1,  $\rho$  is the density of water, and  $f$  is the Darcy-Weisbach friction factor. In general,  $f$  varies from 0.02 to 0.05 depending on surface roughness, channel slope and Reynolds number (Chow, 1959). For Equation 5.10,  $f = 0.025$  is suggested.

4. If  $V_f < V_e$ , then use the geotextile filter.
5. If  $V_f > V_e$ , then design gravel filter using the method suggested below:

$$\frac{d_{50} \text{ (Filter)}}{d_{50} \text{ (Base)}} < 40$$

$$5 < \frac{d_{15} \text{ (Filter)}}{d_{15} \text{ (Base)}} < 40 \quad (5.11)$$

$$\frac{d_{15} \text{ (Filter)}}{d_{85} \text{ (Base)}} < 5$$

Thickness  $t$  should not be less than six to nine inches.

6. Let  $V_f = V_e$  and compute the desired filter thickness  $L$  from Equation 5.8.

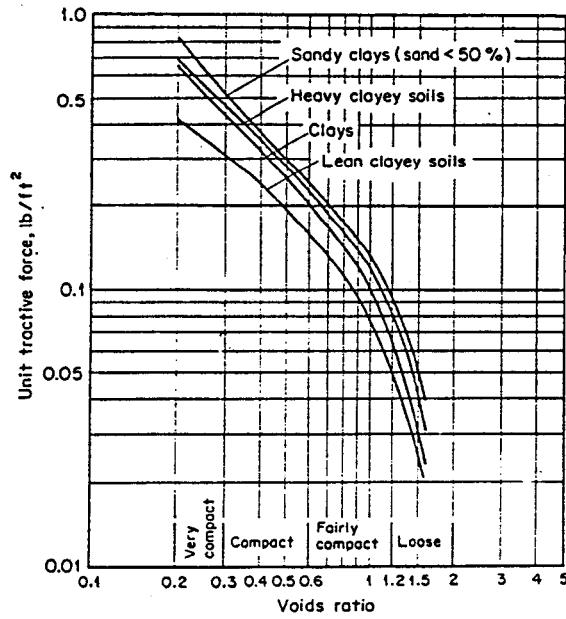


Figure 5.1. Permissible unit tractive force for canals in cohesive material as converted from the U.S.S.R. data on permissible velocities.

7. Compare  $t$  and  $L$  and utilize a larger value.

It is possible to combine geotextile filter and gravel filter to achieve a stable mattress/filter/base soils system under very high velocity.

#### 5.6 Determination of Potential Deformation

The mattress protection structure can protect the channel against flow conditions more severe than design flow conditions based on incipient motion. Test results described in Section 4.4 clearly indicate this. Combining mattresses with suitable filter system can protect the channel against very high flow currents. Figure 4.21 provides a relation to determine the magnitude of mattress deformation.

## VI. SUMMARY AND CONCLUSIONS

Model-scale mattresses with a length scale ratio of 1:3 were tested in an 8-foot flume and in a 4-foot flume. Types of model-scale mattresses tested included 6-inch, 9-inch, 12-inch and 18-inch mattresses and 6-inch grouted mattresses. The largest velocity these mattresses were subjected to was about 12 fps which converted to a prototype velocity of about 20 fps. Also, 6-inch and 9-inch mattresses were tested in an outdoor flume with a 13 percent slope capable of providing a velocity of 21 fps. These tests were analyzed to determine incipient motion of mattresses, hydraulic conditions in mattress channel, velocities at the mattress/filter interface and at the filter/soil interface, pressure variations and extent of mattress deformation when subjected to very high flow current. The analysis results were utilized to develop design criteria.

The major findings of this mattress test program include:

1. The hydraulic conditions in a mattress channel are the same as those in a gravel channel.
2. The roughness of mattresses is mainly caused by filling rocks. The mesh has insignificant effect on mattress roughness. Strickler's equation can be utilized to determine Manning's roughness coefficient.
3. The stability of mattress and riprap structures are highly dependent on flow velocity and weakly dependent on flow depth. The relative effect of velocity and depth on mattress and riprap structure stability is about six to one.
4. Flow velocity and shear stress that cause incipient motion of filling rock within mattress compartment are about twice higher than the same size of unbound rocks. The corresponding Shields parameter is about 0.1 for mattresses comparing to a value of 0.047 for riprap. Mattress mesh greatly enhances the stability of filling rocks. Test results indicate that stability of mattress structure is higher than the stability of riprap structure of the same thickness. To achieve the same degree of stability, the rock size of riprap structure has to be about twice larger than the filling rock within the mattress and the riprap structure has to be thicker. This indicates that the mattresses structure will be more economic than riprap. A comparison with the suggested thickness of riprap shows a savings of 50 to 200 percent for flow velocity up to about 20 fps.
5. When mattresses were subjected to very high flow current, rocks within mattress compartments will propagate downstream and cause rippling deformation surface. However, if the reduced thickness of rocks is larger than median rock size then mattresses are still effective in channel protection. This phenomenon was based on observing the specific head variation at the mattress/filter interface which showed that the specific head remained fairly constant disregard the mattress deformation.

Additional tests are required to confirm this finding. The deformation height can be estimated from Figure 4.19.

6. The velocity at the mattress/filter interface was found to be quite significant for steep channel flow. This interface velocity is highly dependent on the mattress slope and interface spacing, and can be determined by Manning's equation. The velocity immediately underneath the filter fabric is about 1/4 to 1/2 of this interface velocity. This velocity range is about the same for various filter fabrics that are commonly utilized for channel stabilization. This indicates that even if mattresses remain stable, there is a possibility of failure due to high underlying velocity that erodes the base materials. A suitable filter can be utilized to mitigate this problem. For low interface velocities, a filter fabric is recommended because it is effective and easy to install. For large interface velocities, a gravel filter or a combined geotextile/gravel filter can be utilized to assist in stabilizing base soils even under very high flow currents far beyond the incipient conditions.
7. Grouting of the mattresses using sand-asphalt mastic can significantly consolidate the mattresses and reduce interface velocity. Experiments and practical experiences showed that at a velocity of 20 fps, the critical velocity was not reached. Therefore, in case of high velocity (15-25 fps), it may be advisable to grout the reno mattresses with sand-asphalt mastic than to use a larger reno mattress thickness together with a greater size of filling stone.
8. A design procedure has been developed. This procedure is based on test results obtained from this study and theories regarding the mattress bank protection and filter effects. Additional studies are required to confirm or improve the design criteria for designing bank protections in straight channel reaches or around bends using mattress and for designing filter under extremely high flow conditions.
9. All the mattresses tested had a compartment length of three feet. This length is a significant factor affecting mattress stability. It will be beneficial to at least test model-scale mattresses with different compartment lengths to evaluate their effect.

Therefore, to improve design criteria and to increase our knowledge of performance of mattress protection structures, the following additional studies are proposed:

1. Conduct tests of model-scale mattresses of different compartment lengths to evaluate their effect on incipient motion, deformation and stability of mattress.
2. Conduct mattress tests on stream banks and around bends to improve design criteria for bank protection.
3. Conduct study of performance of geotextile filter and gravel filter under extremely high flow to evaluate their performance and to develop design methods that can adequately integrate the filter into mattress and riprap

protection works to improve overall stability of protection works and to avoid unnecessary overdesign.

4. Better evaluate the strength of mattresses to resist deformation. This will provide useful information to relate the mattress deformation to the hydraulic conditions and characteristics of mattresses and thereby to develop ultimate mattress design criteria for more efficient utilization of mattresses.

## VII. REFERENCES

- Agostini R., A. Papetti, 1978. Flexible linings for canals and canalised water courses. Tabulated dimensions for trapezoidal channel sections. Bologna, S.P.A. Officina Maccaferri, 155 p.
- Balsillie, J. H., and R. O. Bruno, 1972. Groins: An annotated bibliography, Army Coastal Engineering Research Center, Washington, D.C., Misc. Paper No. 1-72, 249 p.
- Barton, J. R., and P. V. Winger, 1973, Rehabilitation of a channelized river in Utah in Hydraulic Engineering and the Environment. Proceeding of the 21st Annual Hydraulic Division Specialty Conference, Montana State University, Bozeman.
- Bradt, P. T., and G. E. Wieland, 1978. The impact of stream reconstruction and a gabion installation on the biology, and chemistry of a trout stream. National Tech. Information Service, Springfield, VA, PB-280 543.
- Brown, C. T., 1978. Gabions and reno-mattresses as low cost terminal revetments, in Managing the coast. 4th Austr. Conf. Coastal and Ocean Eng., Adelaide. Barton Inst. Eng. Australia 222-223.
- Brown, C. T., 1979. Gabion report on some factors affecting the use of Maccaferri gabions and reno-mattresses for coastal revetments. Manly Vale, NSW, Univ. NSW, Water Res. Lab., Report No. 156, 75 pp.
- Burroughs, M. A., 1979. Gabions: economical, environmentally compatible erosion control. Civil Engr. (ASCE) 49, 1, 58-61.
- California State Highway Commission, 1922, Rock-and-wire deflectors protect banks against floods. Eng.-News Record.
- Checking river erosion in Columbia. 1973. World Construction, V26, No. 6.
- Chen, Y. H., D. B. Simons, and P. M. Demery, 1981, "Hydraulic Testing of Plastic Filter Fabrics," Journal of the Irrigation and Drainage Division, ASCE, No. IR3, Vol. 107, September, pp. 307-324.
- Chisholm, D. H., 1976. Wellington Airport Extension--additional sea protection. New Zealand Engineering. V. 31, No. 5, pp. 157-161.
- Chow, V. T., 1959, "Open-Channel Hydraulics," McGraw-Hill Book Company, New York.
- Cooper, C. O. and T. A. Wesche, 1976. Stream channel modification to enhance trout habitat under low flow conditions Nat. Tech. Information Service, Springfield, VA. PB-249 858.
- Copeland, R. R., 1980. Old River overbank structure outlet modifications; hydraulic model investigation. National Tech. Information Service, WES/MP/H4-80-5; AD-A092802/8.
- Filter Sheet Used on Working Scheme, 1976. Ground Engineering V. 9, No. 2, p.44.

GangRao, H. V. S., 1978a. The development of standard short-span bridge systems, final summary. National Tech. Information Service. WVD0H-50-F; FHWA/WV-78-1; PB80-120181, 106 p.

GangaRao, H. V., 1978b. Conceptual substructural systems for short-span bridges. ASCE J. of Transportation Engineering, V. 104, No. 1.

Gabions plug side on Tennessee Highway, 1971. Roads and Streets, V. 114, No. 9, p. 62-63.

Gerodetti, M., 1981. Model studies of an overtopped rockfill dam. Water Power Dam Constr., 33, pp. 25-31.

Goodwin, W. A., 1975. Other uses of limestone and dolomite. Limestone, Vol. 12, No. 94, 7 pp. (Tenn. Dept. Transportation).

Gotz, W., 1978. Stabilization of river banks in semi-arid regions. Wasserwirtsch, Vol. 68, No. 5, pp. 147-154.

Harmelink, M. D., and J. J. Hajek, 1973. Performance testing of freeway noise barriers. ASCE J. Transportation Engineering V. 99, No. TE1., pp. 123-138.

Holeman, J. N., and E. F. Sauer, 1969. Conservation in a new town. Soil Conservation, Vol. 35, No. 2, p. 35-38.

Keuther, C., 1935. Die verwendung von Drahtnetzkorpern in Wasserbau. Research Inst. for River Control, Munich, Germany.

Keown, M. P., E. Dardeau, N. R. Oswalt, E. B. Perry, 1977. Literature survey and preliminary evaluation of streambank protection methods. U.S. Army Engr. Waterways Exp. Stn., Vicksburg.

Lavagnino, S., 1974. Gabions guard river banks against 50,000 cfs flow. ASCE Civil Engineering, V. 44, No. 5, pp. 88-89.

Lejecher, T. R., and A. D. Leydecker, 1973. Field notes. Dept. Agr., Forest Service, Washington, D.C., Field notes, Vol. 5, No. 5-6, 16 p.

Leydecker, A. D., 1973. Use of gabions for low water crossings on primitive or secondary forest roads. U.S. Forest Service, Field Notes, V. 5, No. 5-6, pp. 13-6, also in Low-Cost Water Crossings Compendium. Transportation Research Board, Pub., Washington, D.C.

Luedtke, R. J., F. J. Watts, M. A. Brusven, and T. E. Roberts, 1973. Physical and biological rehabilitation of a stream in hydraulic engineering and the environment. Proceedings of the 21st Annual Hydraulic Division Specialty Conference, Mt. State Univ., Bozeman.

Maccaferri Gabions, "Notes on Mastic Grouted Gabions and Reno Mattresses."

Maccaferri Research and Development Department, "Consistency and Viscosity of the Hydraulic Sand Asphalt Mastic and Function of Temperature," Bituminous Products Research Department, Genova.

Maccaferri Research and Development Department, "Sand Asphalt Mastic Grouted Reno Mattresses Revetment, Tests and Controls on the Hot Curable Hydraulic Sand Asphalt Mastic," Bituminous Products Research Department, Genova.

McSwain, K. R., and R. E. Schmidt, 1976. Gabions, perforated pipe and gravel serve as fish screens. ASCE, Civil Engineering, V. 46, No. 5, 73 p.

Maughan, O. E., K. L. Nelson, and J. J. Ney, 1978. Evaluation of stream improvement practices in southeastern trout streams. Okla. Coop. Fisheries Research Unit, Water Resources Research Center, Bull. 115, Stillwater.

Michel, G., 1977. Experience gained at the Service de navigation du nord related to bank protection, in "La defense des berges, des canaux et rivieres, Tenaud, R. (ed). Paris, Ecole Nat. Ponts Chaussees, Assoc. Amical Ing. Anciens Eleves, pp. 57-65.

Nasser, M. S., and J. A. McCorquodale, 1974. Experimental study of wave transmission. J. of the Waterways, Harbors, and Coastal Engineering Division, Proceedings of the Am. Soc. Civil Engineers, V. 100, No. WW4.

Oswald, N. R., J. F. George, and G. A. Pickering, 1975, Fourmile Run Local Flood-Control Project, Alexandria and Arlington County, Virginia, U. S. Army Engineer Waterways Experiment Station, Technical Report, H-75-19, December.

Oswald, N. R., S. T. Maynard, 1978. Bank protection techniques using gabions, in Streambank erosion control evaluation and demonstration, work unit 3, Section 32 Program; Hydraulic Research; Vicksburg, MS, U.S. Army Engineer Waterways Experiment Station, Res. Rep. 3, 9 p.

Parker, T. C., F. A. Kittredge, 1935. Wire-bound rock training walls solve Zion Park Flood problem. Eng.-News Record.

Pernier, M., 1977. Comparative study of different types of bank protection, in "La defense des berges, des canaux et rivieres, Tenaud, R. (ed) Paris, Ecole Nat. Ponts Chaussees, Assoc. Amicale Ing. Anciens Eleves, pp. 13-25.

Pillai, N. N., D. V. S. Verma, 1978. Shore protection using stones enclosed in nets. Coastal Engineering, 1, 4, pp. 349-358.

Poche, D. J. and W. C. Sherwood, 1976. Sediment trapping efficiency of straw and hay bale barriers and gabions. Transportation Research Board Pub., Transp. Res. Record, N594, pp. 10-14.

Posey, C. J., 1969. Erosion prevention experiments. Proc. 13th Congr. Intl. Assoc. for Hydr. Res. V. 2, pp. 211-219.

Posey, C. J., 1957. Flood-erosion protection for highway fills. Trans. ASCE, No. 2871, 531-555.

Quigley, R. M., J. H. L. Palmer, A. Rowland and D. Bere, 1974. Groyne stabilization of slope movements and toe erosion, Lake Huron near Bayfield, Ontario, in Proceedings, 17th Conference on Great Lakes Research, Part 1, McMaster University, Hamilton.

Roth, L., 1977. Erosion control simplified by modernized metal gabion. Dixie Contractor, Vol. 52, No. 8, pp. 17-24.

Royster, D. L., 1975. Tackling major highway landslides in the Tennessee Mountains. ACSE Civil Engr. Vol. 45, No. 9, pp. 85-87.

Saunders, P. A., and J. L. Grace, Jr., 1981. Channel control structures for Souris River, Minot, North Dakota, Hydraulic Model Investigation, Vicksburg, MS, US Army Eng. Waterways Exp. Stn., Hydraulic Lab., TR-HL-81-3, 57 pp.

Schuster, R. C., 1974. Gabions in highway construction. Transportation Research Board Pub. Trans. Research Board Special Rpt. N 148, pp. 97-105.

Serrazanetti, G., 1903. Wasserschutzbauten. Bologna, Italy.

Stephenson, D., 1980. The stability of gabion weirs, Water Power and Dam Constr., 32, 4, 24-28.

Stern, P., 1981. Gabions for hydraulic structures. Appropriate Technol., 7, 4, 6-8.

Tan, K. H., D. Thirumurthi, 1976. Highway Construction impact on water supply lakes. ASCE, J. Environmental Engineering Div., Vol. 104, No. EE5, pp. 997-1011.

Transportation Research Board, 1979. Synthesis 2: Stage Construction. Transp. Research Board Pub., Washington, D.C., 37 p.

U.S. Forest Service, 1979. Proceedings of the Forest Service Geotechnical Workshop held at Ames, Iowa. National Tech Information Service, EM-7170-1; PB80-153612, 472 p.

Velut, D., R. Perpere, and P. Mesnage (et al.) 1977. The Verdon works. The regulation dyke. Travaux 504, pp. 38-51.

Veress, S. A. and J. N. Hatzopoulos, 1979. Monitoring by aerial and terrestrial photogrammetry. National Tech. Information Service, FHWA-WA-80-38-1; PB80-192925, 115 p.

APPENDIX  
DESIGN EXAMPLES

### A.1 Example 1: Protection of a Channel on a Mild Slope

#### Problem

A necessary part of an improvement scheme for a natural water course is to use a drainage channel whose cross section is shown on Figure A.1. The longitudinal bed slope is  $S = 0.001$ . The soil through which the canal passes is sandy clay soil. Determine the protection requirement using mattresses.

#### Solution Procedure

1. A 6-inch Reno mattress is selected for protecting the drainage channel. The filling rocks range from 3 to 6 inches with a median size of 4.5 inches and a  $d_{90}$  of 5.4 inches.
2. The water velocity, discharge capacity, bed shear stress and Froude number of flow in the channel are determined as follows:

- a. The area of the water cross section,  $A$ , the wetted perimeter,  $P$ , the hydraulic radius,  $R$ , and the top width,  $T$ , are:

$$A = (B + ZD)D = (40 + 2 \times 10) \times 10 = 600 \text{ ft}^2$$

$$P = B + 2d \sqrt{1+Z^2} = 40 + 2 \times 10 \times \sqrt{1+4} = 84.7 \text{ ft}$$

$$R = \frac{A}{P} = \frac{600}{84.7} = 7.08 \text{ ft}$$

$$T = B + 2Zd = 40 + 2 \times 2 \times 10 = 80 \text{ ft}$$

- b. The Manning's roughness coefficient (Equation 5.1)

$$n = \frac{d_{90}^{1/6}}{26} = \frac{0.137^{1/6}}{26} = 0.0275$$

- c. The velocity,  $V$ ; discharge,  $Q$ , shear stress,  $\tau$ ; and Froude number,  $F$ , are determined from Manning's equation:

$$V = \frac{1.486}{n} R^{2/3} S^{1/2} = 6.30 \text{ fps}$$

$$Q = AV = 600 \times 6.30 = 3,780 \text{ cfs}$$

$$\tau_b = \gamma DS = 62.4 \times 10 \times 0.001 = 0.624 \text{ psf}$$

$$F = \frac{V}{\sqrt{gA/T}} = 0.405$$

3. Based on Figure 4.10, the design velocity computed above is lower than the critical velocity ( $V_c = 14.5 \text{ fps}$ ) for the 6-inch mattress.

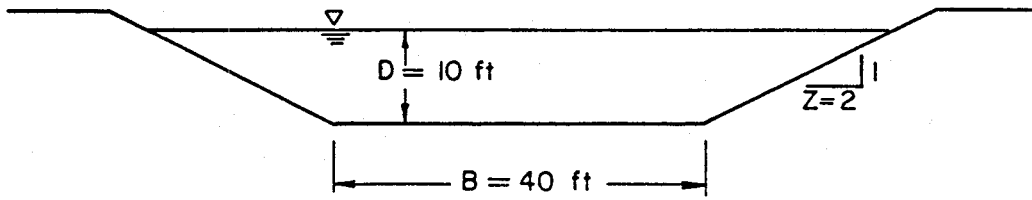


Figure A.1. Cross-sectional shape.

Therefore, the 6-inch mattress is adequate to protect the channel bed based on the incipient motion criteria.

Next, the 6-inch mattresses are evaluated to determine their adequacy for bank protection as follows:

- a. For protecting the channel banks, the permissible critical stress on banks protected by mattresses is (Equation 5.4):

$$\tau_s = \sqrt{1 - \frac{\sin^2 \theta}{\sin^2 \phi}} \tau_c$$

where  $\theta = 26.6^\circ$ ,  $\phi = 41^\circ$  and

$$\begin{aligned} \tau_c &= 0.1 (\gamma_s - \gamma) d \\ &= 0.1 \times (165 - 62.4) \times 4.5/12 = 3.85 \text{ psf} \end{aligned}$$

Then

$$\tau_s = 0.731 \times 3.85 = 2.81 \text{ psf}$$

- b. The maximum shear stress acting on the bank

$$\tau_m = 0.75 \gamma D S = 0.75 \times 62.4 \times 10 \times 0.001 = 0.468 \text{ psf}$$

- c. The permissible critical shear stress  $\tau_s$  is larger than the flow shear stress  $\tau_m$ . Therefore, a 6-inch mattress is suitable for protecting the bank.

4. Determine the filter requirement using the following steps:

- a. Try a filter fabric.

- b. The velocity at the mattress/filter interface is computed based on Equation 5.6:

$$\begin{aligned} V_b &= \frac{1.486}{n_f} \left( \frac{d_m}{2} \right)^{2/3} S^{1/2} \\ &= \frac{1.486}{0.02} \left( \frac{0.375}{2} \right)^{2/3} (0.001)^{1/2} = 0.769 \text{ fps} \end{aligned}$$

- c. The velocity at the filter/soil interface:

$$V_f = 0.5 V_b = 0.385 \text{ fps}$$

- d. For sandy clay soil, the critical shear stress is found from Figure 5.1 to be 0.05 psf. The corresponding critical velocity based on Equation 5.10 is:

$$V_e = \frac{\sqrt{8\tau}}{f_p} = \sqrt{\frac{8 \times 0.05}{0.025 \times 1.94}} = 2.87 \text{ fps}$$

- e. The critical velocity of soil,  $V_e$ , is larger than the flow velocity at the filter/soil interface,  $V_f$ . Therefore, a geotextile filter fabric is adequate for the protection.

## A.2 Example 2: Protection of a Channel on a Steep Slope Problem

The design condition is the same as Example 1 except that the longitudinal bed slope is  $S = 0.01$  and soil is sandy with a  $d_{50} = 0.5$  mm. Determine the protection requirement for using mattresses.

### Solution Procedure

1. A 6-inch Reno mattress is first tried for protecting the channel. The filling rocks range from 3 to 6 inches with a median size of 4.5 inches and a  $d_{90}$  of 5.4 inches.
2. The water velocity, discharge capacity, bed shear stress and Froude number are determined as follows:

$$V = \frac{1.486}{n} R^{2/3} S^{1/2}$$

$$= \frac{1.486}{0.0275} (7.08)^{2/3} (0.01)^{1/2} = 19.9 \text{ fps}$$

$$Q = AV = 600 \times 19.9 = 11,940 \text{ cfs}$$

$$\tau_b = \gamma DS = 62.4 \times 10 \times 0.01 = 6.24 \text{ psf}$$

$$F = \frac{V}{\sqrt{gA/T}} = \frac{19.9}{\sqrt{32.2 \times 600/80}} = 1.28$$

3. Based on Figure 4.10, the design velocity computed above is slightly larger than the critical velocity for 18-inch mattresses. Therefore, 18-inch mattresses with filling rocks ranging 4 to 8 inches are then tried. These filling rocks have a median size,  $d_m = 6$  inches and a  $d_{90} = 7.6$  inches. The corresponding Manning's  $n = 0.0292$ . Therefore, the design flow velocity is 18.7 fps. For this design flow velocity, 18-inch mattresses should be sufficient for protecting the channel bed. Figure 4.13, using the bed shear stress as the parameter, shows the same requirement.

Next, adequacy of using 18-inch mattresses for bank protection is evaluated:

- a. The permissible critical stress on banks protected by mattresses is:

$$\begin{aligned}\tau_s &= 0.731 \tau_c \\ &= 0.731 \times 0.1 \times (165 - 62.4) \times 6/12 \\ &= 3.75 \text{ psf}\end{aligned}$$

- b. The maximum flow shear stress acting on the bank

$$\begin{aligned}\tau_m &= 0.75 \gamma R S \\ &= 0.75 \times 62.4 \times 7.08 \times 0.01 = 4.68 \text{ psf}\end{aligned}$$

- c. The permissible critical shear stress,  $\tau_s$ , is less than the flow shear stress,  $\tau_m$ , by about 20 percent. It is expected that 18-inch mattresses will be sufficient to protect banks. However, some deformation of mattresses may occur.

4. Determine the filter requirement using the following steps:

- a. Try a filter fabric.

- b. The velocity at the mattress/filter interface is computed based on Equation 5.6:

$$\begin{aligned}V_b &= \frac{1.486}{n_f} \left(\frac{d_m}{2}\right)^{2/3} S^{1/2} \\ &= \frac{1.486}{0.02} \left(\frac{0.5}{2}\right)^{2/3} (0.01)^{1/2} = 2.95 \text{ fps}\end{aligned}$$

- c. The velocity at the filter/soil interface,

$$V_f = 0.5 V_b = 1.48 \text{ fps}$$

- d. For sandy soil, the critical shear stress is found from Equation 5.9:

$$\begin{aligned}V_e &= 1.67 d_{50}^{1/2} \\ &= 1.67 (0.5)^{1/2} = 1.18 \text{ fps}\end{aligned}$$

- e. The critical velocity of soil,  $V_e$ , is less than the flow velocity at the filter/soil interface,  $V_f$ . This indicates that even though the mattresses are stable, the interface velocity is capable of moving the base soil to be protected by the mattresses and filter fabric. Either a thin layer (about 2 to 3 inches) of fine gravel can be placed between the base soil and the filter fabric or a gravel filter designed based on Equation 5.11 can be utilized to

assist in stabilizing the base soil.

5. Determine the deformation of the 18-inch mattresses based on the following steps:

- a. Compute the ratio,

$$C_*' = \frac{\tau - \tau_c}{(\gamma_s - \gamma)d_m}$$

For the bed

$$C_*' = \frac{6.24 - 5.13}{(165 - 62.4) \times 0.5} = 0.022$$

For the bank

$$C_*' = \frac{4.68 - 3.75}{(165 - 62.4) \times 0.5} = 0.018$$

- b. From Figure 4.19, for  $C_*' = 0.018 - 0.022$ , the deformation ratio  $\Delta Z/d_m = 1.2$ . Then  $\Delta Z = 6 \times 1.2 = 7.2$  inches. This indicates that the thickness of the upper portion of the 18-inch mattresses would be reduced by  $\Delta Z/2 = 3.6$  inches to a thickness of about 14 inches. This thickness is sufficient to protect the base materials.